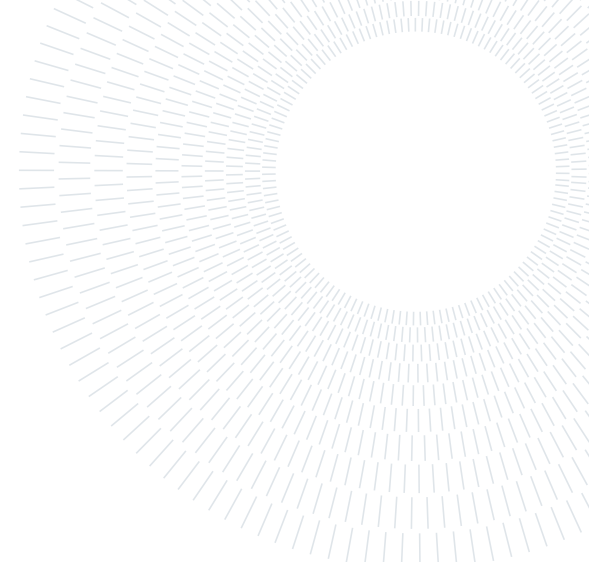




**POLITECNICO**  
**MILANO 1863**

**SCUOLA DI INGEGNERIA INDUSTRIALE  
E DELL'INFORMAZIONE**



EXECUTIVE SUMMARY OF THE THESIS

# PROTOTIPES OF IN VITRO 3D MODEL TO DETERMINE THE ROLE OF PULMONARY MUCUS ON SARS-CoV-2 INFECTION

LAUREA MAGISTRALE IN BIOMEDICAL ENGINEERING - INGEGNERIA BIOMEDICA

**Author: GIULIANA IANNONE**

**Advisor: PROF. PAOLA PETRINI**

**Co-advisor: FRANCESCO BRIATICO**

**Academic year: 2021-2022**

---

## 1. Introduction

Mucus is a dynamic semipermeable barrier that covers several epithelia of the human body acting as a protecting shielding. Airways mucus layer is composed of water (95%), glycoproteins (3%), salts and lipids. Its functions are lungs protection against unsafe particles and chemicals that may enter during inhalation, and maintenance of epithelium hydration level [1],[2]. To guarantee those functions, it is needed the appropriate mucociliary clearance level. However, clearance control is complex because influenced by several mechanisms as epithelial water and ion transport, mucin secretion, cilia action and cough. The worst condition arises under dehydrated conditions or when MUC5AC and MUC5B, the main mucin types, increase their secretion over 6%. In this conditions, mucus osmotic pressure overcomes the one of the periciliary layer causing cilia compression, decreasing in transport leading to mucus adhesion and ducts obstruction [3].

In healthy conditions mucus acts as a high-density mucin fiber network with an average pore size between 100 nm and 1000 nm, that only allows water, nutrients and gasses transition. It has been studied that cells attachment

to the basement membrane is due to the high mucus adhesiveness contribute. Viscosity and elasticity, instead, influence mucus transport capacity and vary through the thickness of the mucus layer. It was discovered the dependence of  $G'$  and  $G''$  on strain and frequency. In a frequency domain between 0.2-1 Hz, the results showed that physiological values for healthy airway mucus are  $G'$  in the range  $14,9 \pm 9,2$  and  $G''$   $4,3 \pm 2,7$  [4].

Unfortunately, mucus changes are the most common lives shortening diseases worldwide. Among those, the most frequent pathological conditions are CF, asthma and COPD. Currently, major interest is given to the respiratory disease caused by novel Coronavirus SARS-CoV-2 which in 2020 brought to the declaration of pandemic state. Coronavirus SARS-CoV-2 stands out for its novelty, aggressivity and velocity in spreading. Patients affected by SARS-CoV-2 show an abnormal increasing of MUC5AC and MUC5B expression, the main mucin types, resulting as strict mucus adhesion to epithelium layer and massive duct obstruction [5]. The reached levels of  $G'$  and  $G''$  show increasing in mucins cross-linking and entanglement.

## 2. Aim of the thesis

The project “Mucus4Covid” arises from the need of founding an *in vitro* model that could be used in biological laboratories for virus studies and mimic the composition and the structural properties of human mucus in healthy and pathological condition due to SARS-CoV-2.

## 3. Materials and methods

A first Mu4Covid formulation was provided at Department of Chemistry, Materials and Chemical Engineering “Giulio Natta” at Politecnico di Milano, Italy. The developed mucus models are composed of alginate, a natural polysaccharide, and mucin, the main protein of pulmonary mucus. GDL and  $\text{CaCO}_3$  were used as crosslinking agents. For each 3D mucus model it always remained unchanged the ratio 1:4:1:1 Alginate:Mucin: $\text{CaCO}_3$ :GDL, what varied was only the concentration of the different components. DMEM, EMEM and TSB have been used as mediums to allow components dissolution.

### 3.0.1 Gel preparation

Alginate and mucin are added slowly in two backer containing medium and have stirred at 250-350 rpm for 4 hours. Then, the double syringe method is hence used to produce the mucus model: firstly, mixing alginate and mucin solutions, then adding the  $\text{CaCO}_3$  suspension and finally the GDL. Before carrying out any test it is necessary to leave the models 20 hours at 4°C. *pH analysis.* The study of the pH of the developed mucus prototype is crucial because an environment similar to the human body has to be set up in order to give the chance to its use in cells experiments. Therefore, using a pH-meter, every composition was stored in syringes of 5mL, and the pH was tested.

### 3.0.2 Rheology

To study the rheological characteristics of the developed gels, it has been used the Anton Paar MCR 502 TwinDrive-Ready SN82235284 rheometer. Through it, frequency and viscosity tests were carried out by changing the upstream plate and the parameter sets.

*Shelf-life assessment.* The study of the shelf-life of the mucus gels was conducted to de-

termine how initial characteristics and performances vary among the conservation time. Different storage modalities were tried: at ambient temperature (22°C), in fridge (4°C) and in freezer (-80°C) and then defrost (initially at -20°C, then 4°C). Mechanical properties were tested for a maximum of 7 days.

### 3.0.3 Stability in medium

Stability tests study if the prototypes change their weights when put in an oven at 37°C. This analysis was crucial because studies conducted with cells are at 37°C. To conduct the experiment, mucus models after production were dispensed in transwells and left crosslinking in them. It was used transwells that fit 24 and 6 multiwells, and respectively 2mL and 400 $\mu$ l of mucus were added. Spent 20 hours, the transwells were weighted (control) and medium was added into the multiwells (respectively 2mL and 800 $\mu$ l). All the empty spaces were filled with dH<sub>2</sub>O and some grains of sodium azide were added. Finally, the overall structure was sealed with parafilm. Weight variation  $w[\%]$  is calculated as follow:

$$w[\%] = \frac{w(t) - w(0)}{w(0)} * 100$$

where  $w(t)$  is the weight at each time-point  $t$  and  $w(0)$  is the initial weight.

### 3.0.4 Collaboration with UniTO and UniPV

UniTO and UniPV collaborated with PoliMI studing cytocompatibility on cellular lines HCT8 and VERO-E6, viral activity using surrogates of SARS-CoV-2 (Human coronavirus, HCoV-OC43) and SARS-CoV-2 (delta variant), bacterial infections and drugs permeability *Material from UniPV.* Were delivered 30 mL of blank TSB (Tryptic Soy Broth), 30 mL of TSB containing *S. Aureus* secretome grown in stationary phase 0.5, 30 mL of TSB containing *S. Aureus* secretome grown in exponential phase 1.7, 30 mL of blank EMEM (Eagles’ Minim Essential Medium), 30 mL of EMEM containing VERO-E6 secretome 0.5, 30 mL of EMEM containing VERO-E6 secretome 1.11. Everything was committed in a freezer and the defrosting was provided leaving the falcons in a hot bath (at 37°C) for 15 minutes.

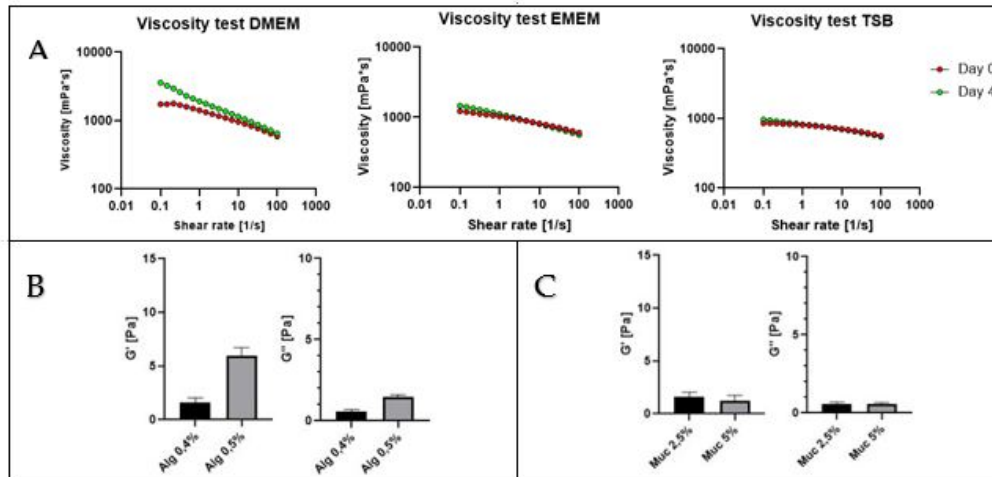


Figure 2: (A) viscosity test of the alginate solution 0,6% conducted on day 0 and day 4 in DMEM, EMEM and TSB; (B) comparison between Mu4Covid 1.5 (alg 0,4%, muc 2,5%) and Mu4Covid 1.8 (alg 0,5%, muc 2,5%). Statistical differences at  $G'$  (0,44Hz) and  $G''$  (0,44Hz) for  $p < 0.05$  have been detected; (C) comparison between Mu4Covid 1.2 (alg 0,4%, muc 5%) and Mu4Covid 1.5 (alg 0,4%, muc 2,5%). No statistical differences at  $G'$  (0,44Hz) and  $G''$  (0,44Hz) for  $p < 0.05$  have been detected

## 4. Results

### 4.1. Optimization

#### 4.1.1 Prerequisites

During the analysis, have been developed several compositions.

Gel Name	Alginate	Mucin	CaCO <sub>3</sub>	GDL
Mu4Covid 1.2	0.4%	5%	0.13%	0.8%
Mu4Covid 1.5	0.4%	2.5%	0.13%	0.8%
Mu4Covid 1.8	0.5%	2.5%	0.13%	0.8%
Mu4Covid 2.0	0.6%	2.5%	0.13%	0.8%
Mu4Covid 2.1	0.6%	2.5%	0.13%	1%
Mu4Covid P 2.2	0.7%	1.25%	0.13%	1%
Mu4Covid P 2.3	0.7%	2.5%	0.13%	1%

Figure 1: more relevant tested compositions

A first skimming of the developed models was based on the compliance to some prerequisites: pH analysis, macroscopic observation and in accordance with UniPV and UniTO studies about cells viability.

#### 4.1.2 Two components system

Alginate and mucin, were selected as the main components of the 3D model. Studies about their characteristics are reported in Figure 2. DMEM, TSB and EMEM have been analyzed as mediums.

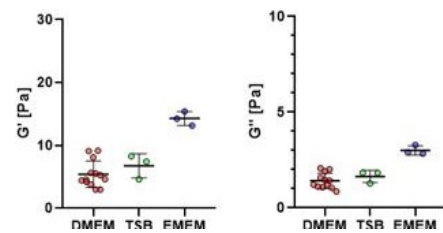


Figure 3: analysis on Mu4Covid 2.0 produced in different mediums

#### 4.1.3 Possibility to be extruded

It has been evaluated if the extrusion mechanism affects the mechanical properties.

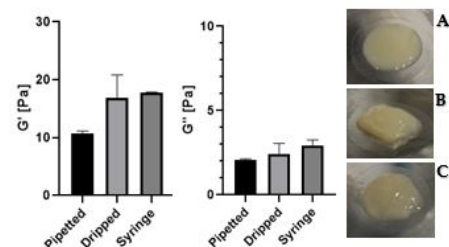


Figure 4: Mu4Covid P 2.2 dispensed by pipetting, dripping and syringing. No statistical differences at  $G'$  (0,44Hz) and  $G''$  (0,44Hz) for  $p < 0.05$  were found between the syringe and dripped modality, while statistical differences were found respect pipetted. (A) pipetted gel, (B) dripped and (C) syringe

4.1.4 Shelf life assessment

Freezing

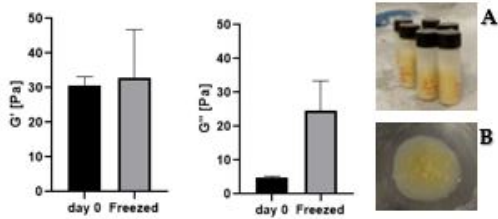


Figure 5: comparison mucus at  $t=0$  and after freezing and defrosting. No statistical differences at  $G'$  (0,44Hz) for  $p<0.05$  have been detected, while statistical differences have been found for  $G''$  (0,44Hz). (A) vials during the storage; (B) on the rheometer plate

Storage in the fridge at 4°C

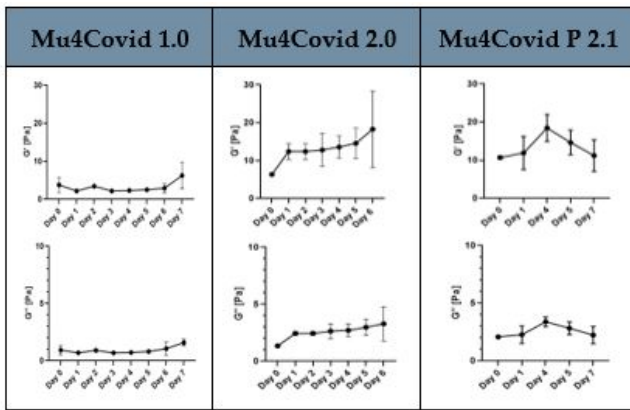


Figure 6: shelf-life over a maximum of 7 days of some studied mucus compositions reported in terms of  $G'$ (0,44Hz) and  $G''$ (0,44Hz)

Storage at  $T_{amb}$

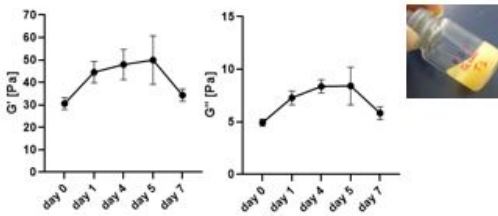


Figure 7:  $G'$ (0,44Hz) and  $G''$ (0,44Hz) when the gel is stored at  $T_{amb}$ . A maximum increasing of 70% of the moduli was detected. Since day 1 the double phase arises, as reported in the image

4.1.5 Stability test

Stability tests have been conducted using 6 transwells support and 24 transwells support.

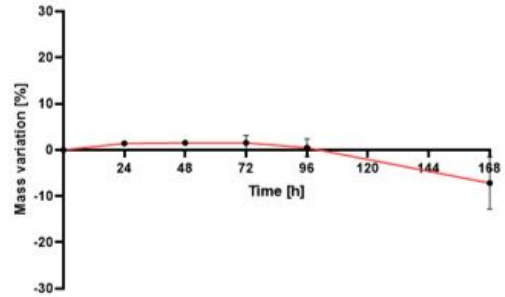


Figure 8: stability test at  $t = 0, 24, 48, 72, 96, 168$  h of Mu4Covid P 2.0 in 24 transwells support

4.2. Bacterial infection

Shelf-life and stability test on Mu4Covid P 2.3 in TSB with *S. Aureus* secretome 0.5 or 1.7 and EMEM with VERO-E6 secretome 0.5 or 1.11.

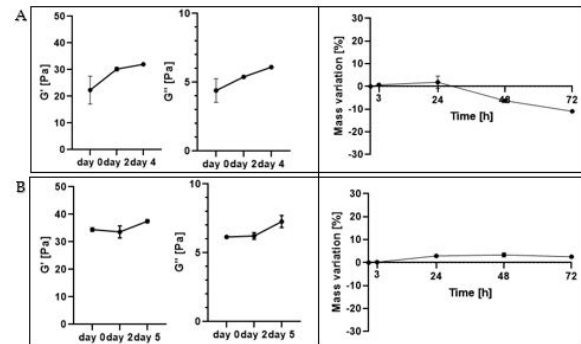


Figure 9: shelf-life in terms of  $G'$ (0,44Hz) and  $G''$ (0,44Hz) and stability at  $t = 0, 3, 24, 48, 72$  h in TSB (A) 0.5 and (B) 1.7

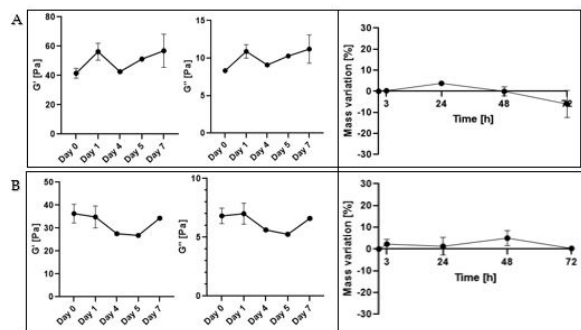


Figure 10: shelf-life in terms of  $G'$ (0,44Hz) and  $G''$ (0,44Hz) and stability at  $t = 0, 3, 24, 48, 72$  h in EMEM (A) 0.5 and (B) 1.11



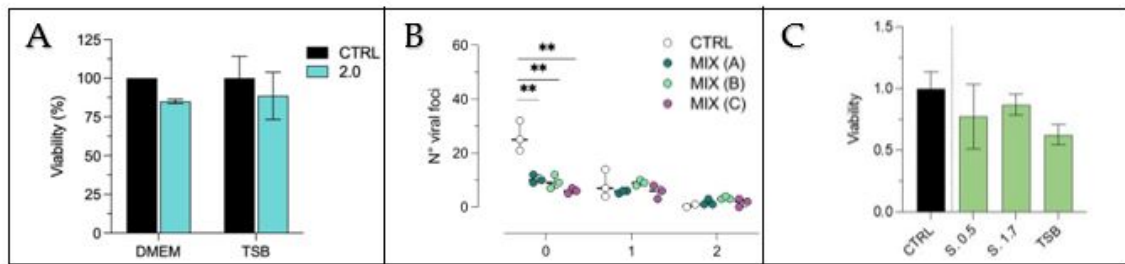


Figure 11: studies conducted in UniPV and UniTO on Mu4Covid 2.0. (A) comparison of the cellular viability of VERO-E6 cellular line using Trypan blue coloration in DMEM and TSB. The control is in absence of Mu4Covid 2.0; (B) virucidal test using HCoV-OC43 on three cellular lines; (C) cytocompatibility of VERO-E6 in Mu4Covid 2.0 containing *S. Aureus* secretome in exponential phase (S. 0.5) and stationary phase (S. 1.7) in TSB and comparison to Mu4Covid in only TSB and the control

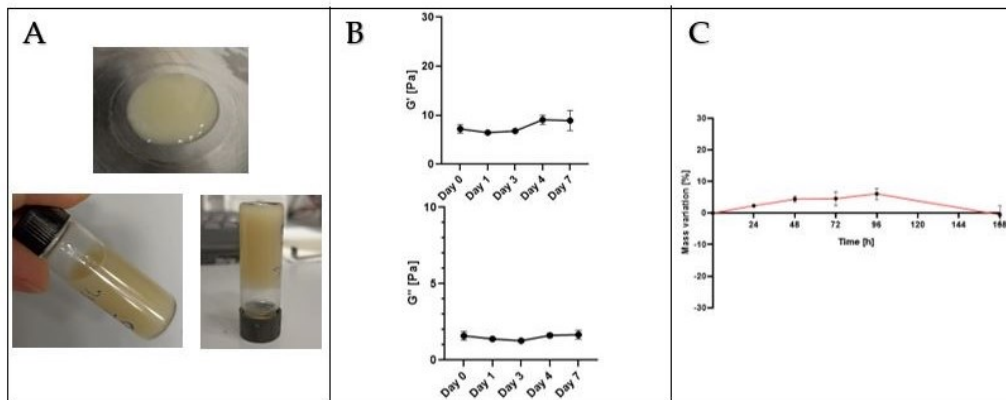


Figure 12: (A) macroscopic view of Mu4Covid 2.1 on the rheometer plate and in the vial during the storage; (B) trends of  $G'$ (0,44Hz) and  $G''$ (0,44Hz) during the 7 days of storage. No statistical differences at  $G'$  (0,44 Hz) and  $G''$  (0,44 Hz) for  $p < 0.05$  have been detected; (C) stability test provided at  $t = 0, 24, 48, 72, 96, 168$  h in 24 transwells support by and calculation of mass variation [%]. The detected pH was 5.84

#### 4.3. Definition of physiological and pathological due to SARS-CoV-2 disease Mu4Covid models

It emerged that Mu4Covid 2.1 (Figure 12) and Mu4Covid P 2.3 (Figure 13) were the models that better mimic respectively healthy and SARS-CoV-2 pathological condition. Their shelf-life was conducted over 7 days and showed the arising of the double phase after 5 days. Tests conducted on the dispensability of the models showed coherent results compared to the general case reported in subsection 4.1.3.

## 5. Discussion

To develop the *in vitro* airway mucus model that better mimics healthy and pathological condi-

tion due to SARS-CoV-2, have been tested several compositions. For each of them pH and macroscopic view have been evaluated. Alginate and mucin have been selected as the main components. While the first one is the determinant of the mechanical properties, change mucin amount and medium type don't causes relevant rheological variations. Pipetting was selected as dispensing modality since dripped and syringed models showed thickness increasing and clots arising. Store the prototypes at  $4^{\circ}\text{C}$  resulted to be the best choice, whereas at  $T_{amb}$  the double phase is immediately displayed and in freezer the model stays too viscous. All models appear stable at  $37^{\circ}\text{C}$  since no variation is beyond  $\pm 7\%$ . Studies conducted at UniTO and UniPV on Mu4Covid 2.0 showed cells viability

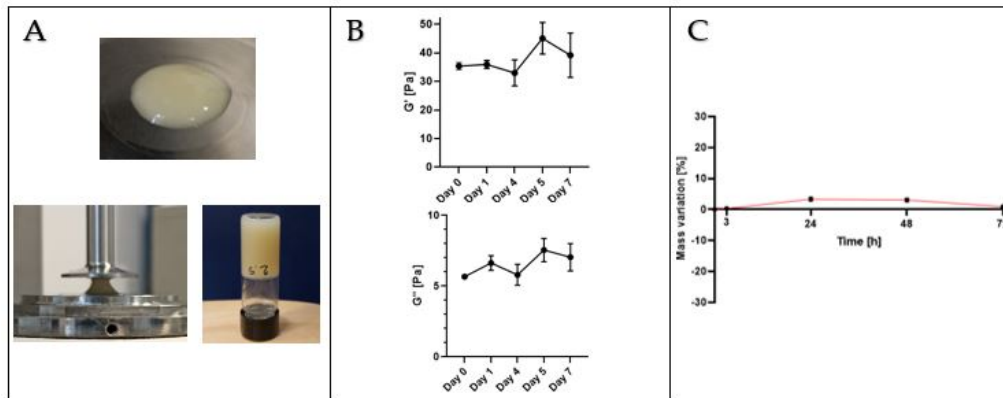


Figure 13: (A) macroscopic view of Mu4Covid P 2.3 on the rheometer plate, when the upper plate is rising and upside down in the vial; trends of  $G'$ (0,44Hz) and  $G''$ (0,44Hz) during the 7 days of storage. No statistical differences at  $G'$  (0,44 Hz) and  $G''$  (0,44 Hz) for  $p < 0.05$  have been detected; (C) stability test provided at  $t = 0, 24, 48, 72, 96, 168$  h in 24 transwells support by and calculation of mass variation [%]. The detected pH was 5.74

over 80%, selective drugs permeability, no differences in viral activity, and that the coexistence of bacteria and virus doesn't affect cells viability. Mu4Covid 2.1 and Mu4Covid P 2.3 were selected respectively as healthy and pathological SARS-CoV-2 mucus model since displaced mechanical characteristics in human range for 5 days from production, adequate dispensability and macroscopic properties, acceptable pH values and great stability at 37°C. TSB and EMEM can be used as mediums, and *S. aureus* secretome can be included being careful that mechanical properties appear slightly varied.

## 6. Conclusion

Mucus acts as a barrier for pathogens, but sometimes this shield isn't enough, and viral and bacterial infections may arise. In SARS-CoV-2, mucus role is fundamental during the progress of the pathology: mucins networks get entangled causing a steep increasing in rheological properties, while pH and mucociliary clearance decrease leading to severe duct obstruction. In this contest, study and develop an *in vitro* mucus layer results topical and of great relevance.

During the study, it has been revealed that high levels of mucin in the prototypes lead to drastic reduction in cell viability and pH. Therefore, the increasing in viscosity typical of SARS-CoV-2 condition must be controlled by alginate concentration. Instead, medium changes don't affect significantly the rheological properties. Data

from UniPV and UniTO give the chance to the use of the model for bacteria and virus studies. The final developed models appear stable in mediums and are characterized by coherent pH values. The mechanical properties match the studies on human mucus, and are preserved for 5 days. The prototypes are also stable at 37°C, giving a chance to their use in cellular experiments. Finally, it was discovered that they are easy to dispense and can adapt to transwells and multiwells of different nature and size. *S. aureus* secretome can be included, but rheological properties increase respect the control (only medium).

## 7. Bibliography

- [1] Mucus: The Body's Unsung Hero. The slimy stuff has a surprisingly wide array of beneficial biological functions, D. Kwon
- [2] Airway Mucus Function and Dysfunction, John V. Fahy, M.D., and Burton F. Dickey, M.D.
- [3] Effective Mucus Clearance Is Essential for Respiratory Health S. Randell, R. Boucher.
- [4] Macro- and Microrheological Properties of Mucus Surrogates in Comparison to Native Intestinal and Pulmonary Mucus, B. Huck, O. Hartwig, A. Biehl, K. Schwarzkopf, C. Wagner
- [5] Alveolar macrophage dysfunction and cytokine storm in the pathogenesis of two severe COVID-19 patients C. Wang, J. Xie, L. Zhao, X. Feia, H. Zhanga, Y. Tanc, X. Nied.



**POLITECNICO**  
MILANO 1863

SCUOLA DI INGEGNERIA INDUSTRIALE  
E DELL'INFORMAZIONE

# PROTOTIPES OF IN VITRO 3D MODEL TO DETERMINE THE ROLE OF PULMONARY MUCUS ON SARS-CoV-2 INFECTION

TESI DI LAUREA MAGISTRALE IN  
BIOMEDICAL ENGINEERING-INGEGNERIA BIOMEDICA

Author: **Giuliana Iannone**

Student ID:	10569833
Advisor:	Paola Petrini
Co-advisor:	Francesco Briatico
Academic Year:	Lorenzo Sardelli
	2021-22





## Abstract

Pulmonary mucus is a dynamic semipermeable barrier mostly composed of water and mucin that acts as a protective shielding for the lining epithelium. In case of adverse events, such as SARS-CoV-2 pathological condition, mucin types MUC5B and MUC5AC secretion increases causing network entanglement and abnormal increasing in rheological properties. The aim of this thesis is to develop, characterize, and validate an *in vitro* model able to mimic healthy and pathological condition due to SARS-CoV-2 infection. The developed prototypes are made of alginate, a natural polysaccharide discovered to be the main responsible of mechanical properties, and mucin, mucus protein incorporated to mimic natural airway biochemistry, and can be dissolved in several mediums. It was found that balance mucin amount is essential to not produce pH decreasing and low cell viability. Studies about cytotoxicity, viral and bacterial infection, and drug permeability on the models were computed at UniTO and UniPV and showed promising results for its use during biological experiments. Mu4Covid 2.1 and Mu4Covid P 2.3 were selected as the compositions to mimic respectively the healthy and SARS-CoV-2 condition. For those optimized models storage, dispensability, wells adaptation, and stability at 37°C have been investigated. Finally, tests conducted in medium containing *S. aureus* secretome showed that bacteria can be included in the pathological mucus model. Components dissolution is guaranteed, but results evident that bacteria secreted components have consequences on mucus viscosity and network entanglement.

**Key-words:** mucus, SARS-CoV-2, alginate, mucin, bacterial medium



## Abstract in lingua italiana

Il muco polmonare è una barriera semipermeabile dinamica principalmente composta da acqua e mucina che funge da schermo protettivo per l'epitelio di rivestimento. In caso di eventi avversi, come per la condizione patologica SARS-CoV-2, la secrezione di MUC5B e MUC5AC aumenta, causando infittimento della rete e incremento anomalo delle proprietà reologiche. Il fine di questa tesi è sviluppare, caratterizzare e validare un modello *in vitro* che simuli la condizione sana e patologica dovuta a SARS-CoV-2. I prototipi realizzati sono composti da alginato, polisaccaride naturale scoperto essere il principale responsabile delle proprietà meccaniche, e mucina, proteina del muco incorporata per imitare la biochimica delle vie aeree, e possono essere disciolti in diversi medium. Si è riscontrato che bilanciare la quantità di mucina è essenziale per non causare una diminuzione del pH e della vitalità cellulare. Studi effettuati in UniTO e UniPV sulla citotossicità, infezione virale e batterica, e permeabilità ai farmaci dei modelli, hanno mostrato risultati promettenti al fine di un loro utilizzo negli esperimenti biologici. Mu4Covid 2.1 e Mu4Covid P 2.3 sono stati selezionati come le composizioni che imitano rispettivamente la condizione sana e da SARS-CoV-2. Per i modelli ottimizzati sono stati studiati lo stoccaggio, la dispensabilità, l'adattamento ai pozzetti e la stabilità a 37 ° C. Infine, test condotti in medium con secretoma di *S. aureus* hanno mostrato che i batteri possono includersi nel modello di muco patologico. La dissoluzione dei componenti è garantita, ma risulta evidente che le componenti secrete dai batteri hanno conseguenze sulla viscosità del muco e sulla fittezza della rete.

**Parole chiave:** muco, SARS-CoV-2, alginato, mucina, medium batterico



# Contents

<b>Abstract.....</b>	<b>i</b>
<b>Abstract in lingua italiana .....</b>	<b>iii</b>
<b>Contents .....</b>	<b>5</b>
<b>1. INTRODUCTION.....</b>	<b>7</b>
1.1 “Mucus: The Body’s Unsung Hero” [1].....	7
1.2 Airway mucus.....	9
1.2.1 Mucin .....	12
1.3 Healthy mucus .....	14
1.4 Pathologic mucus.....	19
1.4.1 Asma, CF and COPD .....	21
1.4.2 Pathological condition due to SARS-CoV-2 .....	26
1.4.3 Pathological condition due to bacterial interaction.....	30
1.4.4 Currently in vitro models.....	33
<b>2. AIM OF THE THESIS .....</b>	<b>36</b>
<b>3. MATERIALS AND METHODS.....</b>	<b>37</b>
3.1 Materials.....	37
3.2 Mu4Covid preparation .....	37
3.3 Rheology .....	39
3.4 Shelf-life assessment.....	39
3.4.1 Freezing.....	40
3.5 Stability in medium .....	40
3.6 pH analysis .....	42
3.7 Multiwell adaptability .....	42



3.8	Dissolution method .....	43
3.9	Collaboration with other universities.....	43
3.9.1	Materials from Pavia.....	44
<b>4.</b>	<b>RESULTS .....</b>	<b>45</b>
4.1	Optimization.....	45
4.1.1	Study of the composition .....	45
4.1.2	pH analysis.....	46
4.1.3	Macroscopic observation.....	46
4.1.4	Cells viability .....	48
4.1.5	Two components system.....	49
4.1.6	Possibility to extrude .....	57
4.1.7	Shelf-life assessment .....	59
4.1.8	Stability test.....	62
4.2	Collaboration with UniPV and UniTO.....	64
4.3	Definition of physiological Mu4Covid model.....	67
4.4	Definition of pathological Mu4Covid model .....	71
4.5	Bacterial infection .....	80
<b>5.</b>	<b>DISCUSSION .....</b>	<b>84</b>
<b>6.</b>	<b>CONCLUSION.....</b>	<b>96</b>
	<b>Bibliography.....</b>	<b>99</b>
<b>A.</b>	<b>Appendix A .....</b>	<b>111</b>
<b>B.</b>	<b>Appendix B.....</b>	<b>113</b>
	<b>List of Figures.....</b>	<b>118</b>
	<b>List of Tables.....</b>	<b>129</b>

# 1. INTRODUCTION

## 1.1 “Mucus: The Body’s Unsung Hero” [1]

Mucus is a complex hydrogel that acts as a protective barrier in several parts of the human body. Its composition and its structure play a crucial role in maintaining the shielding properties and, at the meantime, allow molecules and nanomaterial diffusion [1]. The mucus layer covers and protects all the wet epithelia of the human body, counterbalancing the higher level of exposure to the environment of those districts. Its presence is found in pulmonary airways, in the whole gastrointestinal (GI) tract, including the stomach and the small and large intestines, in cervicovaginal tract and in oculo-rhino-otolaryngologic tracts.

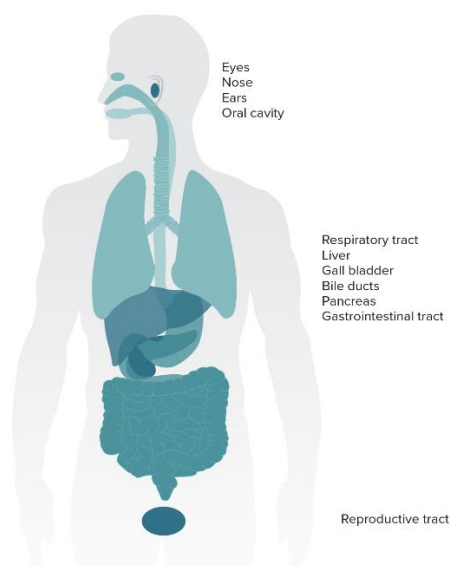


Figure 1.1: Anatomic view of mucus coating of the tissues lining all the body internal organs and cavities (adapted from [1])

Depending on where it is placed, mucus performs different functions among which are lubricant to protect epithelia against shear induced by mechanical forces during

digestion and blinking, maintenance of an enough hydrated layer over the epithelium, shielding to pathogens and noxious substances and allow the formation of a permeable gel layer for the exchange of gases and nutrients with the underlying epithelium [2]. Having a deficient mucous barrier leaves the underlying epithelium vulnerable to infections and injuries but, at the meantime, an excessive mucus production lead to altered rheologic properties and ducts obstruction. This is an important factor in the morbidity and mortality of chronic airways and GI diseases. Mucus is continuously secreted by submucosal glands and specialized epithelial secretory cells. Depending on the body district, it can show different features in matter of chemistry, physical and structural characteristics. Some examples are the reached thickness (form a 100– 800  $\mu\text{m}$  thick layer in the GI tract and a smaller 2–10  $\mu\text{m}$  thick layer in the pulmonary airways), the gas diffusion and the nutrients and drugs penetration [3]. Mucus composition is relatively conserved across different epithelia. It is mostly made up of water (95%) and mucin glycoproteins, but also contains DNA, salts, cell debris, lipids and proteins which have defensive purpose such as lysozyme, immunoglobulins, defensins, growth factors and trefoil factors [4]. Through all the components, mucins are the main responsible for the viscous and elastic gel-like properties. They are large and viscous glycoproteins mostly composed by carbohydrate, which in some cases can constitute until the 80% of the weight of the whole molecule, and amino acids.

Mucus from healthy subjects is very difficult to obtain because, in absence of trauma or disease, very little amounts are produced. Due to the limited availability of native mucus of human origin, the scientific community has started operating in developing artificial mucus surrogates. Ideally, those surrogates should be able to mimic both composition and structural properties of the natural mucus, in order to provide robust experimental models that can be used for studies about drug, virus and bacteria permeance.

## 1.2 Airway mucus

A mucus layer covers the airway tract. It is mostly composed of water (95%) and glycoproteins, but also molecules as salts and lipids which possess the protective functions such as anti-microbial, anti-protease, and antioxidant activity. The main mucus function is to protect the lung against unsafe particles and chemicals that may enter during inhalation as air pollutants among which ozone, sulfur dioxide, nitrogen dioxide, and cigarette smoke [5]. The mucus covers all the tract starting from the larynx, then the lungs, the bronchioles and finally the alveoli as showed in the below Figure 1.2.

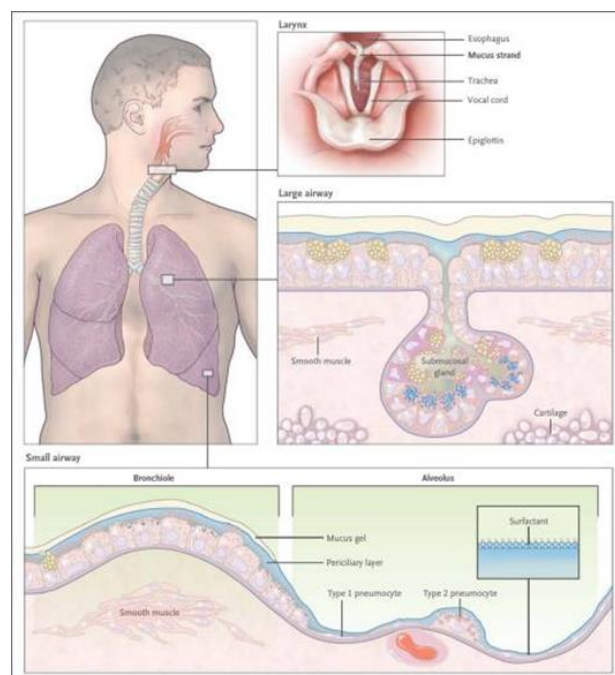


Figure 1.2: mucus distribution in normal airways (adapted from [20])

Mucus is continuously transported from the lower respiratory tract to the more proximal airways. This movement is allowed by the ciliary motion of the ciliated cells lining the airways that behave as renewable and transportable barrier against inhaled particulates and toxic agents. Considering that an adult approximately inhales 11000L

of airway every day, this represents a significant exposure to the surrounding medium and entails potential risks such as inhaled pathogens, pollutants, allergens and other particles [6], [7]. This transport is due to the mucociliary clearance mechanism, also known as the mucociliary escalator, that continuously wipes away and neutralizes the inhaled materials out of the airways. Thanks to mucus viscoelastic properties, it is allowed the conversion of energy from beating cilia into vectorial mucus transport. Under normal conditions, the mucus transport rate is  $60\mu\text{m/s}$ . Hence, particles get trapped in the viscous mucus layer and get removed due to the constant beating of the cilia present on the surface of underlying epithelial cells. Among the removed substances there are alveolar macrophages, the principal resident phagocytic cell in the lungs [5], [7], [8].

The mucus clearance is a complex mechanism that includes several mechanisms as epithelial water and ion transport, mucin secretion, cilia action and cough. Mechanical clearance is the dominant defense of the airways, and its failure produces obstructions that contributes to the pathogenesis of COPD and predisposes to chronic bacterial infection. The major determinants of the mechanical transport are hydration of mucosal surfaces, the coordinated activity of the cilia and mucin secretion [9]. Under normal conditions water content is enough to hydrate the periciliary layer, immediately over the epithelium, and the below mucus layer. The periciliary layer is an epithelial cell exudate,  $6\mu\text{m}$  in depth, that has low viscosity and an ionic content that is tightly maintained by the movement of sodium and chloride by the airway cells [10]. If the water content (and so even salts) increases too much, the mucus layer progressively starts swelling causing a clearance acceleration that reflects as a major mucus transport ( $100\mu\text{m/s}$ ). Inversely, under dehydrated conditions, clearance decreases and this results as a mucus adhesion to the cell surfaces [11]. The worst condition appears when it's shown an airway surface dehydration. In fact, it's



essential, in order to have a normal mucociliary clearance, that mucus contains around 2% of solids. In case of dehydrated condition, an increasing of secreted mucins (MUC5AC and MUC5B) is noticed and this brings to an increase in osmotic pressure generated by the mucus layer overlying the cilia. Exceeded a critical threshold ( $> 6\%$  of solids), the osmotic pressure of the mucus layer overcomes the one of the periciliary layer causing a cilia compression that reflects to a decrease in transport and ultimately the mucus stasis and adhesion to the airway surface [12].

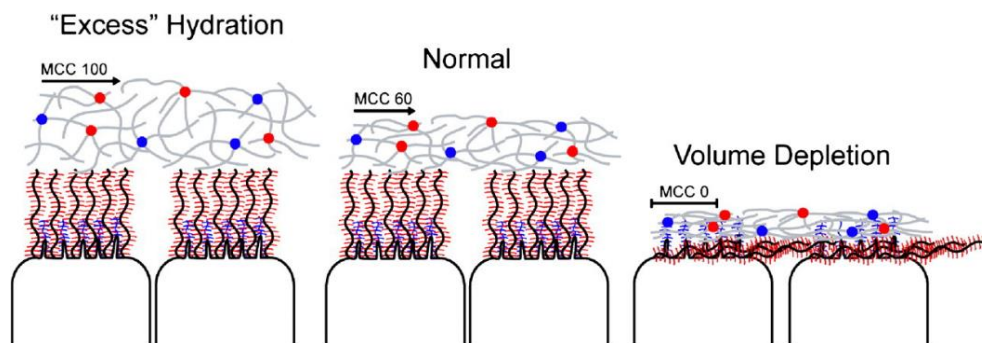
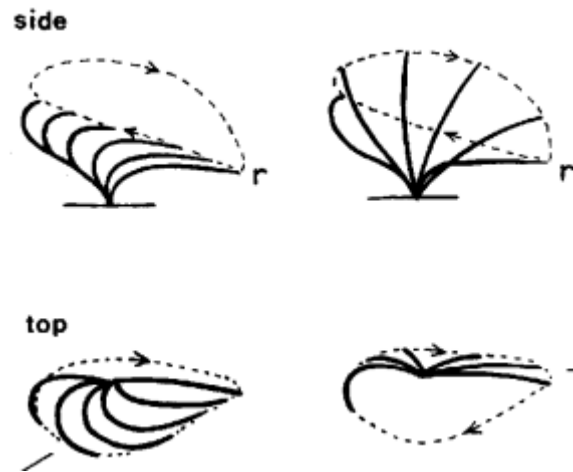


Figure 1.3: impact of water amount in the clearance studies in a "two layers system" made of pericellular environment and overlying mucus layer. The left panel reports the condition of hyperhydration, the central panel reports the normal physiological condition, the right panel the dehydrated condition (adapted from [11])

Another important factor that allows mucus transport is the coordinated activity of the cilia. They are the responsible of the propulsive function thanks to their tips which move in a low viscosity layer beyond the mucus. Cilia propel mucus through their asymmetric movements during the ciliary beat cycle. This cycle can be subdivided into two parts: the effective stroke of the cycle, in which cilia are fully extended and move in a plane perpendicular to the cell surface, and the recovery stroke, in which cilia swing around, near the cell surface, in order to reach again the starting position [13], [14].



**Figure 1.4:** beat cycle of the cilia seen from the side and top view. The recovery stroke starts on the left from the resting position (r) and continues unrolling clockwise. The effective stroke on right, shows how they remain extended until reaching the resting position (adapted from [14])

Beyond this, the reduction in mucus clearance can be also associated to primary ciliary dyskinesia that may induce mutations in genes that reflect to a not proper formation or function of cilia or to a decrease in MUC5B mucin secretion. Furthermore, glycoproteins, or mucins, are also the principal determinant of the mucus viscoelastic properties [11]. Viscosity and elasticity are the fundamental parameters to study both in healthy and pathological condition because enable mucus transport through ciliary movements [15].

### 1.2.1 Mucin

Mucins are high-molecular-weight glycoproteins that constitutes the major component of the airway mucus. Their function is to help eliminating inhaled pathogens and toxic elements under normal circumstances. The mucin structure presents regions of small and globular hydrophobic domains alternated with highly glycosylated unstructured regions [16]. This compresence of the two structures, allows the formation of an interconnected three-dimensional elastic network with a mesh-like

structure. The result is an intertwined network that both physically and in a size-dependent manner hinders nanoparticles diffusion acting as a barrier. For this reason, bacteria and virus penetration result attenuated. Unfortunately, also drug diffusion, epithelial absorption, and therapeutic outcomes of mucosal drug delivery, if not correctly dimensioned, are impeded [17]. On the other side, being a dense network, numerous interaction sites are also provided.

Mature mucins can belong to two different classes: the membrane-bound mucins and the secreted mucins. Among the first ones are included MUC1, MUC4 and MUC16. They allow cellular adhesion, pathogen binding, and signal transduction. Instead, the second ones can be further divided into insoluble gel-forming mucins, including MUC2, MUC5AC, MUC5B, MUC6 and MUC19, and soluble mucins, that involve MUC7, MUC8 and MUC9. They influence the viscoelastic and gel-forming properties of the mucus [18], [19]. MUC5AC and MUC5B are the main mucin types present in pulmonary mucus. They are structured as long single chains and form the mucus gel both by entanglement in a mesh and by noncovalent calcium-dependent crosslinking of adjacent polymers [20]. MUC5AC results abundant in tracheal and bronchial sections, and it's also present in bronchiolar epithelium and distal airways [21]. MUC5AC secretion changes significantly under stressing conditions such as inhalation of air pollution and tobacco smoking. Its structure contributes to host immunity and fight bacterial colonization [22]. Indeed, in case of infections, the level of MUC5AC rises steeply, creating much more bonding and that results in a much more tenacious structure. However, the formed sticky mucus is harder to clean from airways. MUC5B, instead, is majorly present in the submucosal gland duct epithelium, but is also localized in bronchiolar epithelium and distal airways. It's expressed in healthy airway and its function is to maintain immune homeostasis and provide anti-bacterial defence acting as a baseline barrier [21].

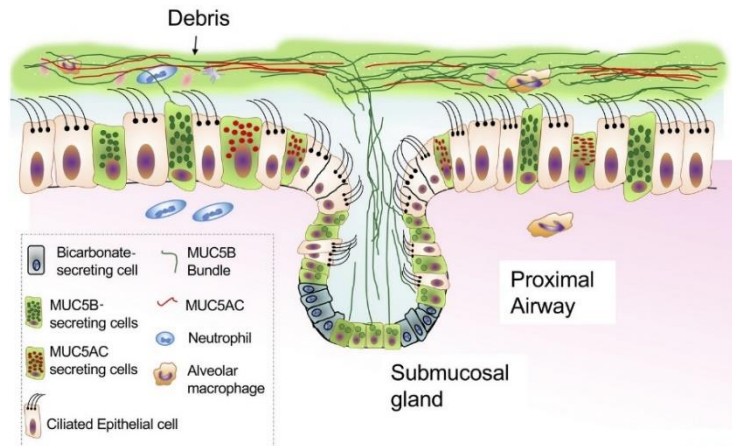


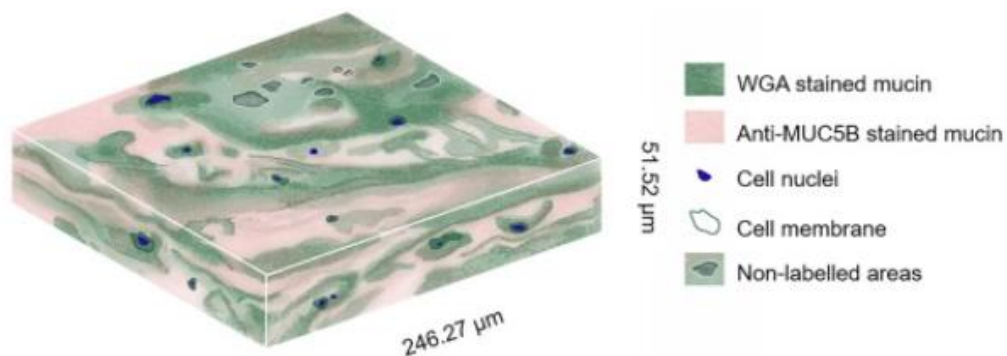
Figure 1.5: representation of the airways mucus layer focusing on MUC5AC and MUC5B, the most relevant membrane-bound mucins (adapted from [23])

The membrane-bounded are transmembrane mucins that normally dominate the apical surface of simple epithelia. Their glycan structure attracts water, creating a fluid layer, called periciliary, that surrounds the microvilli and the cilia. This layer is essential for ciliary action on mucus removal from airways. Since the transmembrane mucins have high levels of sialic acid and sulphate content, they provide a strongly negatively charged layer around the airway epithelia. This assures the formation of mucin bindings of secreted mucins MUC5AC and MUC5B and their continuous removal from the lungs. Transmembrane mucins form themselves a barrier that prevents pathogen invasion of the underlying epithelium [24].

### 1.3 Healthy mucus

In healthy conditions airway mucus plays a key role in protection of the lining epithelium against unsafe particles and chemicals that may enter during inhalation as air pollutants and cigarette smoke. Mucus is present in airways from the level of the trachea to the bronchioles and is characterized by a balanced production and mucin secretion [25]. Lipids and glycoproteins interact together affecting the wettability and hydrophobicity, and therefore the barrier functions of the mucus layer [26].

Through the major experiments conducted on airway mucus it's important to underline the fluorescence microscopy analysis, which provide information on the mucus material. In this way, MUC5AC, MUC5B and other mucin components are labeled and it has been evaluated their presence in mucus layer. As example it's below reported a schematic illustration prepared by using Illustrator Photoshop that depicts how MUC5B is distributed [27].



**Figure 1.6:** MUC5B distribution in mucus layer. WGA is referred to the samples that were treated with 10 $\mu$ g/mL of wheat germ agglutinin, while anti-MUC5B for the ones treated with antibodies (adapted from [27])

The mucus barrier can be considered as a high-density mucin fiber network whose average pore size is between 100nm and 1000nm. This structure is very functional and allows water, nutrients and gasses to pass through it, while if the particles are too big, their passage is not allowed. Moreover, MUC2 is the mucin type deputed not to permit bacteria or particles of more than 0.5 $\mu$ m to enter the layer. In this way a sterile environment is guaranteed. The so that formed barriers, prevent the passage of harmful particles, but unfortunately, they also provide difficult access to pharmaceuticals [28].



The airway mucus is considered as a very complex non-Newtonian biological material with flow and deformation rheological properties, characterized by nonlinear and time-dependent viscoelastic and physical properties of adhesiveness and wettability. Cells attachment to the basement membrane is due to mucus adhesiveness contribute. Instead, viscosity and elasticity are fundamental and directly involved in mucus transport capacity [29]. They vary as function of shear stress, time of shearing and length scale. If any change in mechanical properties occurs, it may be affected mucus function as a lubricant, selective barrier, and the defense against infection will be reduced. For example, if mucus becomes too thick, mucus clearance decreases resulting in bacterial overgrowth. On the other side, if it becomes too less viscous, as in women with bacterial vaginosis, it may be responsible for the increased risk of infection by HIV and *Neisseria gonorrhoeae*, as well as other adverse gynecological conditions [51]. To fully describe physical properties of the mucus layer it's important to identify: the elastic or storage modulus ( $G'$ ) and the viscous or loss modulus ( $G''$ ). The first one determines the solid-like characteristics of a polymer and considers the elastic behavior, the second one determinate the liquid-like characteristics and accounts for the viscous component. In order to determine them two different tests are usually done: oscillatory shear tests and frequency tests. The first one is generally performed over a range of small strain magnitudes (0.02–10% strain) at constant frequency (in physiological range) to determine the strain at which the viscoelastic moduli deviate by more than 10% from the plateau value indicating the linear viscoelastic regimen (LVR) [30]. The second one is conducted in order to analyze its rheological frequency-dependent properties. The obtained results showed that physiological values for healthy airway mucus are  $G'$  in the range  $14,9 \pm 9,2$  and  $G''$   $4,3 \pm 2,7$  [31]. The reason of those studies is that in heathy humans there are several factors that affect the rate of mucus flow such as relative humidity of inspired air,

gravity, and precisely the ciliary beat frequency. Typical ciliary beat frequencies range are from 7 cycles/sec in the peripheral airways to 25 cycles/sec in the trachea. Higher tracheal frequencies are needed to prevent mucus accumulation and clogging [6].

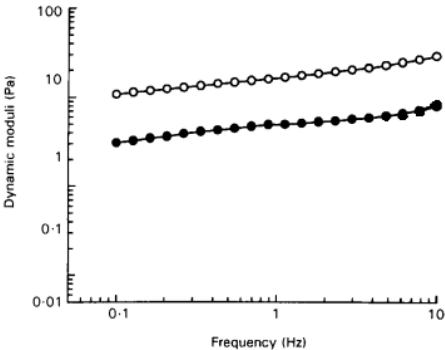


Figure 1.7: study on native airway mucus.  $G'$  (white dots) and  $G''$  (black dots) are here reported in function of frequency [Hz] (adapted from [32])

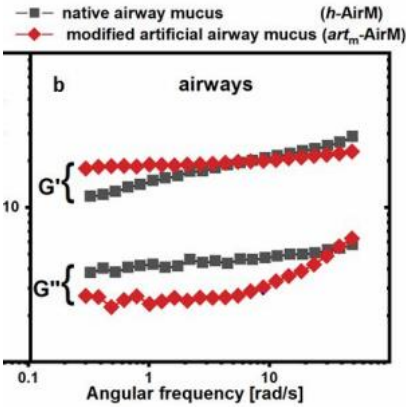


Figure 1.8: study on native airway mucus and modified one.  $G'$  (red squares) and  $G''$  (red squares) are referred to the modified artificial airway mucus,  $G'$  (grey squares) and  $G''$  (grey squares) are referred to the native. Both the trends are reported in function of frequency [Hz] (adapted from [31])

It has been noticed that the average shear rate to which the mucus is subjected in large bronchi (diameters 7–11.1mm) was  $0.9079 \text{ s}^{-1}$ , that in medium bronchi (diameters 4.3–7mm) was  $0.7817 \text{ s}^{-1}$  and that in small sized airways (2.8–3.5mm) was  $0.2494 \text{ s}^{-1}$ . The

below Figure 1.9 reports all the shear rates experienced for the whole tracheobronchial tree in healthy patients [33].

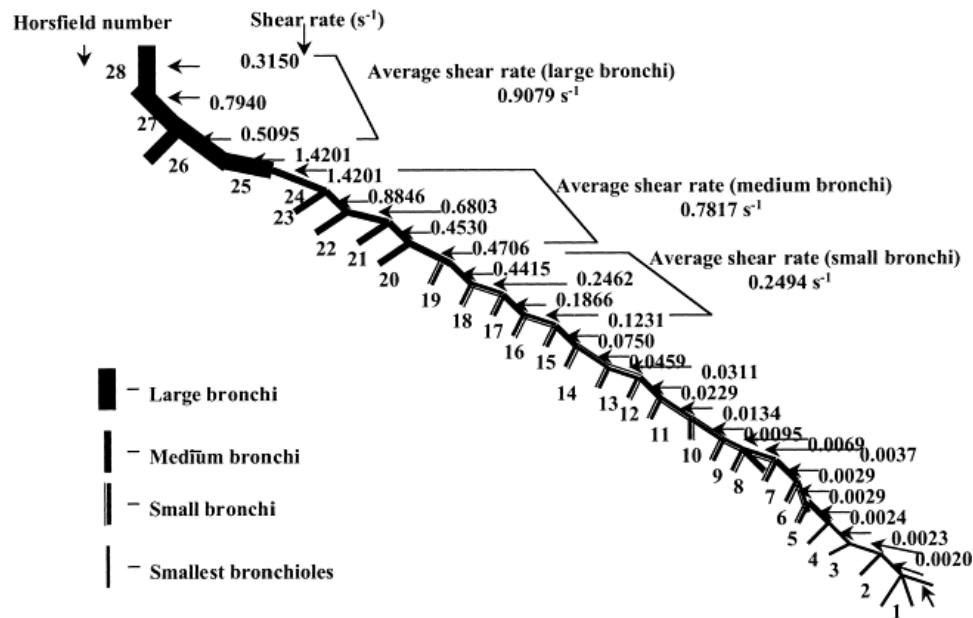


Figure 1.9: Shear rates experienced through the tracheobronchial tree (adapted from [33])

Another important parameter is viscosity. Mucus viscosity of healthy airways changes depending on where it is calculated: the more superficial mucus layer is characterized by gel-like properties and it's responsible of adsorbing and entrapping inhaled particles, while the below mucus layer is in contact with the epithelial cells and has lower viscosity so that cilia can easily provide its transport [34]. Mucus viscosity variation through the layers is controlled at the biochemical level [35].

However, healthy mucus references are very difficult to obtain because in absence of trauma or disease, very little is produced by the lung [6]. Currently, healthy human airway mucus is sourced from induced sputum (IS) and through bronchoscopy or using endotracheal tube. Instead, in subjects with disease, mucus is withdrawn from spontaneous sputum or from human bronchial epithelial (HBE) cell culture surfaces.

If sputum is induced in healthy subjects, even if the procedure is minimally invasive, it is necessary a dilution of the mucosal material and requires a trained health care team to perform the procedure. The main problem related to this is that since rheology is highly dependent on concentration, the measurement may be perturbed. Instead, for pathological patients, sputum can be obtained easily, spontaneously and in large volumes [36].

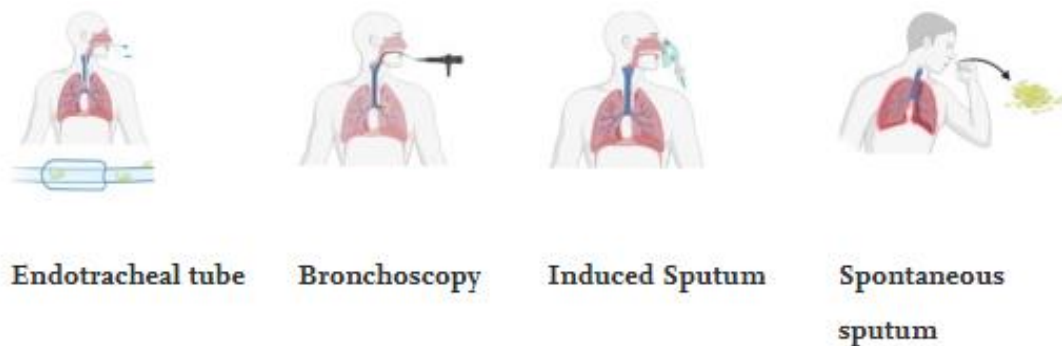


Figure 1.10: Sources for native human pulmonary mucus (adapted from [37])

## 1.4 Pathologic mucus

Mucus changes can bring to some dangerous pathological conditions. Those variations can be both qualitative, e. g. changes in mucus composition or structure, or quantitative, e. g. changes in amount of mucus in the lung. Changings in mucus composition could be due to alteration in glycoprotein biosynthesis, electrolyte transport, or water content, while structural modifications are due to interactions between normal mucus and pathogens. Quantitative changes, instead, involve hypersecretion of airway mucin that brings to duct obstructions [7].

Airway mucus obstruction can lead to many chronic lung diseases including genetic disorders as cystic fibrosis (CF), acute viral and bacterial infections such as primary

ciliary dyskinesia, non-cystic fibrosis bronchiectasis and pan-bronchiolitis, common lung diseases such as asthma and chronic obstructive pulmonary disease (COPD). Those pathologies have emerged as the leading causes of morbidity and mortality associated to airway failure [11]. The common factor of those pathologies is the reduction of mucociliary clearance and the increasing in mucus secretion. The coexistence of those conditions leads to airway mucus obstruction and plugging causing deleterious effects on lung function and homeostasis. In healthy conditions, cilia-dependent mucus transport is very efficient and successful, but, when it fails brings to intrapulmonary mucus accumulation. In addition, hydration and biochemical constituents are altered in pathologic mucus. Some examples are abnormal salts secretion, increased production of mucins and infiltration of mucus with inflammatory cells. Even the amount of serum proteins, mostly MUC5AC and MUC5B expressions, get increased in pathological conditions. MUC5AC overproduction, for example, is the major cause of the harmful build-up of mucus in the airways related to asthma, CF and COPD conditions [15]. However, also MUC1, MUC4, and MUC16 showed an overexpression in various diseases including CF, asthma, and cancer [38]. It's been studied that the mucus glycoproteins increasing is responsible for alterations in the rheology characteristics.

Through the conducted studies on pathological mucus, it has also been investigated how pH influences rheological properties and mucin concentration. It has been discovered that acidic pH brings to higher protein content, promoting the structural organization of mucins from random coil to form gel-like phase [39]. This mutated structural organization confers higher mechanical properties to the whole structure. Instead, the effects of pH and  $\text{Ca}^{2+}$  on viscosity were not statistically significant [40].



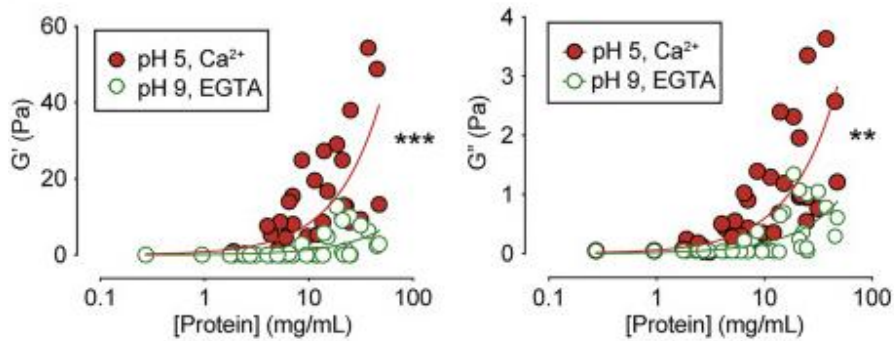


Figure 1.11: Relationship between mucus gel protein concentration and elastic modulus and viscous modulus at pH 5 with 10-mM  $\text{Ca}^{2+}$  and at pH 9 without  $\text{Ca}^{2+}$  (adapted from [40])

#### 1.4.1 Asma, CF and COPD

Asthma is one of the more common chronic diseases related to the airway tract. It affects ~334 million people (more male than female) of all ages, races, and ethnicities worldwide. The symptoms include cough, breathlessness (dyspnea), chest tightness and wheezing. Asthma results from obstruction in airflow, arising from a combination of inflammation-induced airway smooth muscle constriction and decreasing in mucociliary clearance [41]. The reduction in mucociliary clearance is present even in patients with mild stable disease, but the decreasing is highlighted in presence of severe airways mucus plugging found in fatal asthma. It has been discovered a correlation between asthma disease and the MUC5B expression reduction and MUC5AC increasing [42]. Moreover, Epidermal Growth Factor Receptor (EGFR) levels are increased and directly proportional to asthma severity [43]. Finally, a mild increasing has been detected also in goblet cells. During severe asthmatic events, related to the increasing in MUC5AC expression, the secreted mucus has higher viscous and elastic moduli and appears macroscopically abnormal compared to the physiological condition. This rheological variation is characteristic of an increase of the

cross-linked mucin polymers in the mucus gel. Consistently with this, it has also been noticed that the density of mucin polymers in asthmatic patients is shown to be increased [44].

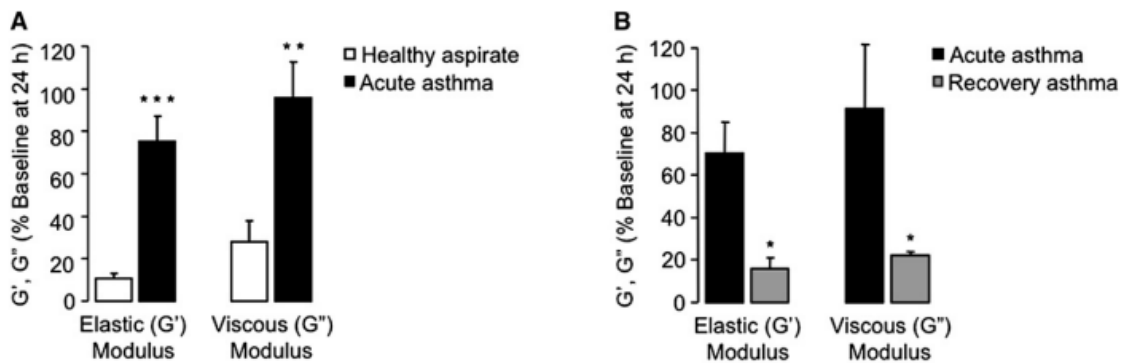


Figure 1.12: comparison between elastic and viscous moduli of healthy subjects and asthmatic during studies about time and temperature dependence. Data are collected from four healthy subjects and five patients with asthma. (A) Airway mucus collected from patients with early asthma stage. \*\*\* $P < 0.001$  and \*\* $P < 0.01$  versus healthy control subjects. (B) Comparison of airway mucus collected during the acute asthma stage and after the recovery in the hospital. \* $P < 0.05$  versus acute asthma (adapted from [44])

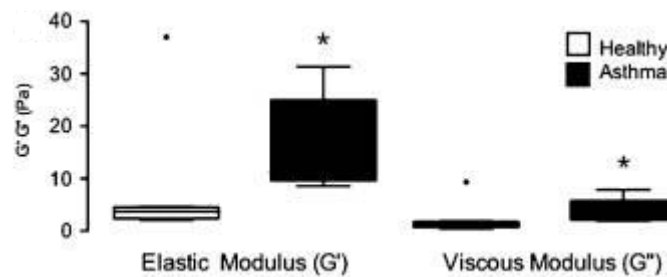


Figure 1.13: comparison between elastic and viscous moduli of healthy subjects and asthmatic ones during studies about frequency dependence (adapted from [44])

In case of patients affected by CF, some anomalies have been founded too. CF is one of the most common lives shortening autosomal recessive disorder in the white population. It is caused by mutations in the Cystic Fibrosis Transmembrane

Conductance Regulator (CFTS) gene which results in increased sodium absorption and decreased chloride and bicarbonate secretion at the apical cell membrane. The decreasing in chloride secretion brings to a defective transport in the epithelial cells present in the respiratory, hepatobiliary, gastrointestinal, and reproductive tracts and in pancreas [45]. Symptoms related to CF disease are cough, elevated sputum production, wheeze, chest tightness, difficulty in breathing and fever. Those symptoms are also accompanied by some emotional impacts that include frustration, depression, irritability and by activity impacts as difficulty in sleeping, sitting and lying down [46]. CF disease is strongly associated to an airway surface dehydration. In CF disease, mucus becomes significantly more concentrated respect the healthy condition, reaching values of solids content up to 21%. This dizzying increasing brings to a compression of the pericellular layer caused by the mucus layer, to a decrease of mucociliary clearance and finally mucus layer adherence to the airways surfaces. Increasing the solids concentration, also the adhesion between the mucus itself and the pericellular layer will enhance because further connections are created and this results as an increase in adhesion strength [47], [48]. In patients affected by CF it has been showed MUC5B decreases in bronchi, but they've been showed in abundance in the airway epithelial lining, due to the attached mucus. Indeed, MUC5AC appeared to be more abundant [49]. Due to mucin increasing in concentration, it starts self-assembling and forming high-density non-swellable structures called flakes. Those flakes, in healthy conditions, account for around 5% of the mucins, while in case of advanced CF disease they can reach up to 50% [50].

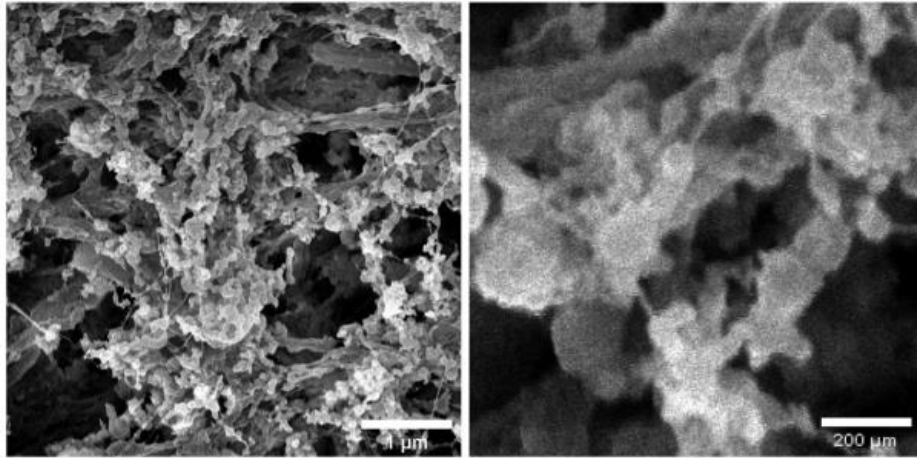


Figure 1.14: SEM images of a network of mucus samples for the healthy condition at two different zoom levels (adapted from [50])

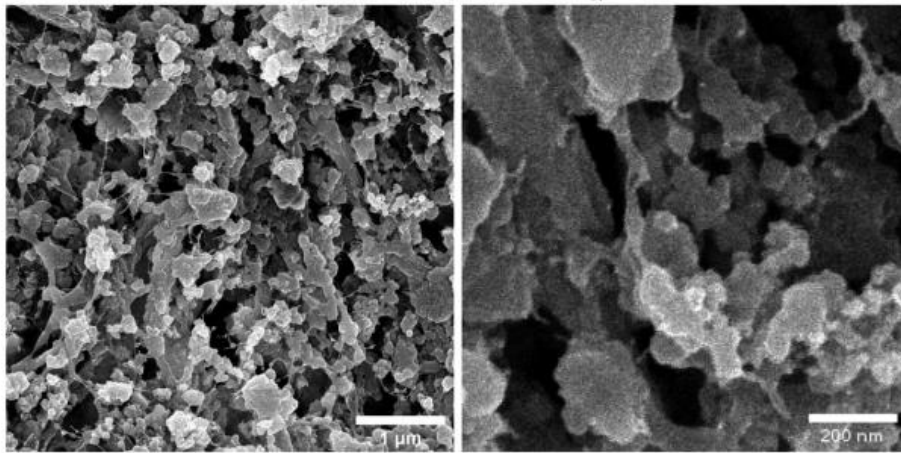


Figure 1.15: SEM images of a network of mucus samples for the CF pathologic condition at two different zoom levels (adapted from [50])

The massive mucus amount secreted in in patients affected by CF condition, also brings to an increasing in rheological properties. Under oscillatory, controlled strain shear, CF sputum is significantly more elastic than viscous during the whole frequency and strain ranges [51].

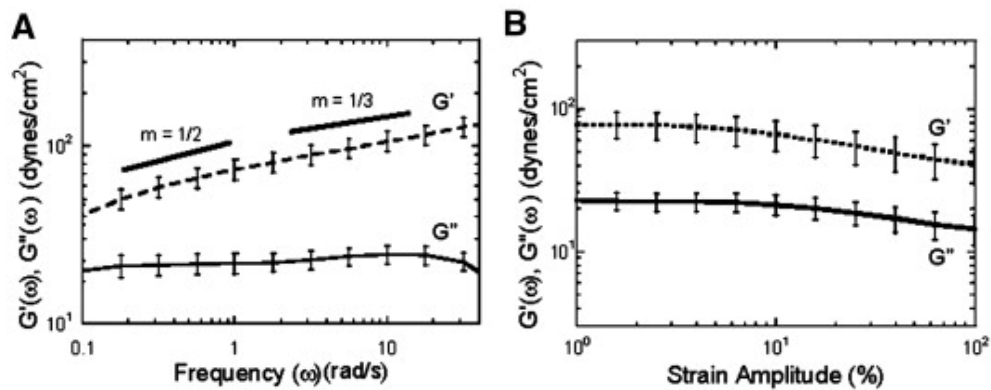


Figure 1.16: Macro-rheology of human cystic fibrosis sputum. (A) The frequency-dependent elastic and viscous moduli of CF samples (conducted on 6 patients). (B) Strain-dependent elastic and viscous moduli from 0.1–100% strain amplitude (adapted from [51])

COPD is the major public-health problem related to airways [52]. The main risk factors are long-term exposure to cigarette smoke and environmental pollution, but also exposure to biomass fuel, as well as genetic susceptibility. Therefore, in some cases, it can be considered as a quite preventable disease. However, it is responsible of a large proportion of hospitalization for acute care and brings to high percentages of disability and premature deaths. Treatments provided on patients with COPD affect their quality of life and include long-term oxygen therapy, lung volume reduction surgery and pulmonary rehabilitation, but also pharmacological agents.

During the last studies, it has been proposed to abandon the concept of COPD as a unique pathological condition and refer to it as a series of disorders that contribute to the arising of several impair conditions [53]. Because of this huge variety, more and more personalized treatments and therapies should be implemented [54]. The condition related to COPD is based on airflow obstruction not completely reversible with inhaled bronchodilators, presence of chronic cough and sputum and emphysematous changes in lungs [55]. Mucus accumulation in epithelium and lumen

of small airways are considered the main related problems. In more critical cases, COPD is associated to airway mucus hypersecretion, aggravated airflow obstruction, high airway resistance and chronic cough [16]. Characteristics of airway mucus hypersecretion including sputum production, increased luminal mucus, goblet cell hyperplasia and submucosal gland hypertrophy are present in those conditions. However, mucus COPD differs to asthma because mucus here is less viscous, and the ratio between MUC5AC and MUC5B is generally reduced [56]. COPDs are related to MUC5AC increasing in secretion. MUC5AC couples with unique sialylation and sulfation and causes acidification of the airway microenvironment reducing the efficacy of common antibiotics [57].

#### 1.4.2 Pathological condition due to SARS-CoV-2

Coronavirus infections are studied worldwide since 1960s. Initially, they were related to innocuous respiratory human conditions that weren't life-threatening. In the last twenty years, caught on several serious and deadly respiratory disorders attributed to beta-coronavirus subfamily. Those conditions are associated to severe acute respiratory syndrome (SARS) and the middle east respiratory syndrome (MERS) that respectively brought to 9.6% and 36% mortality rates [58]. The recent soaring of respiratory disease COVID-19 caused by novel coronavirus SARS-CoV-2 is a severe and urgent global concern, so that The World Health Organization (WHO) declared SARS-CoV-2 to be a pandemic on March 11, 2020 [59].

Coronavirus SARS-CoV-2 enters in the cell with the same mechanism of all the other viruses: interacting with mucins and mucin glycans. Depending on the phases of cells infection, the clinical stages that bring to the advance of the pathology can be divided into three phases: the asymptomatic state, followed by the upper airway and conducting airway response and finally progression to acute respiratory distress

syndrome (ARDS) [60]. SARS-CoV-2 spike (S) protein binds ACE2 and promotes its entrance in cells. Mucins pores, in fact, are sufficiently large (approximately 500nm) to allow the virus (generally 30 to 200nm in diameter) to enter [61].

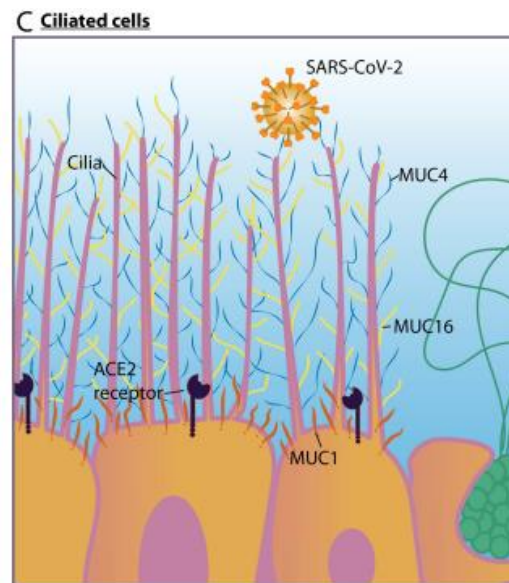


Figure 1.17: representation of the ciliated epithelial cells focusing on the produced mucins MUC1 (red), MUC4 (blue), and MUC16 (yellow) and how SARS-CoV-2 enters in binding to the receptor ACE2 (adapted from [62])

Time by time, virus starts propagating and migrating along the conducting airways tract, generating infections that are increasingly difficult to eradicate. If the acute stage is reached less mucus is produced due to damage of glandular epithelial cells [62].

Disease severity was found to be associated with demographic factors, such as older age (over 66) and male gender. Diabetes, obesity, arterial hypertension, immunodeficiency and allergic, COPD and asthmatic history were found as risk factor for the progress of the disease and its possibility to cause severe damages [63]. In case of some severe illness, dyspnea may arise and lead to hospitalization, intensive care treatment or, in more critical conditions, resulting in death.



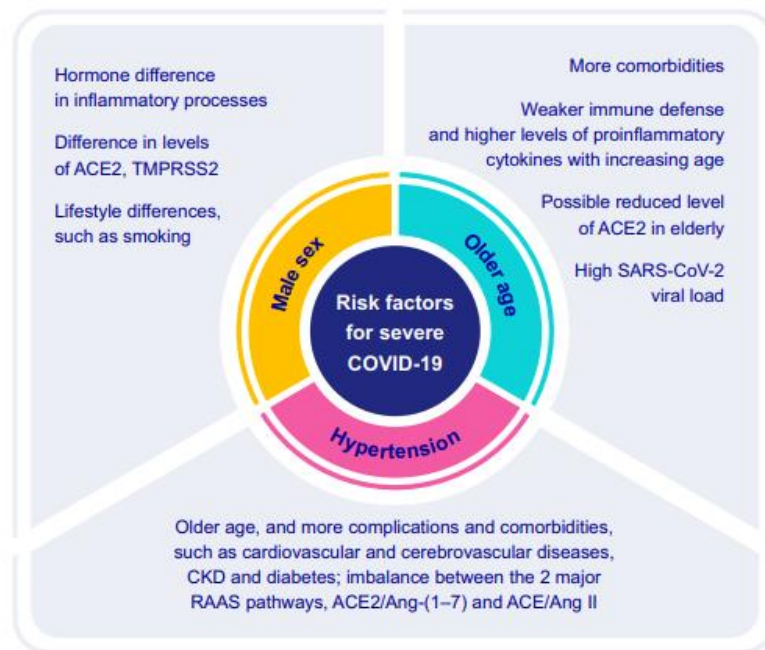


Figure 1.18: age, gender and hypertension as risk factors on SARS-CoV-2 severity (adapted from [63])

The more common symptoms associated to SARS-CoV-2 condition are fever (body temperature of 38 °C or more), cough (dry cough or cough with sputum), muscle soreness, pneumonia, diarrhea, runny nose and lung infection [64]. Autopsy studies revealed that the pathological condition related to SARS-CoV-2 brings to atypical and abnormal accumulation of airway mucus. This alarming condition on some occasions may get worse when patients are treated with intubation, since intubation may cause mucus accumulation [64]. Among the observed consequences of this pathological condition can be alveolar damage and neutrophilic inflammation, dense mucoid material and mucus plugging observed in airway lumens of bronchi and bronchioles and sputum that gets stiffer increasing with the critical condition [64], [65]. Biopsy showed that Coronavirus SARS-CoV-2 mainly involves injuries at small airways and alveoli causing partial detachment of bronchial epithelium, gelatinous mucus attachment in the bronchial lumen, and large amount of sticky mucus and sputum



plugs in small airways. In case of some critical conditions, excessive mucus amount is produced and stands in the alveolar structure causing their obstruction and decrease in gas exchange [66].

As for the previously discussed airway diseases, even for this pathological condition the abnormal mucus composition is associated to elevations in MUC5AC and/or MUC5B expression. Since the viral infections are transmitted mainly as aerosols that allow droplets to enter the human lungs and lay at the mucosal surface, the mucus structure, to protect the surface, starts overproducing mucin substructures [67]. From autopsy studies conducted in those years all over the world, it has emerged that 40% of patients affected by SARS-CoV-2 exhibited an increase in sputum volume and mucus hypersecretion, while and 33% of autopsies conducted on SARS-CoV-2 patients, detected severe mucoid tracheitis in the lower respiratory tract. As part of the host immune defence, in patients affected by Coronavirus SARS-CoV-2 it has been showed MUC1 and MUC5AC increased levels in trachea sputum, hence in the whole airway tract MUC5AC, MUC1, and MUC1-CT are evaluated higher than the control [67]. Hence, it's evident a similarity in disease progression of SARS-CoV-2 with typical mucus hypersecretory diseases such as asthma, CF and COPD [68]. Protein concentration in SARS-CoV-2 samples has been detected 5.5 times greater than the one in healthy samples. It has been found that the solid percentage in those pathological patients is close to the one of CF patients also in terms of reached thickness and tenacious respiratory secretions [69].

The extreme danger related to Coronavirus SARS-CoV-2 is also due to its very rapid contagiousness. Super spreader events (SSEs) play an important role in accelerating the spread of the pandemic. It is essential to study its super spreading behavior to control the epidemic and set up a management strategy [70]. Super-spreading events

may have different nature: can be generated by host, pathogen, and environmental factors and their outbreak can be implied by several factors at the same time.

#### 1.4.3 Pathological condition due to bacterial interaction

The mucus layer in healthy conditions is structured in a way that the periciliary layer remains relatively devoid of microbes, whilst the above layer contains a different community of commensal bacteria, necessary to ensure good health [71]. Those healthy bacteria dwell in the mucus layer without causing harmful inflammation, but rather have the ability to raise an inflammatory response against harmful pathogenic attacks [72]. In healthy airways, in case of invasion of small numbers of pathogenic bacteria, neither injury nor local colonization generally arise. Indeed, mucus transport, allowed by mucociliary clearance, in concert with antimicrobial proteins and other proteins such as IgA and collectins eradicate inhaled toxic bacteria and provides their expulsion [73]. Instead, in chronic obstructive pulmonary disease, since local condition is changed resulting as an impairment of the local defence system, the development of the infections is facilitated.

Some predisposing conditions for bacterial infection are: factors that promote bacterial adherence and growth, changes in geometry due to the aggravating airway obstruction caused by an increase in mucus secretion and viscosity, and subversion of normal protective defence mechanism into damaging host tissue at mucosal level [74]. However, it's also true that impairment of mucociliary clearance and local immune defence due to smoke, bad habits and injurious quality of the inhaled air allow bacterial pathogens to gain a foothold in the lower respiratory tract [75]. In addition to the previously enounced predisposing conditions and bad behaviours, there's the aggravating circumstance, developed in recent times, due to antibiotic resistance. The Centres for Disease Control and Prevention in 2019 has stated that the world is on the verge of entering the "post-antibiotic era", where the number of people that die due

to bacterial infections is higher than the one that die from cancer [76]. The reason of this critical situation is due to the rising of multidrug resistance in opportunistic pathogens, resulting in reduced effectiveness of antibiotics. As consequence, there is the growing necessity to develop some innovative approaches to tackle infection in order to avoid falling back into a pre-antibiotic era [77], [78]. The main problem is due to respiratory pathogens such as *Pseudomonas aeruginosa*, *Staphylococcus aureus*, *Haemophilus influenzae*, *Streptococcus pneumoniae* and *Streptococcus pyogenes* that have evolved virulence factors able to interact with mucins and mucin glycans during the development of airway infection [62]. The coexistence of chronic obstructive pulmonary disease and antibiotics resistance may bring to some even more dangerous conditions for the patients. When the pathological condition due to bacterial infection is associated to CF airway disease, reflects in a reduction of airway surface liquid (ASL) volume in both the mucus and periciliary layers. ASL produces thickened of mucus gels that adhere to airway surfaces and causes a decreasing in clearance becoming the site for the chronic intraluminal infection [79].

Several recent published studies have also found out a correspondence between the viral respiratory tract infections and the increased risk of bacterial coinfections. Coronavirus SARS-CoV-2 disease results, unfortunately, isn't an exception. Indeed, one patient out of seven hospitalized due to Coronavirus SARS-CoV-2 has contracted a dangerous secondary bacterial infection that, for the 50% of the cases, results fatal [80]. In case of patients that due to their critical infective condition have been intubated, it has been showed patient-specific lung microbiome communities with prominence of *Staphylococcus* [81].

#### 1.4.3.1 *Staphylococcus aureus*

*Staphylococcus aureus* is cocci-shaped, Gram-positive bacteria that tend to be arranged in clusters as “grape-like” structures. *S. aureus* can be found in the environment, as well as in normal microbiota that mostly arises in moist squamous epithelium of the anterior nares, but also skin and GI mucus membrane. If contracted on healthy skin it doesn't cause serious infections, but a different treatment should be done if enters the bloodstream or internal tissues where it may cause a real danger [82]. In fact, *S. aureus* is also a dominant cause of infective endocarditis, osteoarthritis, skin, soft tissue, pleuropulmonary and device-related infections. Healthy individuals have a small but finite risk of contracting an invasive infection caused by *S. aureus*. Instead, hospitalized patients, especially if have been treated surgically, that have impairments in immune system or that suffer of debilitating conditions, such as type 1 diabetes, have a significantly higher rate of contract the infection [83]. Depending on the clinical history of the subject and on where it is contracted, it may cause severe illness condition or not. For these reasons, *S. aureus* is considered at both time a commensal bacterium and a human pathogen [84]. In developed countries, many nosocomial infections are caused by *S. aureus* strains that are multiply resistant to antibiotics, known as Methicillin-Resistant Staphylococcus Aureus (MRSA) [83]. This infection is hugely present in CF patients due to the frequent hospitalizations they should undergo since early childhood [85]. Doing immunofluorescence and transmission electron microscopy test, *S. aureus* bacterium present in CF patients was discovered to be very little attached to the lung epithelium, whereas abundant amounts were detected in the mucus of obstructed airways [86]. The worst condition associated to *S. aureus* infection is due to establishment of biofilms. This state generates a self-produced extracellular matrix (ECM) composed of proteins, carbohydrates and extracellular DNA which encases the cells within a sticky matrix and enhance the survival in hostile

environment [87]. In this conditions, the infection becomes almost impossible to be treated with antimicrobial agents, since the bacterium reacts by adapting its phenotype to express the so-called “small-colony variants” (SCVs) [88]. In the last few years, more and more the genome-wide studies leave room for the detection and quantification of the actual secreted proteins by a cell, tissue, organism or bacteria [89]. The general secretory (Sec) pathway plays a key role in bacterial protein secretion and is responsible for translocation of a multitude of proteins across the cytoplasmic membrane [90].

#### 1.4.4 Currently *in vitro* models

Until recently, mucus was considered as a passive physical barrier that protects from hosts, but mounting evidence suggests that mucus plays additional biological and immunological roles in homeostasis maintenance. Mucus, in fact, acts in concert with the immune system, the lining epithelium and the present microbiota, to provide physical, biological, and chemical defense against potentially harmful pathogens [91]. However, only in the last decades massive interest is given to studies on mucus functions and characteristics.

The development of *in vitro* and *in silico* tissue models and the elimination of animal-testing from drugs and medical devices development is highly encouraged by experts of different fields (materials science and engineering, cell and molecular biology, chemistry, biomedical engineering, pharmacy and regulation) [92]. *In vitro* models have the target to improve scientists understanding of organ biology, such as investigating the effect of growth factors, oxygen availability, cell development and differentiation, but also organ pathophysiology. They are able to recreate a proper mucus environment and allow a better comprehension of human disease processes and mechanisms, especially the more recent.

The first studies conducted on airway mucus were set withdrawing patient mucus through endotracheal tubes or bronchoscopy analyses. The main feature of this kind of mucus models is that chemical, structural and rheological composition are exactly the *in vivo* ones. However, the poor reducibility due to subject-to-subject variability and the poor stability due to the enzymatic degradation, are the main drawbacks of this technique. Instead, if sputum is induced through medical techniques, even if the procedure results as a minimally invasive one, it is necessary a dilution of the mucosal material and requires a trained health care team to perform the procedure. Nevertheless, the main disadvantage is that since rheology is highly dependent on concentration, the measurements result perturbed [36].

In recent years, deep interest in vitro model is given by human co-culture of inflamed airway mucosa that allow to mimic the interactions through mammalian–microbial co-culturing techniques. Those models study neutrophil migration across the airway epithelial barrier on immortalized human lung epithelial cell lines. However, the main limitation of this method is the low volume of mucus that is manufactured and the long periods of culture needed to produce them [93].

Another approach, typically used in GI tract, is to simulate a mucin-producing human epithelium through the “Organ-on-a-Chip” system. This developed environment allows the formation of 3D intestinal villi like the ones of the small intestine, and the differentiation of Caco-2 cells into absorptive enterocytes, but also includes enteroendocrine cells, Paneth cells and mucus-producing goblet cells. Although the Organ-on-a-Chip devices have been mostly used for long-term co-culture and exclusively under healthy conditions. However, the main limitation of this approach is the use of plastic substrates, such as PDMS that aren’t representative of human tissue structure [94].

Only extremely recent studies have focused their attention on founding biomaterials that, when placed in contact with porcine stomach or bovine submaxillary gland mucins, allow the mimicking of *in vivo*-like biophysical properties. The mainly used cross-linking agents are poly(acrylic) acid (PAA) and thiolate-star polyethylene glycol (PEG) polymers. Those developed models are applied to study lung diseases as COPDs, CF and asthma to understand airway dysfunction and provide the basis for new therapeutic interventions [95].

## 2. AIM OF THE THESIS

The “Mucus4Covid” project arises from the intent of founding an *in vitro* model that was able to mimic as faithful as possible the composition, the action and the structural properties of the natural airway mucus in healthy and pathological condition due to Coronavirus SARS-CoV-2 disease. The developed models should be compliant with biological experiments leaded at Università degli studi di Pavia and Università degli studi di Torino allowing studies about cells vitality, virus and bacterial infection and drug permeability. All the collected data are shared and discussed between the three involved universities in order to give higher completeness and scientific value to the obtained results.

To develop the mucus-like hydrogel layer it was chosen alginate due to its ease of use, cytocompatibility and non-cell adherent properties, and mucin, incorporated to mimic the biochemical properties of natural airway mucus. Characterization of the models is provided in terms of storage, dispensing modality, adaptability to the wells and stability at 37°C. Finally, it will be indagated the possibility to include bacterial medium in the pathological developed model to understand if *S. aureus* secretome can be included in the prototype and what it involves.



# 3. MATERIALS AND METHODS

## 3.1 Materials

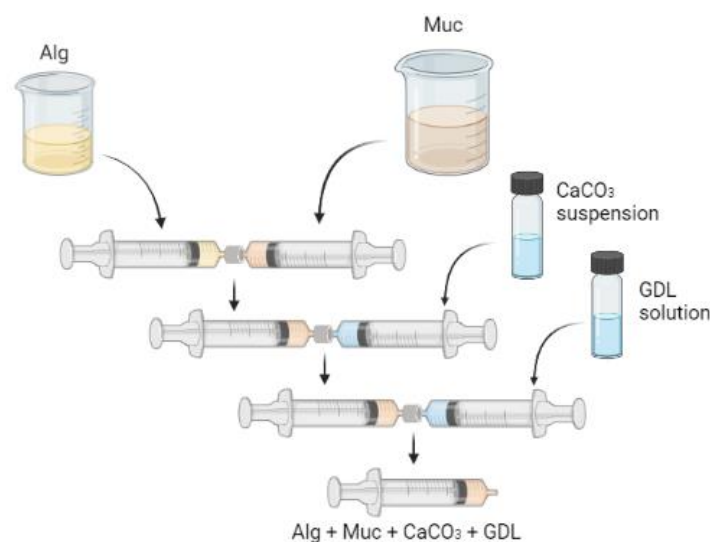
A first Mu4Covid formulation was provided at Department of Chemistry, Materials and Chemical Engineering “Giulio Natta” at Politecnico di Milano, Italy. Changing the concentration of Alginic acid sodium salt (Alginate; Sigma-Aldrich, Lot.# MKCJ8027, Germany), Mucin from porcine stomach Type III (Mucin; Sigma-Aldrich, Lot.# SLCC7224, Germany), Calcium Carbonate ( $\text{CaCO}_3$ ; Sigma-Aldrich, Lot.# BCCD5575, Germany) and D-(+)-Gluconic acid  $\delta$ -lactone (GDL; Sigma-Aldrich, Lot.# SLCF8971, Germany) it has been possible develop several 3D-models of pulmonary mucus.

For every 3D mucus model it always remained unchanged the ratio 1 : 4 : 1 : 1 Alginate : Mucin :  $\text{CaCO}_3$  : GDL, what has varied is only the concentration of the different components. Dulbecco’s Modified Eagle’s Medium (DMEM; Lonza, Lot.# 0000929445, USA) was used as medium to allow the components dissolution. Sodium Azide (Sigma-Aldrich, Lot.#STBH0657, USA) was added to the DMEM in order to assure no bacterial proliferation during the more prolonged studies. Sodium citrate tribasic dihydrate (Sodium citrate; Sigma-Alfrich, Lot.#BCCD3229, Belgium) was used as dissolving agent. Parafilm (Sigma-Aldrich, PARAFILM® M, PM-996) was used to cover the backer containing the solutions while stirring.

## 3.2 Mu4Covid preparation

Using a balance (Sartorius Lab Instruments Gmbh & Co. KG, 37070 Goettingen, Germany) it has been possible to weight the correct amount of alginate, mucin,  $\text{CaCO}_3$  and GDL depending on the mucus 3D-model that it is wanted to be prepare. Then, the medium is spilled in two different beakers that are put on a Heating Magnetic Stirrer

(IKA® RCT basic S000 or VELP Scientifica Code F20500162) and very slowly the alginate grains and the mucin powder are respectively added. Wait the right time is crucial in order not to allow the accumulation of the components and clusters formation. The stirrer heating is deactivated while the stirrer rpm has to be 250-350 for both the solutions. To obtain the homogenization of both the hydrogel and the protein, the solutions need to be stirred until no more grains are present. This would happen after a minimum of 4 hours. Spent this time it's possible to go on with the gel production. The alginate and mucin are taken from the beakers and transferred in two different syringes of 10mL each (TERUMO® SYRINGE without needle). The double syringe method, reported in Figure 3.1, is hence used to produce the mucus model: firstly, mixing the alginate and mucin solutions, then adding the  $\text{CaCO}_3$  suspension and finally the GDL, which must be prepared immediately before using it. Before carrying out any test it is necessary to wait 20 hours so that the gel gets crosslinked. The crosslinking is provided leaving the prototypes in the fridge (SCIENTIFIC REFRIGERATOR-Fiocchetti) at the controlled temperature of  $4^\circ\text{C}$ .



**Figure 3.1:** graphical representation of the mucus model production using the double syringe method: alginate and mucin solutions are firstly added in two different syringes that are put in contact using a connector, then  $\text{CaCO}_3$  suspension is added and finally GDL solution

### 3.3 Rheology

To provide information on the rheology of the prototypes, it has been used the Anton Paar MCR 502 TwinDrive-Ready SN82235284 rheometer (measuring system PP25 SN52890; measuring cell P-PTD200+H-PTD200 SN82317201-82718077).

RheoCompass™ version 1.30.1064-Release is the software used for its control. For all the experiment it has been set a measuring position of 0.5 mm and the below plate (INSET I-PP50/SS Diameter 50mm; STAINLESS STEEL; Cat. No. 16222) is put at controlled temperature of 25°C. Two different tests are carried out at the rheometer. The frequency sweep test, that needs the parallel plate (Part. No: 79044, Serial No: 52890) whose diameter is 24.998mm and gives as output the storage modulus ( $G'$ ) and loss modulus ( $G''$ ) in MPa at various frequencies. The rheometer sets up the frequency range at 0.1-20Hz, but data between 1.9-20Hz were cut and not reported because not significative for this analysis [33]. Instead, for the viscosity test it was necessary to use the parallel plate (Part. No: 79045; Serial No: 52530) whose diameter is 49.971mm. This tests carry out the viscosity (MPa·s) depending on the shear rate  $\gamma\text{-dot}$  (1/s) in a range 0.1-100 1/s.

### 3.4 Shelf-life assessment

The study of the shelf-life of the mucus prototypes has been conducted in order to determine how the initial characteristics and performances vary among the conservation time. After their production, all the prototypes were stored in vials of 4mL and left in a fridge at a controlled temperature of 4°C. For a maximum of seven consecutive days, one single vial per time is tested at the rheometer with the frequency test investigating the rheological properties. Per each test 1mL of mucus was picked up from the vial using a pipette (GILSON® PIPETMAN, P1000 100-1000 $\mu$ L) and

deposited on the rheometer plate. In each vial were present at least 3mL of solution in order to allow to lead three experiments per time point.

### 3.4.1 Freezing

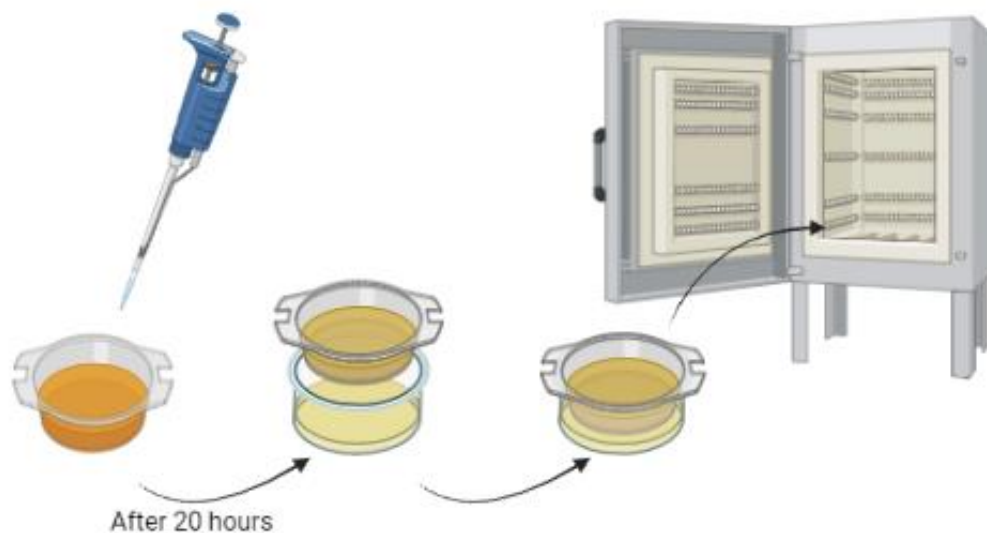
It has been experimented another way of storing by freezing the different mucus 3D-models. In doing so it has been analyzed if the freezing and defrosting processes may affect the characteristics of the prototypes. Gels, after their productions are put in several vials 4mL and left reticulating in a fridge at 4°C, then spent 20 hours, are transferred in a freezer (Eppendorf CryoCube® F740hi, Eppendorf Italia, No. 724734). They are left in it at the controlled temperature of -80°C for a minimum of 72 hours. Then, a several smooth defrosting in time is provided. After these procedures, the prototypes have been tested at the rheometer with a frequency sweep test in order to verify if their characteristics were equal or not to the ones found immediately after their reticulations.

## 3.5 Stability in medium

It was requested to make the stability test in to study if the prototypes change their weights when put in an oven at the controlled temperature of 37°C. This analysis was crucial because all the studies conducted with the cells are at 37°C.

To conduct this experiment, two different transwells have been used: transwells (Griner bio-one ThinCert™-6 Well, Art. No. 657640 Lot.# 21090316) that fit 6 multiwells (Griner bio-one, Lot.# E19023AM) whose pores diameter is 0.4 um, translucent PETMembrane (RoTrac®) and transwells (Griner bio-one ThinCert™-24 Well, Art. No. 662630) that fit 24 multiwells (Griner bio-one, Lot.#131216-076). Ended the mucus production, the solution was directly transferred in the transwells inside the multiwell (MW) plate, and it is left reticulating in them leaving the compound 20 hours in the

fridge. Depending on the size of the transwells they are filled with different amounts of mucus: the one that fits the 6MW is filled with 2mL of solution, the other with 400 $\mu$ L. Spent the 20 hours of reticulation in the fridge, all the transwells were weighted. Then, the medium was added in the multiwells: in the first case 2 mL, in the second 800 $\mu$ L. All the empty spaces were filled with 1mL of dH<sub>2</sub>O and some grains of sodium azide, and the overall structure was sealed with parafilm to avoid the sample drying. Finally, the multiwell with the transwells inside is put in the oven (New Brunswick™ Innova® 42/42R) and left at 37°C.



**Figure 3.2:** graphical representation of how the stability test was carried out: using a pipette the transwells were filled of mucus solution and left crosslinking in a fridge for 20 hours. Spent this time, they are put in contact with the medium deposited in the below MW and the structure is moved in an oven at 37°C. At each timepoint the weight of each transwell is controlled

Every 24 hours and for a maximum of 168 hours (7 days) the gels were weighted using a balance and 1mL of dH<sub>2</sub>O and sodium azide were added in the empty spaces.

The weight variation  $w$  [%] is calculated as the difference between the weight at each time-point and the initial weight divided by the initial weight:

$$w[\%] = \frac{w(t)-w(0)}{w(0)} * 100 \quad \text{Equation 1}$$

where  $w(t)$  is the weight at each timepoint  $t$  and  $w(0)$  is the initial weight.

It has also been calculated the standard deviation and the standard deviation [%]:

$$Sd.Dev. [\%] = \frac{Sd.Dev.}{Mean\ weight} * 100 \quad \text{Equation 2}$$

where mean weight is given by the mean of the weights collected for each timepoint.

## 3.6 pH analysis

The study of the pH of the developed mucus prototype is crucial because an environment similar to the human body has to be set up in order to give the chance to its use in cells experiments. To conduct these experiments, the different compositions of the mucus 3D-models, after their production, were stored in syringes of 5mL (TERUMO® SYRINGE without needle). After waited the 20 hours of reticulation in the fridge at 4°C, it has been used a pH-meter (HANNA Instruments, CHEMIFARM srl. Code: HI 5522-02) to analyze the pH value of every prototype.

## 3.7 Multiwell adaptability

To provide the multiwell adaptability, several amounts of mucus were picked up using pipettes of different volumes and placed on a petri dish (Thermo SCIENTIFIC, Nunclon™ Delta Surface, Lot.# 163333). Macroscopic considerations have been done immediately after dropping the mucus. For more accurate considerations it has been used the App ImageJ version 1.8.0 and the calculation of the maximal reached height and of the diameter of each drop were provided.

### 3.8 Dissolution method

The 3D-models of the mucus showed themselves like gels and not always it's easy to remove them from the laboratory components. In case of vials, syringes or multiwells of any dimension it is enough to wash them with plenty of water. Instead, for the transwells it has been necessary to study a dissolution method. It has been discovered that Sodium Citrate 5% solution 50mmol works good for this need. Transwells, depending on their size were placed in their appropriate MW. If it dealt with 24 MW, 1mL of Sodium Citrate solution was added in the transwells and 1mL in the below wells. Instead, if it was 6 MW, 2mL were added inside the transwells and 2mL below them. The compound stayed like this overnight under static conditions. Spent this time, it was very easy to eliminate the gel from the transwells, that were finally washed with plenty water, and were ready to be used again.

### 3.9 Collaboration with other universities

Università degli Studi di Torino (UniTO) and Università degli Studi di Pavia (UniPV) collaborated with Politecnico di Milano (PoliMI) in order to develop the project.

Compatibility tests were carried out at UniTO and UniPV. Those experiments have been conducted using two different epithelium cellular lines HCT8 and VERO-E6, used for studies about SARS-CoV-2. In order to quantify cells viability, with the first cellular line it has been used the luminescence assay, while for the second the Trypan Blue colouring. The virucidal tests were provided at Virology Laboratory IRCSS San Matteo, Pavia. Those experiments used surrogates of SARS-CoV-2 (Human coronavirus, HCoV-OC43) and SARS-CoV-2 (delta variant) that infected the gels prototypes deposited on VERO-E6 cells. At UniTO the prototypes were also employed for several drugs permeability studies using Parallel Artificial Membrane Permeability Assay (PAMPA) assay. This is an *in vitro* model introduced by Kansy, et al. that is

widely used in the pharmaceutical industry as a high throughput permeability assay to predict oral absorption [71]. It consists of a donor and an acceptor compartment separated by a phospholipid membrane that mimics the cell membrane. Drug concentration in the acceptor compartment was obtained by LC-MS.

### 3.9.1 Materials from Pavia

UniPV delivered to PoliMI some falcons containing mediums of different origin, so that it was possible provide tests about shelf-life and stability at 37°C. The materials were committed in a freezer and when necessary, they were defrosted leaving the falcons in a hot bath (at 37°C) for 15 minutes. The delivered materials were: 30mL distributed in 3 falcons of blank TSB (Tryptic Soy Broth), 30mL distributed in 3 falcons of TSB containing *Staphylococcus Aureus* secretome grown in stationary phase 0.5, 30mL distributed in 3 falcons of TSB containing *Staphylococcus Aureus* secretome grown in exponential phase 1.7, 30mL distributed in 3 falcons of blank EMEM (Eagles' Minim Essential Medium), 30mL distributed in 3 falcons of EMEM containing VERO-E6 secretome 0.5, 30mL distributed in 3 falcons of EMEM containing VERO-E6 secretome 1.11.



# 4. RESULTS

## 4.1 Optimization

### 4.1.1 Study of the composition

During the analysis, several compositions have been studied in order to discover which was the one that better fits the characteristics of the native mucus. For a sake of clarity, the below table shows some of the most significant studied concentrations that brought to the developed healthy mucus 3D-models.

Gel Name	Alginate	Mucin	CaCO <sub>3</sub>	GDL
<b>Mu4Covid 1.0</b>	0.4%	5%	0.13%	1%
<b>Mu4Covid 1.2</b>	0.4%	5%	0.13%	0.8%
<b>Mu4Covid 1.3</b>	0.5%	2.5%	0.13%	1%
<b>Mu4Covid 1.4</b>	0.5%	5%	0.13%	1%
<b>Mu4Covid 1.5</b>	0.4%	2.5%	0.13%	0.8%
<b>Mu4Covid 1.8</b>	0.5%	2.5%	0.13%	0.8%
<b>Mu4Covid 2.0</b>	0.6%	2.5%	0.13%	0.8%
<b>Mu4Covid 2.1</b>	0.6%	2.5%	0.13%	1%
<b>Mu4Covid P 1.0</b>	0.3%	2.5%	0.13%	1%
<b>Mu4Covid P 2.0</b>	0.3%	1.25%	0.13%	1%
<b>Mu4Covid P 2.1</b>	0.6%	1.25%	0.13%	1%
<b>Mu4Covid P 2.2</b>	0.7%	1.25%	0.13%	1%
<b>Mu4Covid P 2.3</b>	0.7%	2.5%	0.13%	1%

**Table 4.1:** some of the more interesting tested gels and their composition<sup>1</sup>

---

<sup>1</sup> See appendix A for the graphical behavior at t=0 of each composition of G' (0,44Hz) and G'' (0,44Hz).

### 4.1.2 pH analysis

One of the parameters that was necessary to consider is the pH. In order to study it, after the mucus production it has been stored in syringes of 5mL and by means of a pH-meter it has been possible to detect the pH value of each composition. The below table reports all the obtained results.

<b>Gel Name</b>	<b>pH</b>	<b>Medium</b>
<b>Mu4Covid 1.0</b>	5.56	DMEM
<b>Mu4Covid 1.2</b>	5.62	DMEM
<b>Mu4Covid 1.5</b>	5.85	DMEM
<b>Mu4Covid 1.8</b>	5,69	DMEM
<b>Mu4Covid 2.0</b>	6	DMEM
<b>Mu4Covid 2.1</b>	5.84	DMEM
<b>Mu4Covid P 1.0</b>	5.73	DMEM
<b>Mu4Covid P 2.0</b>	5.73	DMEM
<b>Mu4Covid P 2.1</b>	5.92	DMEM
<b>Mu4Covid P 2.3</b>	5.74	DMEM









**Table 4.2:** all the tested pH values obtained during the analysis


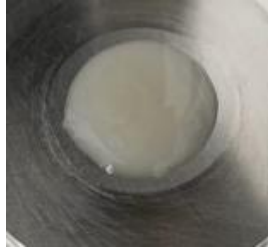


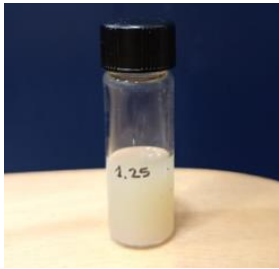

### 4.1.3 Macroscopic observation

The macroscopic observation has been conducted in two different ways. In Table 4.3 is reported how the mucus 3D models appear both inside the vial used for the storage and on the rheometer plate where are put in order to provide the experiments. All the photos are taken after 20 hours of crosslinking in fridge.

From the macroscopic analysis it has been showed that some gels with low amount of alginate and mucin exhibit the presence of a liquid phase since the first day of

production. Increasing the crosslinking agent and/or the alginate amount, gels are showed to be more compact and able to keep the shape also when not on a flat surface. Moreover, for higher mucin concentrations the compound has shown to be more in shades of yellow and less transparent.

Gel name	Inside vial	On rheometer plate
Mu4Covid 1.0		
Mu4Covid P 1.0		
Mu4Covid 1.2		
Mu4Covid 1.8		

<p><b>Mu4Covid P 2.0</b></p>		
<p><b>Mu4Covid 2.1</b></p>		
<p><b>Mu4Covid P 2.1</b></p>		

**Table 4.3:** macroscopic view of several tested gels: the first column reports the nomenclature, the second how the gel looks like inside the vials used for the storage, and the third one how it looks like when pipetted and placed on the rheometer plate before performing any test

#### 4.1.4 Cells viability

Through the drafting of a step-by-step protocol<sup>2</sup>, it has been possible to drive from afar an expert team based at Università degli studi di Pavia on the realization of several mucus prototypes. The more interesting compositions were told to those specialists

---

<sup>2</sup> See the Appendix B for the complete document.

where, following the delivered protocol, they realized the 3D models and then conducted experiments about cells viability. Two different cellular lines (HCT8 and VERO-E6) and two different tests (luminescence assay and Trypan blue) were used. Finally, the team based in Pavia sent the analyzed results. Interfacing with this team and match the results about cells vitality and the mechanical properties was a crucial point of the study. In this way it has been possible to develop a prototype that wasn't harmful for the cells, but that rather allows their proliferation in it.

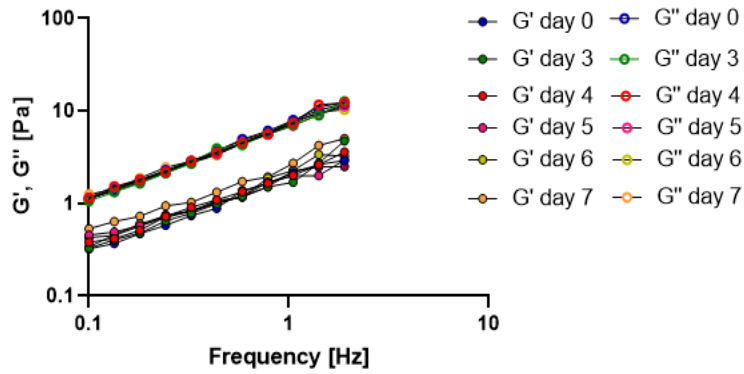
#### 4.1.5 Two components system

In order to create a final product that was simple to manufacture and easily reproducible using a clear protocol, alginate and mucin have been selected as the two main components of the 3D model. Below are reported the studies conducted on those components.

##### 4.1.5.1 Alginate

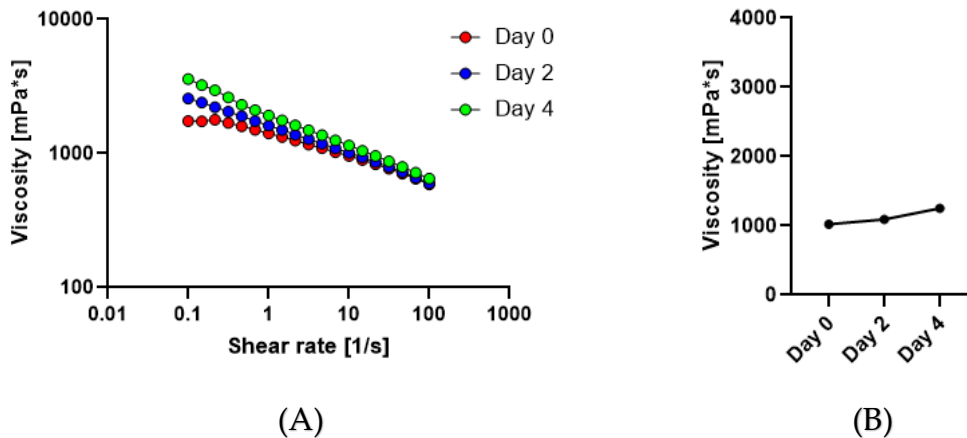
Two kinds of tests, the frequency and the viscosity ones, were used in order to study the alginate properties, how they vary in time and for how long the alginate solution could be stored in a fridge without changing its characteristics.

From the frequency test it has been investigated how the rheological properties vary in time. Until day 7 from the production,  $G'$  and  $G''$  have been analyzed respect frequency.

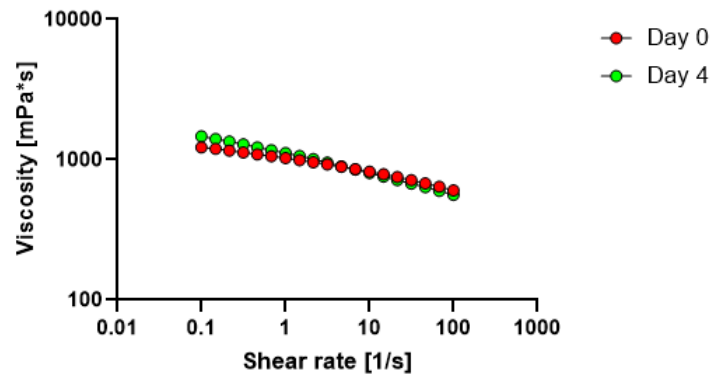


**Figure 4.1:** frequency test of the alginate solution 0,6% conducted on the same alginate solution stored for 7 days from its production

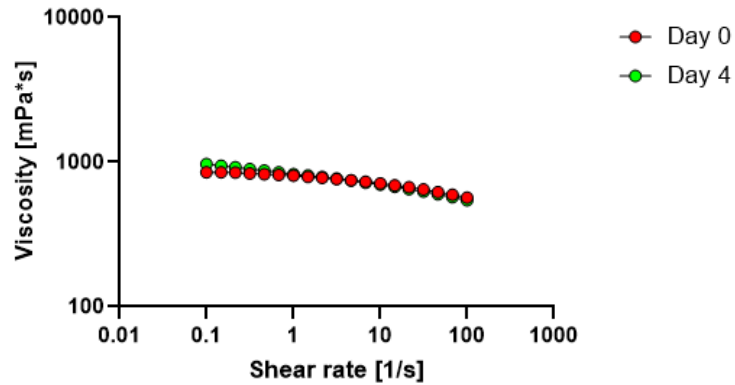
From the viscosity test instead, the viscosity has been calculated respect the shear rate. Those kinds of tests have been conducted until day 4 from the production of the alginate solution.



**Figure 4.2:** viscosity test of the alginate solution 0,6%. (A) reports the viscosity [mPa\*s] against the shear rate [1/s], (B) selected the shear rate value at 6,81 [1/s] it has been reported the correspondent viscosity value during the testing days

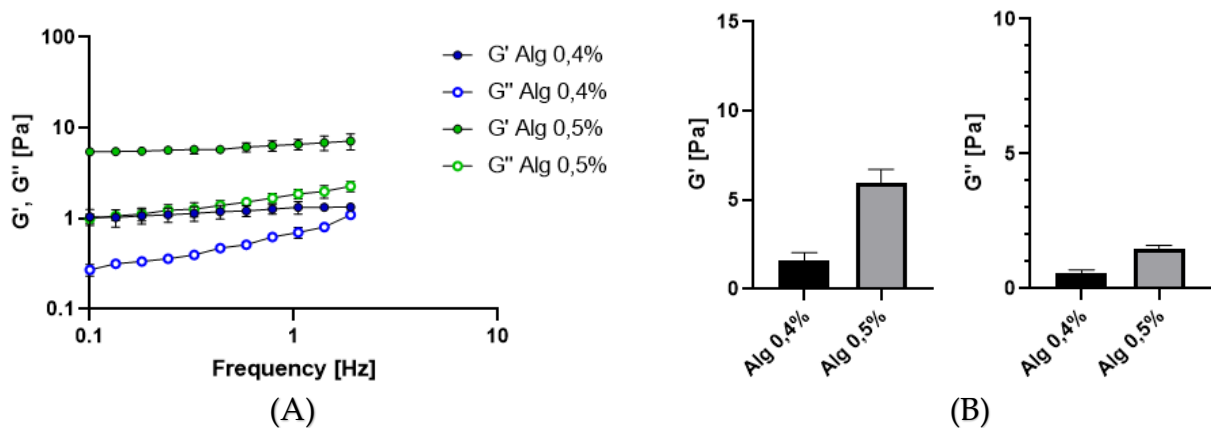


**Figure 4.3:** viscosity test of the alginate solution 0,6% dissolved in EMEM. Comparison between day 0 and day 4

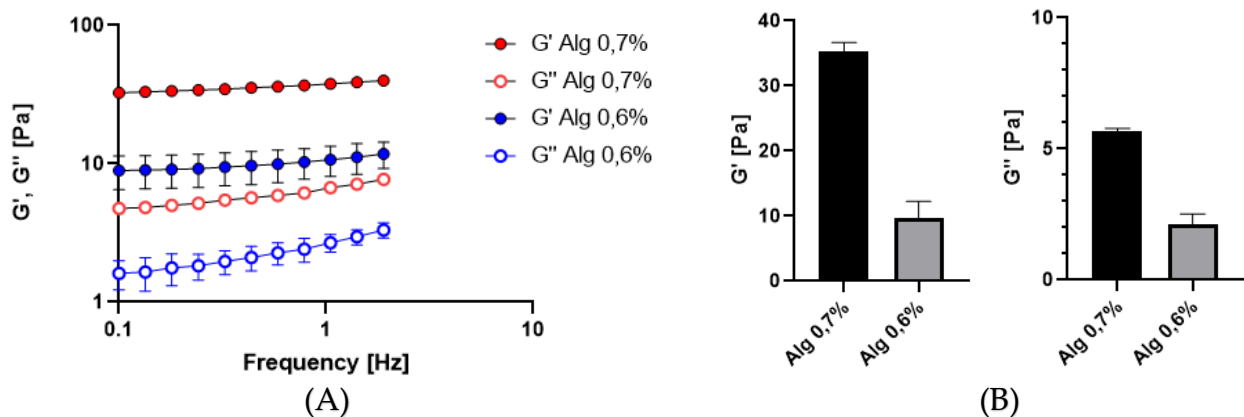


**Figure 4.4:** viscosity test of the alginate solution 0,6% dissolved in TSB. Comparison between day 0 and day 4

In order to study how the alginate properties affect the overall mucus structure, here are reported some comparison between gels in which the only variation is given by the alginate percentages. This analysis showed that increasing the alginate concentration also the rheological properties increase.



**Figure 4.5:** comparison between Mu4Covid 1.5 and Mu4Covid 1.8 in which the respective alginate concentrations are 0,4% and 0,5%, while mucin is kept constant at 2,5%. (A) Reports the whole curve, (B) fixed the frequency at 0,44 Hz reports the correspondent storage and loss moduli. Statistical differences at  $G'$  (0,44 Hz) and  $G''$  (0,44 Hz) for  $p < 0.05$  have been found between the two compositions



**Figure 4.6:** comparison between Mu4Covid 2.1 and Mu4Covid P 2.3 in which the respective alginate concentrations are 0,6% and 0,7%, while mucin is kept constant at 2,5%. (A) Reports the whole curve, (B) fixed the frequency at 0,44 Hz reports the correspondent storage and loss moduli. Statistical differences at  $G'$  (0,44 Hz) and  $G''$  (0,44 Hz) for  $p < 0.05$  have been found between the two compositions



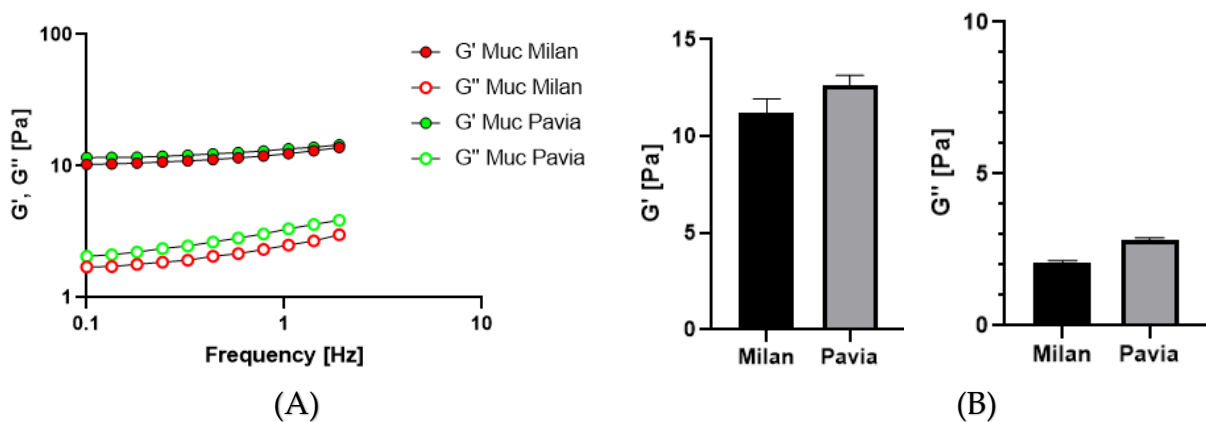
#### 4.1.5.2 Mucin

Similar studies have also been conducted on mucin to study its behaviour.



**Figure 4.7:** how mucin appears after weighted

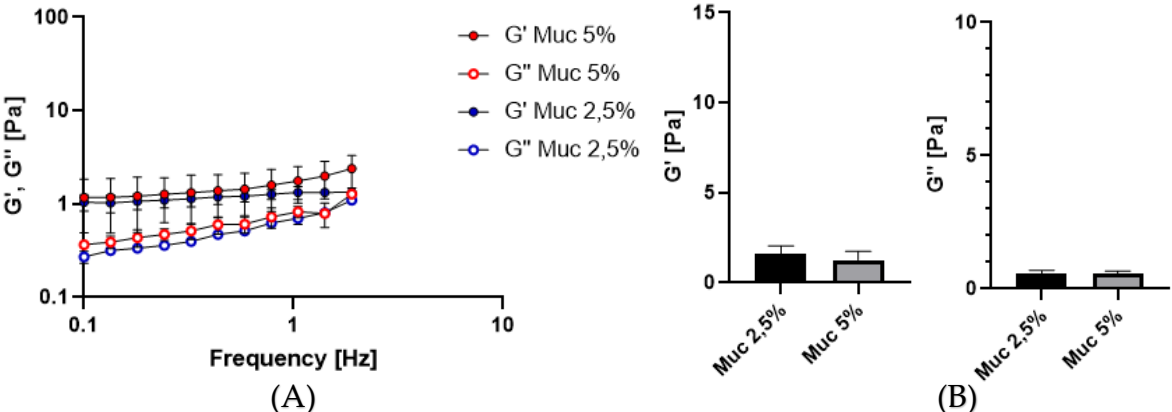
Since the mucin used for the studies in Pavia had been stored differently, it has been necessary to compare the one coming from UniPV and the one present at PoliMI. Therefore, two different gels with the same composition have been tested.



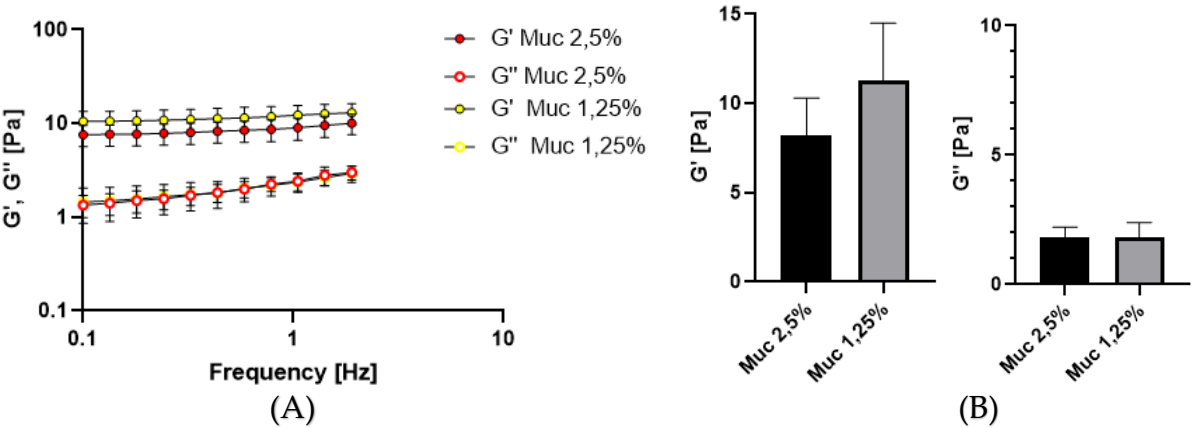
**Figure 4.8:** comparison between two gels produced with the same components amount, the only difference is the used mucin: the one present at Politecnico di Milano and the one from Università degli studi di Pavia. (A) shows the whole curve, (B) fixed the frequency at 0,44 Hz reports the correspondent storage and loss moduli. No statistical differences at  $G'$  (0,44 Hz) and  $G''$  (0,44 Hz) for  $p < 0.05$  have been found between the two compositions

In order to study how the mucin properties affect the overall mucus structure, have been produced several gels in which the only variation is given by the mucin percentages. Finally, they've been compared in pairs.

From this study it has been showed that no statistically significant variations in terms of storage and loss moduli are revealed when changing the mucin concentration. Therefore, it is possible to produce gels with different amounts of mucin, depending on the need, and obtain comparable properties.



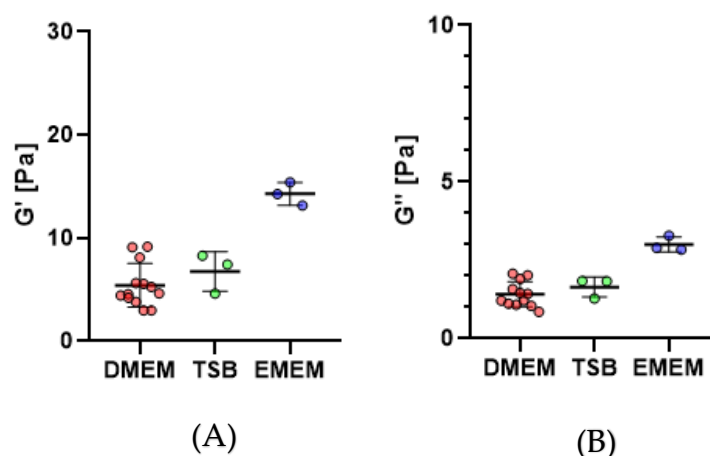
**Figure 4.9:** comparison between Mu4Covid 1.2 and Mu4Covid 1.5 in which the respective mucin concentrations are 5% and 2,5%, while alginate is kept constant at 0,4%. (A) shows the whole curve, (B) fixed the frequency at 0,44 Hz reports the correspondent storage and loss moduli. No statistical differences at G' (0,44 Hz) and G'' (0,44 Hz) for  $p < 0.05$  have been found between the two compositions



**Figure 4.10:** comparison between Mu4Covid 2.1 and Mu4Covid P 2.1 in which the respective mucin concentrations are 1,25% and 2,5%, while alginate is kept constant at 0,6%. (A) shows the whole curve, (B) fixed the frequency at 0,44 Hz reports the correspondent storage and loss moduli. No statistical differences at G' (0,44 Hz) and G'' (0,44 Hz) for  $p < 0.05$  have been found between the two compositions

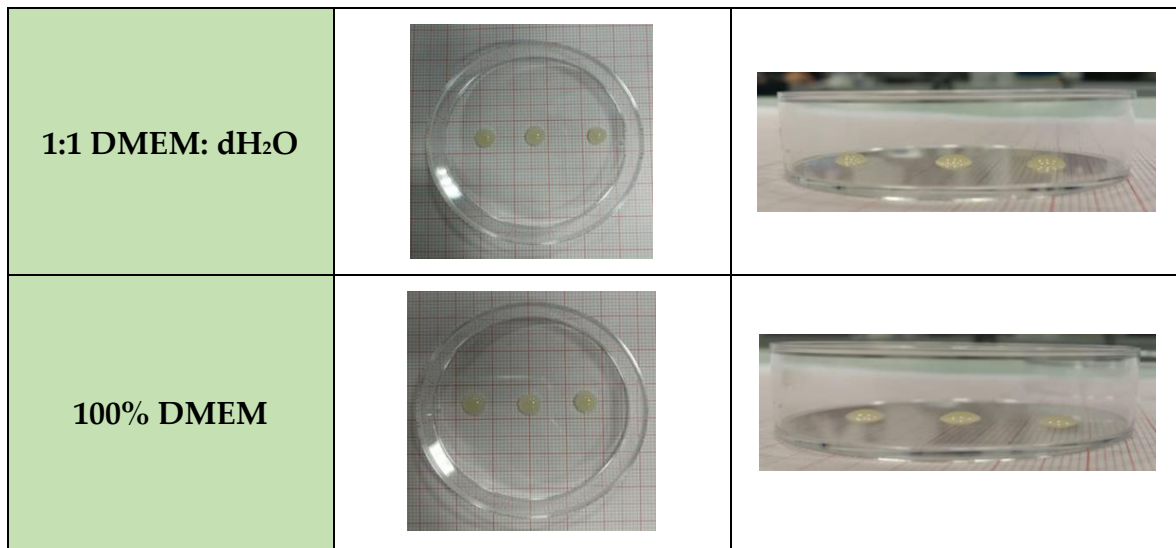
#### 4.1.5.3 Medium

It was necessary to study if it was possible to include mediums in the gel and which was the best medium composition for this analysis. Three different mediums have been analyzed: DMEM with 1% L-glut, 1% PS and 10% FBS, TSB and EMEM. Therefore, it has been analyzed if the three of them could be used for components dissolution. It has been noticed that all the mediums were able to dissolve the components, so three mucus models identical in composition have been developed and their mechanical properties have been compared.



**Figure 4.11:** Mu4Covid 2.0 produced in DMEM, TSB and EMEM as mediums. Here reported a comparison in terms of (A)  $G'$  (0,44 Hz) and (B)  $G''$  (0,44 Hz)

Moreover, it has also been investigated if gel properties vary if the medium is the only DMEM (hereinafter named 100% DMEM) or diluted in distilled water 1:1 DMEM:dH<sub>2</sub>O.



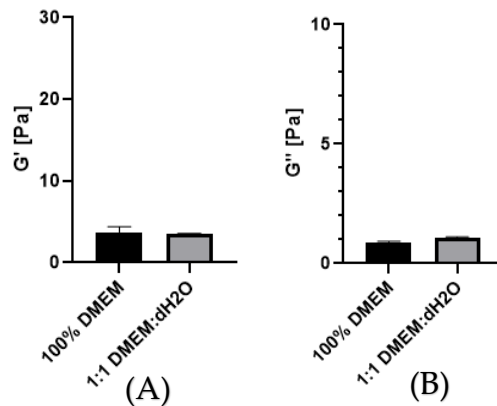
**Table 4.4:** macroscopic view of the mucus dissolved in DMEM and in 1:1 DMEM:dH<sub>2</sub>O. Each drop has been deposited withdrawing 20 $\mu$ l of gel after its reticulation

Using the App ImageJ, it was possible to calculate the height and the diameter of the drops and make a comparison between the ones produced in only DMEM and the ones produced in 1:1 DMEM:dH<sub>2</sub>O.

	1:1 DMEM:dH <sub>2</sub> O	100% DMEM
Height	1,8 $\pm$ 1,5	1,7 $\pm$ 0,5
Diameter	5,6 $\pm$ 0,3	6 $\pm$ 0,1

**Table 4.5:** diameter and height of each drop calculated using the App ImageJ. Here reported the mean and the standard deviation

In addition, they have also been studied the rheological properties using the frequency sweep test at the rheometer.

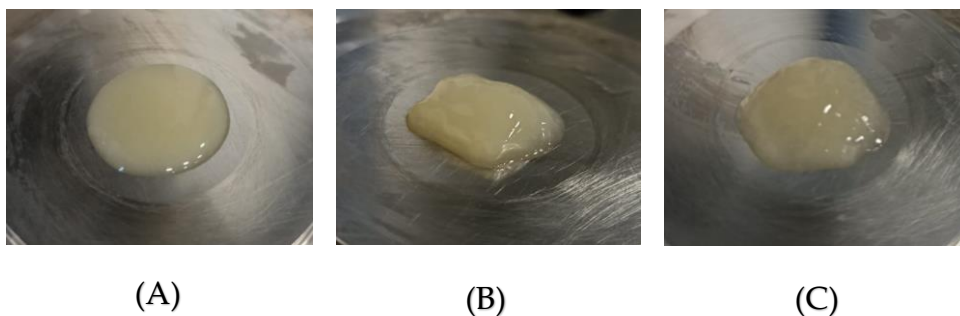


**Figure 4.12:** comparison between two gels of the same composition but dissolved in different medium: one using DMEM with 1% L-glut, 1% PS and 10% FBS and the other in distilled water 1:1 DMEM:dH<sub>2</sub>O. No statistical differences at (A)  $G'$  (0,44 Hz) and (B)  $G''$  (0,44 Hz) for  $p < 0.05$  have been found between the two compositions

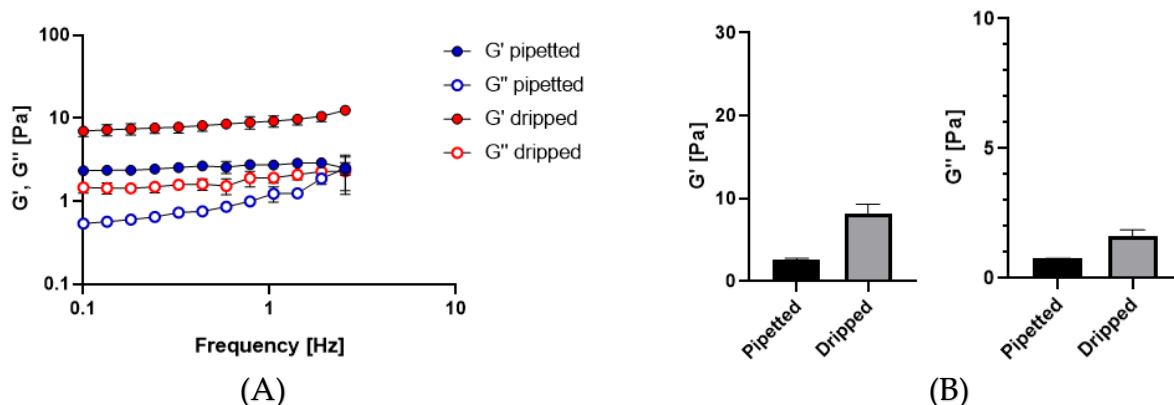
#### 4.1.6 Possibility to extrude

It has been evaluated if the extrusion method affects the mechanical properties of the mucus. Different extrusion methods have been tested and their properties have been evaluated macroscopically and at the rheometer through the frequency test. The sample has been pipetted (1mL), dripped and syringed (1mL).

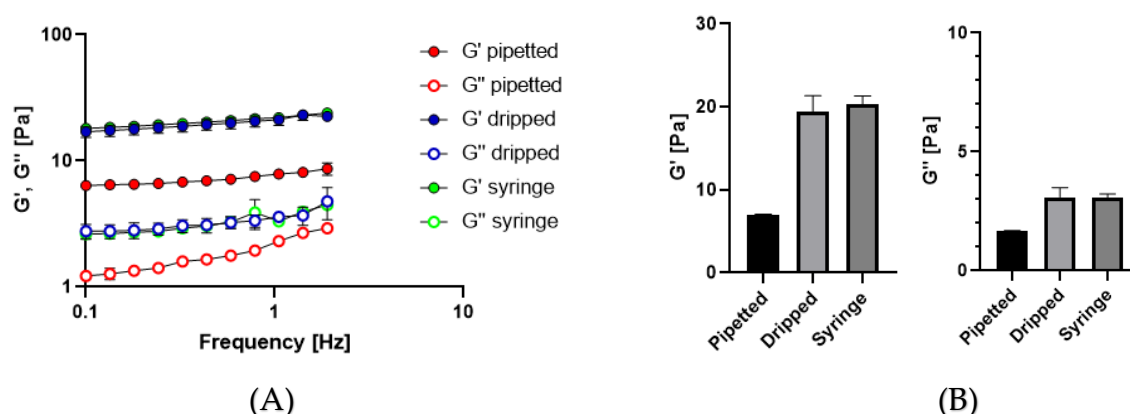
Considering this analysis, it's possible and easy for the user to choose the dispensing modality that better fits the requirements.



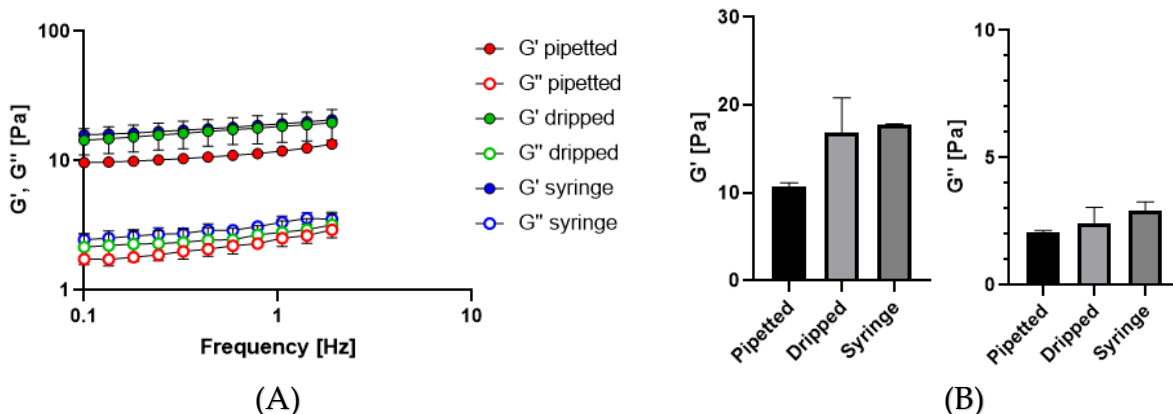
**Figure 4.13:** macroscopic view of the gels on the rheometer plate immediately before providing the frequency test. (A) pipetted gel, (B) dripped and (C) syringe



**Figure 4.14:** comparison of the same gel (Mu4Covid 1.0) dispensed by pipetting and dripping. (A) shows the whole curve, (B) fixed the frequency at 0,44Hz reports the correspondent values of storage and loss moduli. Statistical differences at  $G'$  (0,44Hz) and  $G''$  (0,44Hz) for  $p < 0.05$  have been found between the two compositions



**Figure 4.15:** comparison of the same gel (Mu4Covid 2.1) dispensed by pipetting, dripping and syringing. (A) shows the whole curve, (B) fixed the frequency at 0,44Hz reports the correspondent values of storage and loss moduli. No statistical differences at  $G'$  (0,44Hz) and  $G''$  (0,44Hz) for  $p < 0.05$  have been found between the syringe and dripped modalities, while statistical differences have been found between the syringe and dripped respect pipetted



**Figure 4.16:** comparison of the same gel (Mu4Covid P 2.2) dispensed by pipetting, dripping and syringing. (A) shows the whole curve, (B) fixed the frequency at 0,44Hz reports the correspondent values of storage and loss moduli. No statistical differences at  $G'$  (0,44Hz) and  $G''$  (0,44Hz) for  $p < 0.05$  have been found between the syringe and dripped modalities, while statistical differences have been found between the syringe and dripped respect pipetted

#### 4.1.7 Shelf-life assessment

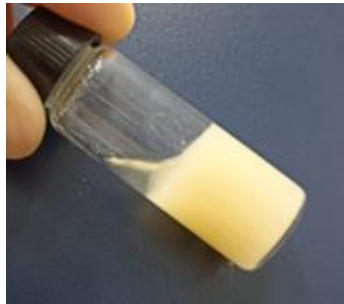
After the gel production, 3mL of gel have been pipetted in each vial. All the vials have been stored in a fridge at 4°C waiting for the crosslinking to occur. For a maximum of 7 consecutive days, every 24 hours one vial was opened, and its content was tested at the rheometer doing frequency sweep tests. In the Table 4.6 are reported some of the obtained results making a distinction between the detected storage and loss moduli. All those data were studied in terms of reached values of  $G'$  and  $G''$  during conservation time, deviation from the average and preservation of the initial properties.

Gel name	$G'$ [Pa]	$G''$ [Pa]
Mu4Covid 1.0		
Mu4Covid 2.0		
Mu4Covid P 2.0		
Mu4Covid P 2.1		
Mu4Covid P 2.2		

**Table 4.6:** shelf-life over a maximum of 7 consecutive days of several mucus compositions. Fixed the frequency at 0,44Hz, all data are reported in terms of storage and loss moduli and their time evolution



Going on with the shelf-life a remarkable result is the presence of the double phase. Some mucus models such as Mu4Covid P 1.0 and Mu4Covid P 2.0 show its appearance immediately, all the others after few days (from 3 to 5 days).



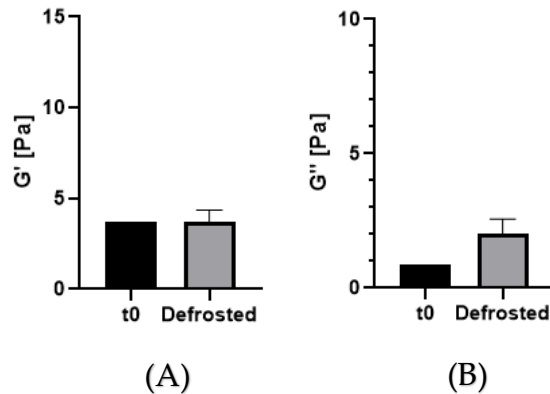
**Figure 4.17:** the presence of the double phase didn't spare any gel production, here reported how Mu4Covid P 2.3 looks like after being stored for 7 days at 4°C

#### 4.1.7.1 Freezing process

It has also been investigated the freezing as storage modality. The experiment has been conducted after the mucus crosslinking by leaving the samples in a fridge at a controlled temperature of -80°C for 72 hours. Then, in order to defrost it, the samples were left 30 minutes at -20°C and 3 hours at 4°C. Finally, it was provided the test at the rheometer and the obtained macroscopic properties were compared to the ones of at  $t=0$  that were obtained after 20 hours of crosslinking.



**Figure 4.18:** macroscopic view of frozen and successively defrosted samples when pipetted on the rheometer plate

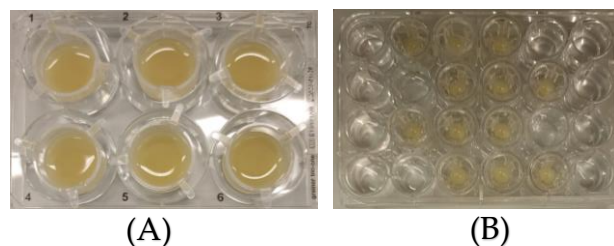


**Figure 4.19:** comparison between rheological properties of the mucus Mu4Covid 1.0 at  $t_0$  and after the freezing and the defrosting in terms of  $G'$  (A) and  $G''$ (B). No statistical differences at  $G'$  (0,44Hz) for  $p < 0.05$  have been found between the two storage modalities, while statistical differences at  $G''$  (0,44Hz)

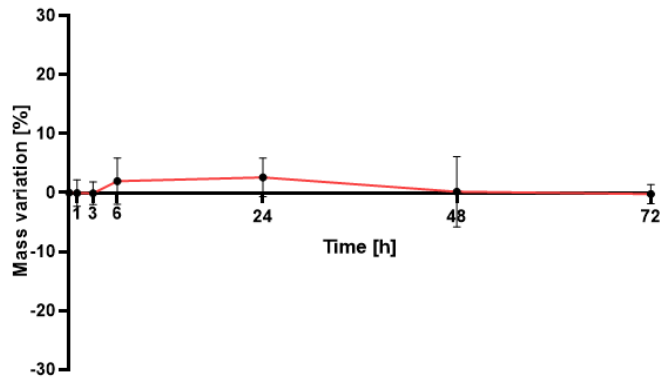
#### 4.1.8 Stability test

To understand if the medium interacts with the 3D structures, stability tests were performed. Transwells were filled with the mucus prototype, medium was added in the below multiwells and finally the whole structure was placed in the oven at the controlled temperature of 37°C. At each time point the weights of the samples had been collected and then mass variation [%] has been calculated. For most of the studied compositions it has been showed very smooth initial increasing in mass variation and a consequent decreasing in time. All data are never beyond  $\pm 7\%$ .

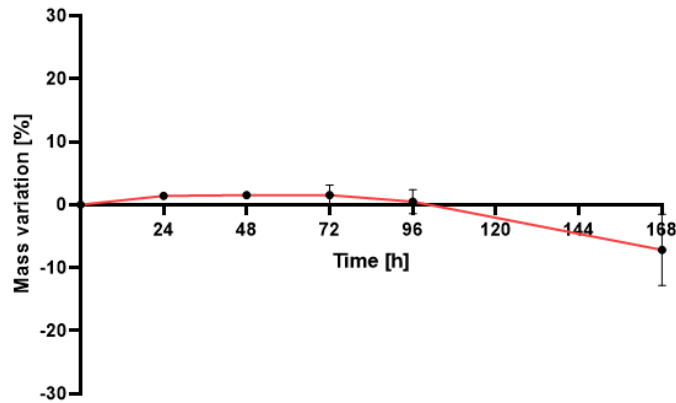
Since the 3D mucus models were able to adapt themselves to transwells of different sizes, stability tests have been conducted using 6 transwells support and 24 transwells support.



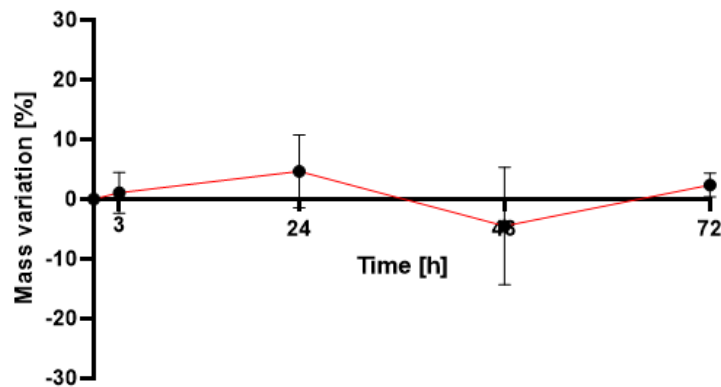
**Figure 4.20:** macroscopic view of how the 3D model adapt itself to transwell of different sizes. (A) 6 transwells support, (B) 24 transwells support



**Figure 4.21:** stability test provided at  $t = 0, 1, 3, 24, 48, 72$  hours of Mu4Covid 2.0 in a 6 transwells support by weighting the samples and calculating the mass variation [%]



**Figure 4.22:** stability test provided at  $t = 0, 24, 48, 72, 96, 168$  hours of Mu4Covid P 2.0 in 24 transwells support by weighting the samples and calculating the mass variation [%]



**Figure 4.23:** stability test provided at  $t = 0, 3, 24, 48, 72$  hours of Mu4Covid P 2.2 in a 6 transwells support by weighting the samples and calculating the mass variation [%]

## 4.2 Collaboration with UniPV and UniTO

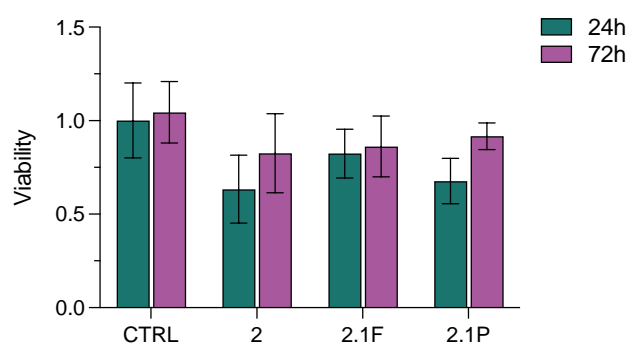
During the Mucus4Covid project development, UniTO and UniPV collaborate with PoliMI in order to give greater consistency to the obtained model. At PoliMI have been conducted tests to optimize the concentration of the mucus prototype and the rheological analysis. At UniTO and UniPV the cytocompatibility and viral activity were studied, but also bacterial infections (UniPV) and drugs permeability (UniTO).

All the below reported data are referred to mucus composition Mu4Covid 2.0.

Gel name	Alginate	Mucin	CaCO <sub>3</sub>	GDL
Mu4Covid 2.0	0.6%	2.5%	0.13%	0,8%

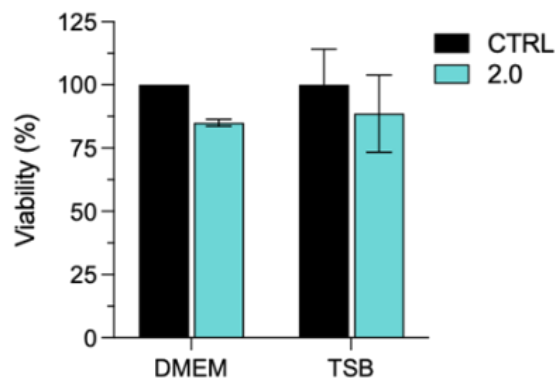
**Table 4.7:** here reported the composition of Mu4Covid 2.0 used for the tests in UniTO and UniPV

Cytocompatibility tests were provided using two different epithelial cellular lines: HCT8 and VERO-E6, specific cellular line used during SARS-Cov-2 studies.



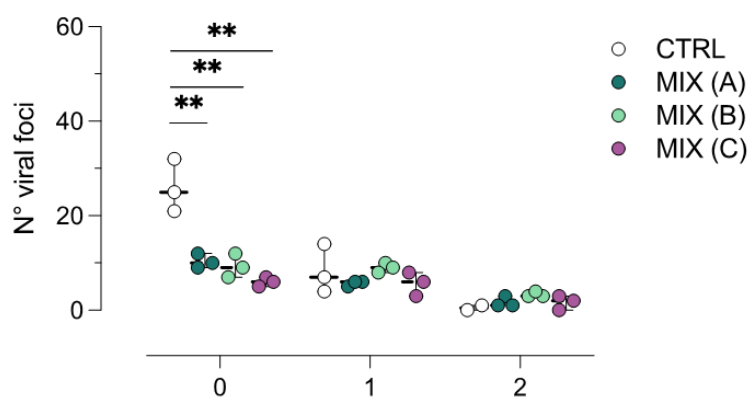
**Figure 4.24:** cellular activity at 24 and 72 hours of VERO-E6 cellular line. Cell viability has been quantified using Trypan blue coloration

During cytocompatibility tests it has also been studied if changing the medium brings to any difference in cell viability.

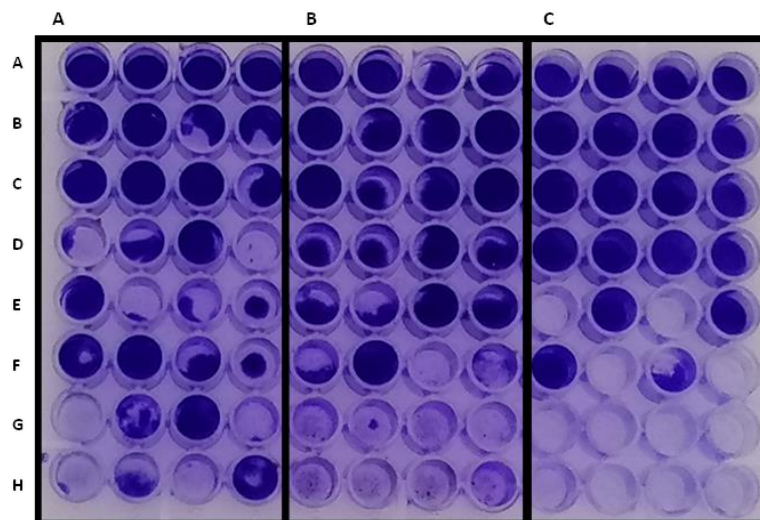


**Figure 4.25:** comparison of the cellular viability of VERO-E6 cellular line using Trypan blue coloration when the dissolving agent is DMEM and TSB. The control is given by the cells culture in absence of Mu4Covid 2.0

Viral activity and virucidal tests were provided using virus considered surrogates of SARS-CoV-2 (Human coronavirus HCoV-OC43) and SARS-CoV-2 (delta variant). Those tests were conducted by loading the viral suspension in Mu4Covid 2.0, leaving in the incubator for 2 hours, lay the compound on the cellular layer and incubating again. Then it has been evaluated the replicate activity of the virus (N° foci).

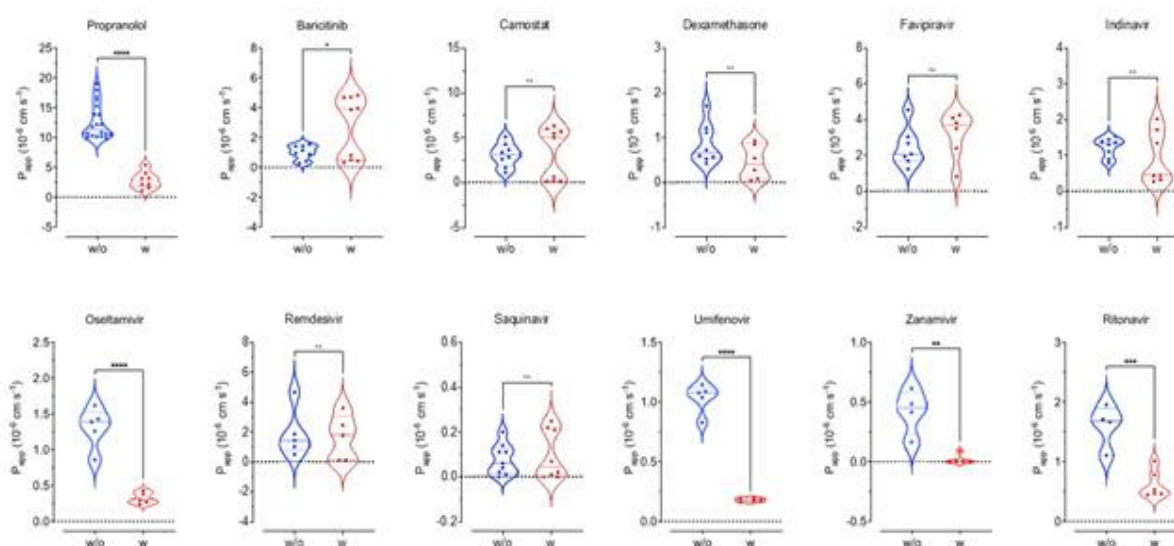


**Figure 4.26:** virucidal test using HCoV-OC43 on three different cellular lines



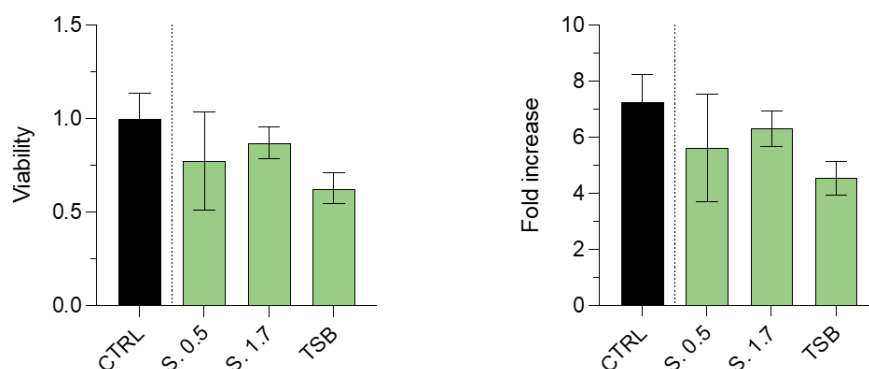
**Figure 4.27:** virucidal test using Sars-CoV-2 with different mucin amounts (A) 2,5% and (B) 1,25% and in absence of Mu4Covid 2.0 (C)

It has been evaluated mucus behavior when in contact with several antiviral drugs. Those permeability tests were conducted using PAMPA assay.



**Figure 4.28:** drug permeability tests. Blu, reports data when mucus is absent while red in mucus presence

Finally, overcoming the limits present in current literature, it has been produced a mucus model containing bacterial secretome and placed in contact with the virus. To provide the experiment *Staphylococcus Aureus* secretome has been produced in stationary and exponential phase.



**Figure 4.29:** cytocompatibility using VERO-E6 present in Mu4Covid 2.0 containing *S. aureus* secretome in exponential phase (S. 0.5) and stationary phase (S. 1.7) dissolved in TSB and comparison with Mu4Covid 2.0 in only TSB and the control in absence of Mu4Covid 2.0

### 4.3 Definition of physiological Mu4Covid model

From all the preliminaries conducted studies, it emerged that the composition that better mimics the healthy condition was the following:

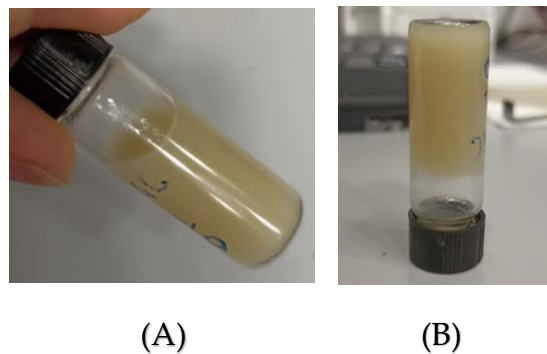
Gel name	Alginate	Mucin	CaCO <sub>3</sub>	GDL
Mu4Covid 2.1	0.6%	2.5%	0.13%	1%

**Table 4.8:** here reported the composition of Mu4Covid 2.1, the mucus model that has showed to better mimic the physiological healthy condition

To reach this result, several experiments have been done and they are here reported. In order to verify all the preliminary requisites, it has been conducted the pH analysis. After the solution production, it was dropped in a 5mL syringe and left crosslinking

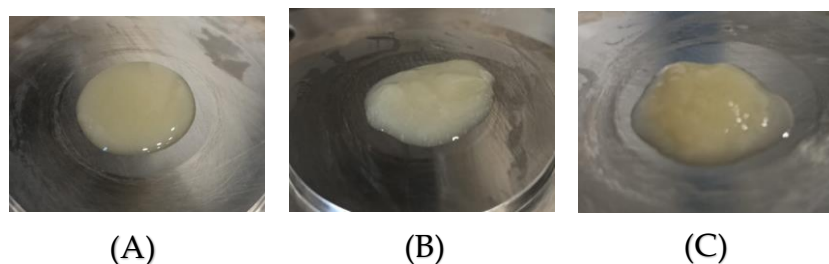
in fridge overnight. After spent 20 hours, the pH was detected using a pH-meter. The found value was  $\text{pH} = 5.84$ , compatible with the physiological environment and cell vitality.

Another prerequisite was the macroscopic view. Below it is reported how Mu4Covid 2.1 looks like in the vial used for the storage.



**Figure 4.30:** macroscopic view of Mu4Covid 2.1 when inside the vial used for the storage. (A) shows how the gel is like when the vial that contains it is slightly inclined (B) shows how it is like when the vial is put upside down

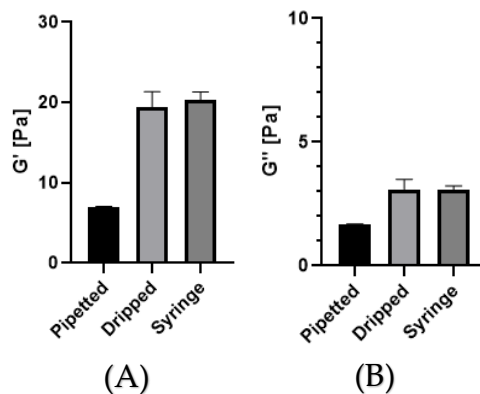
The studies about the dispensing modality showed that when pipetted, the gel appears with a smooth, compact and homogenous surface and is very easy to dispense. Instead, when dripped or syringed the gel is much thicker and has not homogenous surface.



**Figure 4.31:** macroscopic view of how Mu4Covid 2.1 appears when dispensed in different ways: (A) pipetted, (B) dripped and (C) syringed

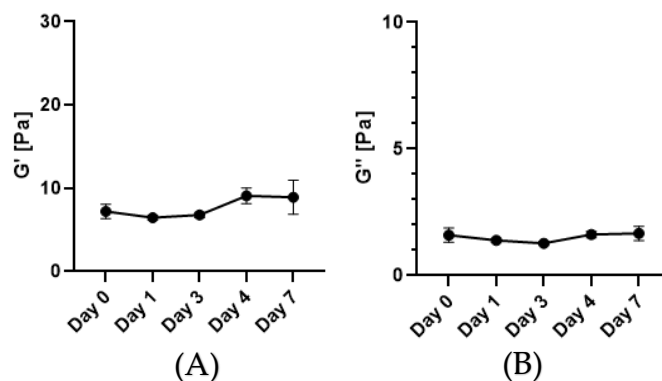
Moreover, the rheological test on the 3 different dispensing modalities has been provided in order to catch the differences.





**Figure 4.32:** comparison of Mu4Covid 2.1 dispensed by pipetting, dripping and syringing. Fixed the frequency at 0,44Hz (A) shows the trend of  $G'$ , while (B) the trend of  $G''$ . No statistical differences at  $G'$  (0,44Hz) and  $G''$  (0,44Hz) for  $p < 0.05$  have been found between the syringed and dripped modality, while statistical differences have been found between the syringed and dripped respect pipetted

The rheological properties have been investigated over 7 days in order to study for how long mechanical properties of the prototype are stored<sup>3</sup>. Moreover, one vial has been stored for 30 days and then the rheological properties have been evaluated.

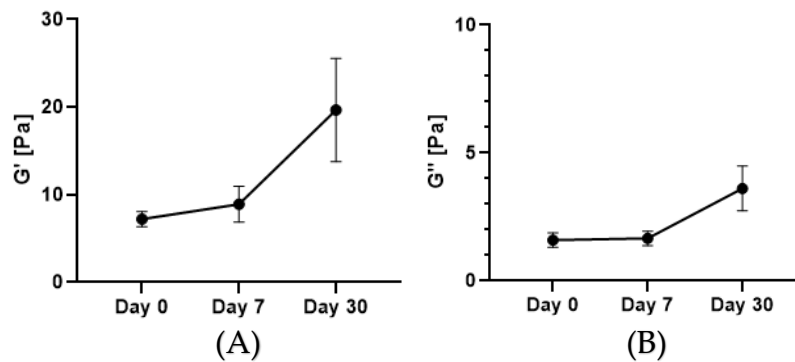


**Figure 4.33:** fixed the frequency of 0,44Hz (A) reports the trend of  $G'$  during the 7 days of storage (B) reports the trend of  $G''$  during the 7 days of storage. No statistical differences at  $G'$  (0,44Hz) and  $G''$  (0,44Hz) for  $p < 0.05$  have been found during the conducted shelf-life

<sup>3</sup> See Appendix A for the complete behaviour of Mu4Covid 2.1 during the shelf-life assessment

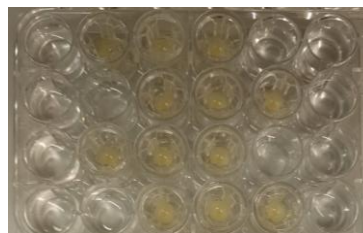


**Figure 4.34:** macroscopic view of how the mucus model appears after 30 days of storage in the vial and on the rheometer plate before providing the test

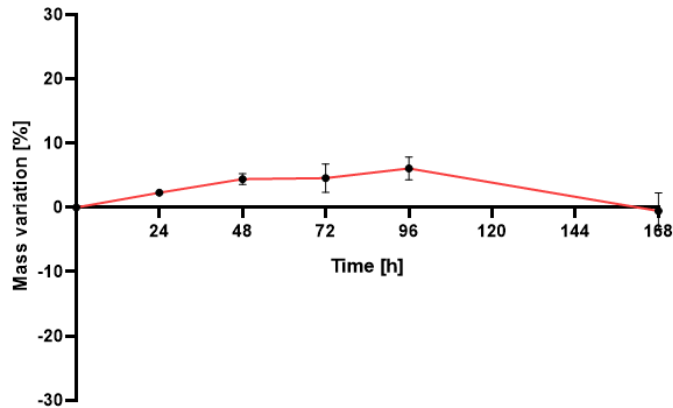


**Figure 4.35:** fixed the frequency of 0,44Hz (A) reports the trend of  $G'$  at  $t = 0, 7, 30$  days (B) reports the trend of  $G''$   $t = 0, 7, 30$  days. Statistical differences at  $G'$  (0,44Hz) and  $G''$  (0,44Hz) for  $p < 0.05$  have been found between the obtained values at  $t = 30$  days and  $t = 0$  day or  $t = 7$  days

The stability test has been conducted using the same protocol. Here reported the obtained results.



**Figure 4.36:** to provide the stability test, the gel was dispensed in transwells that fit 24 transwells support. Here reported the macroscopic observation of how Mu4Covid 2.1 looked like and how it adapted to the walls



**Figure 4.37:** stability test provided at  $t = 0, 24, 48, 72, 96, 168$  h of Mu4Covid 2.1 in 24 transwells support by weighting the samples and calculating the mass variation [%]

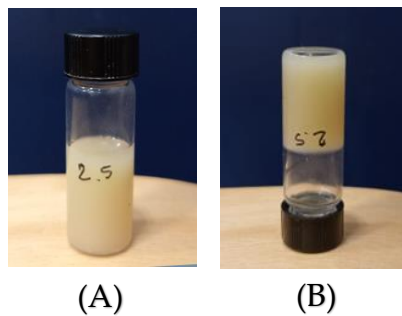
#### 4.4 Definition of pathological Mu4Covid model

From all the preliminaries conducted studies, it emerged that the composition that better mimics the SARS-CoV-2 pathological condition was the following:

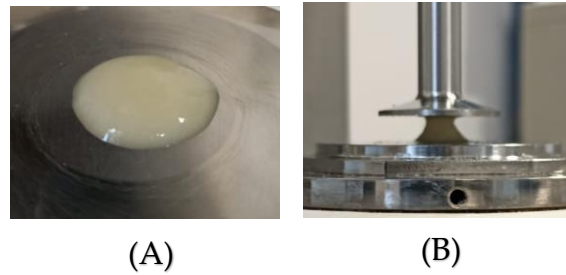
Gel name	Alginate	Mucin	CaCO <sub>3</sub>	GDL
Mu4Covid P 2.3	0.7%	2.5%	0.13%	1%

**Table 4.9:** here reported the composition of Mu4Covid P 2.3, the one that has showed to better mimic the SARS-CoV-2 pathological condition

To reach this result, several experiments have been carried out and they are here reported. Firstly, it has been conducted the pH analysis that showed  $\text{pH} = 5,74$ .

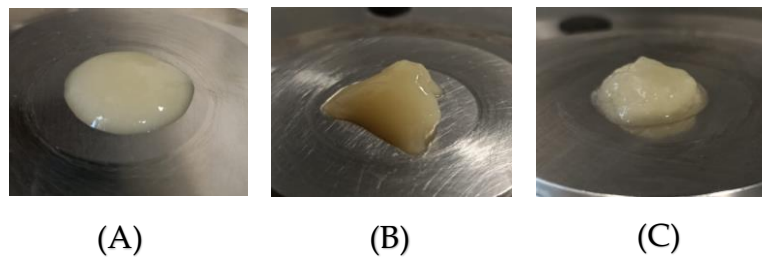


**Figure 4.38:** macroscopic view of Mu4Covid P 2.3 in the vial for the storage showing how the gel is like when (A) the vial is on a flat surface (B) the vial is upside down



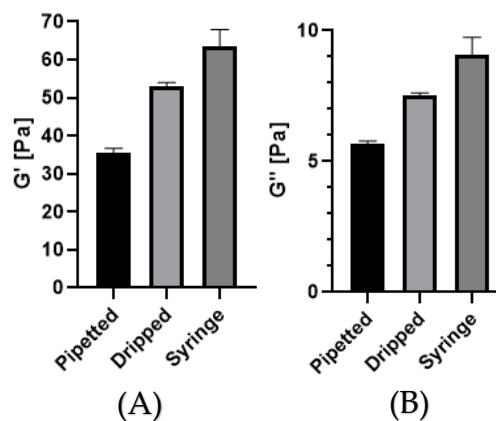
**Figure 4.39:** macroscopic view of Mu4Covid P 2.3 when is put on the rheometer plate before performing any experiment (A) and when the experiment is concluded and the upper plate of the rheometer is rising up (B)

The studies about the dispensing modality showed that when pipetted, the gel appears with a smooth, compact and homogenous surface and is very easy to dispense. Instead, when dripped or syringed the gel is much thicker and hasn't an homogenous surface.



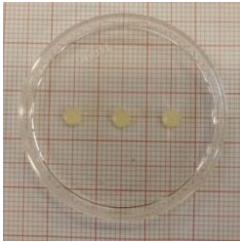

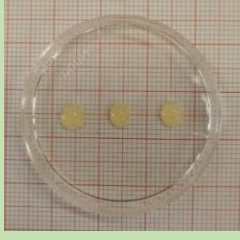

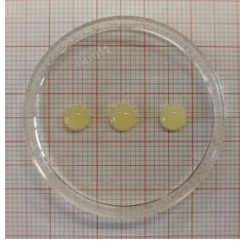

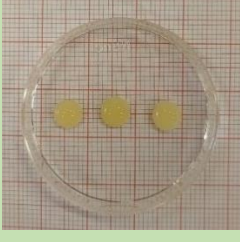

**Figure 4.40:** macroscopic view of how Mu4Covid P 2.3 appears when dispensed in different ways: (A) pipetted, (B) dripped and (C) syringe

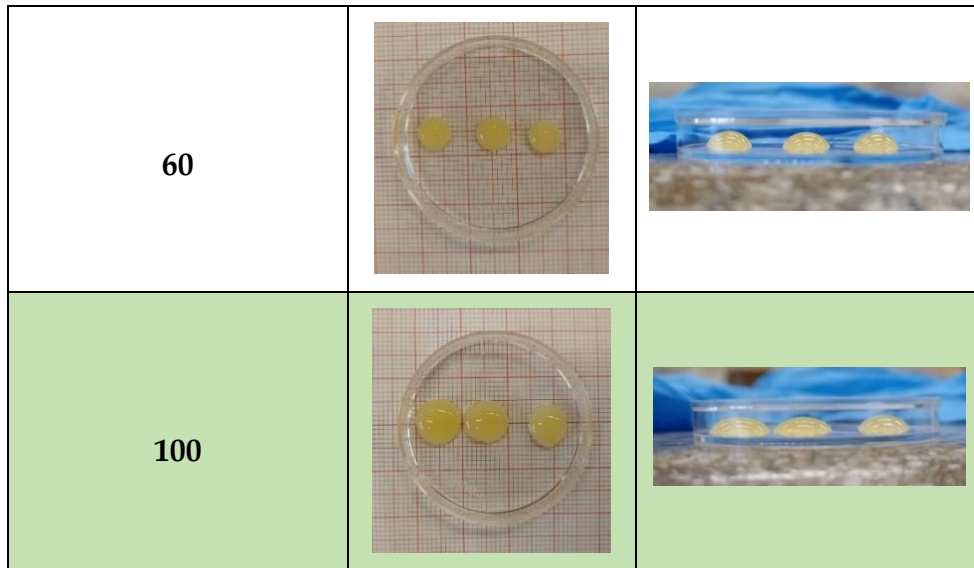
Moreover, the rheological test on the 3 different dispensing modalities has been provided in order to catch the differences.



**Figure 4.41:** comparison of Mu4Covid P 2.3 dispensed by pipetting, dripping and syringing. Fixed the frequency at 0,44Hz (A) shows the trend of  $G'$  (B) the one of  $G''$ .  
 Statistical differences at  $G'$  (0,44Hz) and  $G''$  (0,44 Hz) for  $p < 0.05$  have been found between the three dispensing modalities

It has been studied how the gel adapts itself to the surface. Drops of different amounts have been placed on a petri dish and then using App ImageJ the height and the diameter have been calculated and reported in the below table.

Mucus quantity [ $\mu\text{L}$ ]	Diameter [mm]	Height [mm]
10		
20		
30		
50		

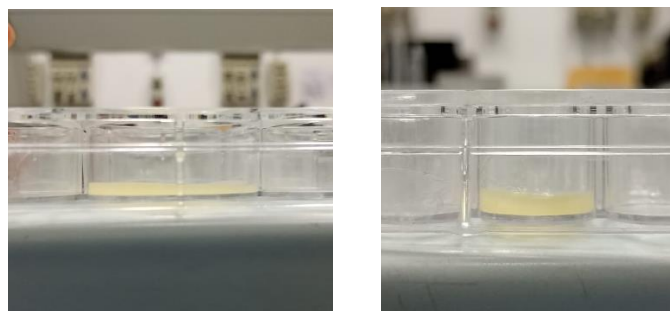


**Table 4.10:** macroscopic observation of several mucus quantities on a petri dish using a pipette. Each drop has been pipetted three times. For each mucus quantity, here reported the photos of the side and top view

	10 $\mu\text{L}$	20 $\mu\text{L}$	30 $\mu\text{L}$	50 $\mu\text{L}$	60 $\mu\text{L}$	100 $\mu\text{L}$
Diameter [mm]	3,7 $\pm$ 0,1	4,6 $\pm$ 0,2	5,6 $\pm$ 0,1	6 $\pm$ 0,1	6,8 $\pm$ 0,1	9,2 $\pm$ 0,5
Height [mm]	1,6 $\pm$ 0,1	1,9 $\pm$ 0,1	2 $\pm$ 0,1	2 $\pm$ 0,2	2,5 $\pm$ 0,2	2,5 $\pm$ 0,1

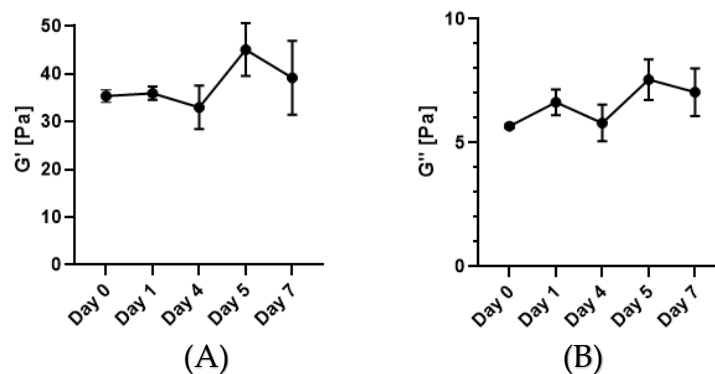
**Table 4.11:** diameter and height of each drop calculated using the App ImageJ. Here reported the mean and the standard deviation

It has been analysed which amount of Mu4Covid P 2.3 was necessary to fully cover a well that fits the 6 and 24 multiwells. Respectively 1mL and 0,3 mL were necessary.



**Figure 4.42:** macroscopic view of 1mL of gel in a well of the 6 multiwells and 0,3 mL of gel in a well of the 6 multiwells

The rheological properties have been investigated over 7 days and below reported<sup>4</sup>.



**Figure 4.43:** fixed the frequency of 0,44Hz (A) reports the trend of  $G'$  during the days (B) reports the trend of  $G''$  during the days. No statistical differences at  $G'$  (0,44Hz) and  $G''$  (0,44Hz) for  $p < 0.05$  have been found during the conducted shelf-life

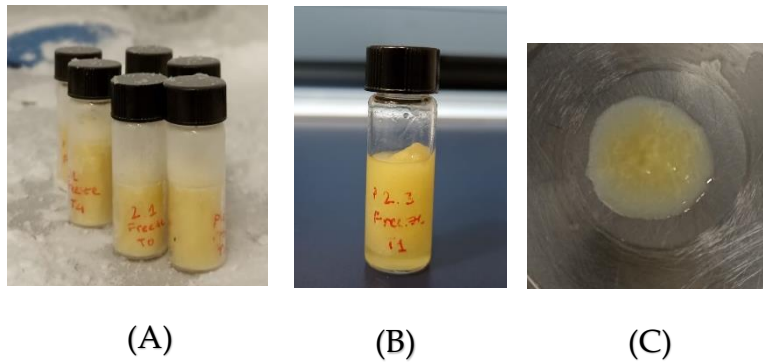


**Figure 4.44:** appearance of the liquid phase in Mu4Covid P 2.3 after being stored at 4°C after 5 days

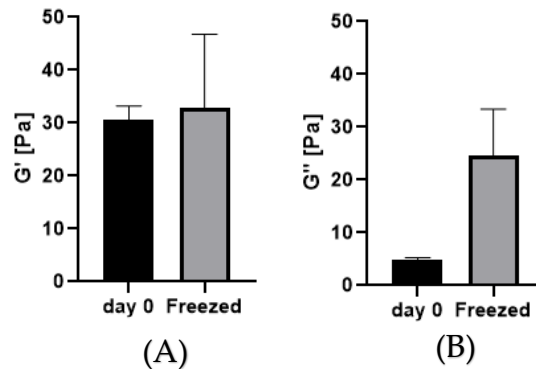
It has also been investigated the freezing as storage modality leaving the samples at -80°C for 96 hours and then smoothly defrost the mucus leaving it at -20°C for 20 minutes and at 4°C overnight. Below are reported the macroscopic views and the tests conducted.

---

<sup>4</sup> See Appendix A for the complete behaviour of Mu4Covid P 2.3 during the shelf-life assessment



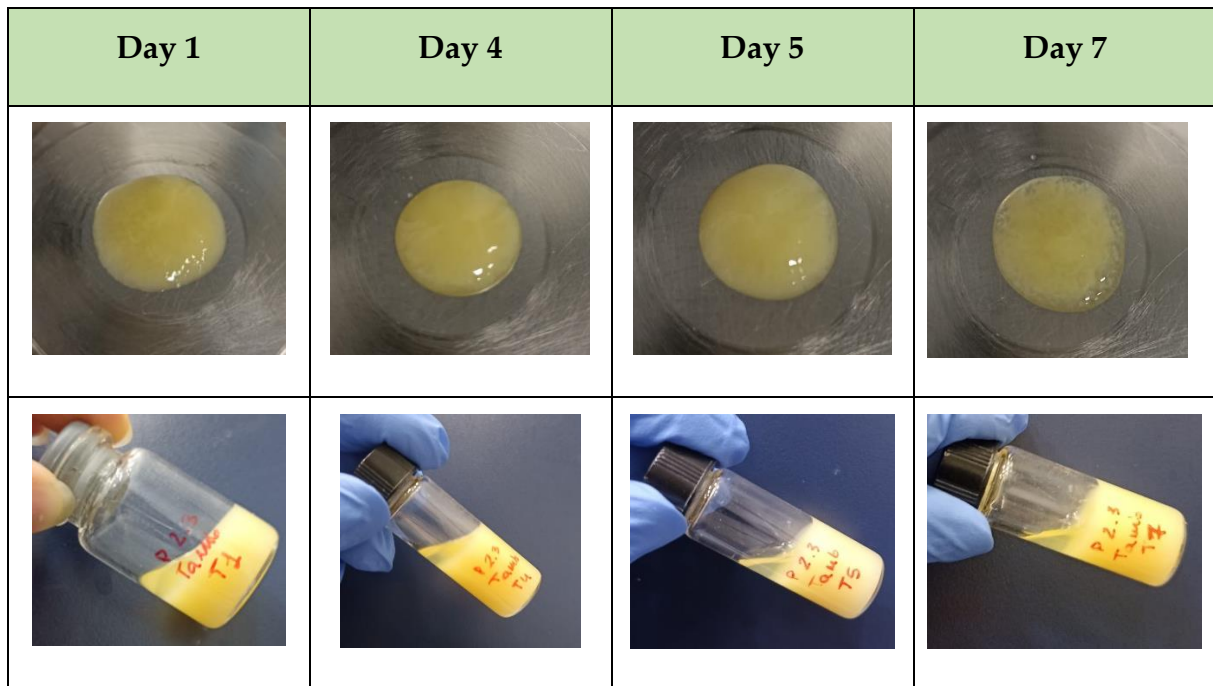
**Figure 4.45:** macroscopic view during the freezing/defrosting process: (A) when vials were freeze at  $-80^{\circ}\text{C}$ , (B) mucus in the vial after leaving the sample overnight at  $4^{\circ}\text{C}$  to provide the defrost, (C) mucus deposited on the rheometer plate before performing any operation



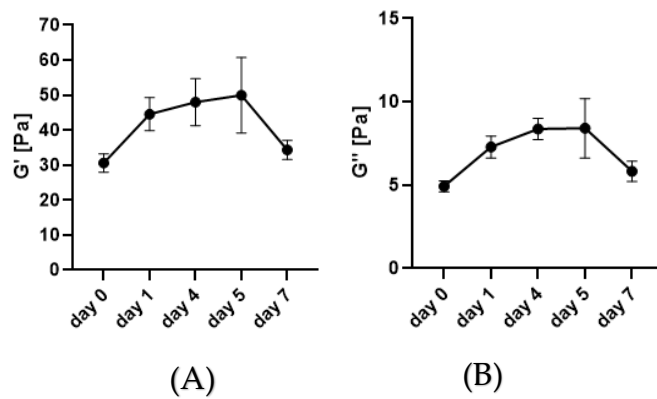
**Figure 4.46:** comparison between rheological properties of Mu4Covid P 2.3 at  $t=0$  and after the freezing and the defrosting in terms of (A)  $G'$  (0,44Hz) and (B)  $G''$ (0,44Hz). No statistical differences at  $G'$  (0,44 Hz) for  $p < 0.05$  have been found between the conducted shelf-lives, while statistical differences have been found in terms of  $G''$  (0,44 Hz)

It has also been investigated the storage at ambient temperature ( $T_{\text{amb}}$ ) of  $22^{\circ}\text{C}$ . Mucus models have been left reticulating, after their production, in fridge at  $4^{\circ}\text{C}$  and then tested at the rheometer. Values of  $G'$  and  $G''$  were acquired for  $t=0$ . All the other samples have been moved from the fridge and left at  $T_{\text{amb}}$  for the storage. During the subsequent 7 days rheological and macroscopic properties have been evaluated.





**Table 4.12:** macroscopic view on the rheometer plate and inside the vials of Mu4Covid P 2.3 when stored at  $T_{amb}$



**Figure 4.47:** fixed the frequency of 0,44Hz (A) reports the trend of  $G'$  (B) reports the trend of  $G''$  during the storage at  $T_{amb}$ . Statistical differences at  $G'$  (0,44Hz) and  $G''$  (0,44Hz) for  $p < 0.05$  have been found during the conducted shelf-life

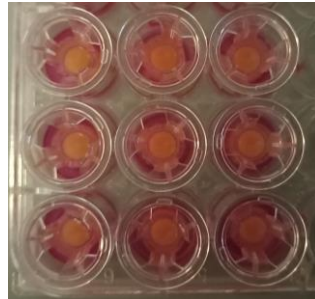
	G' (0,44Hz)	Mean	Standard deviation	Increasing [%]
T0	29,4 33,6 28,7	30,6	2,6	0
T1	49,9 42,8 41,0	44,6	4,7	45,7
T4	51,9 51,8 40,2	48,0	6,7	56,8
T5	61,9 40,9 47,1	50,0	10,8	63,4
T7	36,2 32,4	34,3	2,7	12,2

**Table 4.13:** here reported the values of each measurement of  $G'$  (0,44 Hz) during the shelf-life conducted at  $T_{amb}$ , its mean value, the calculated standard deviation and finally the increasing [%]

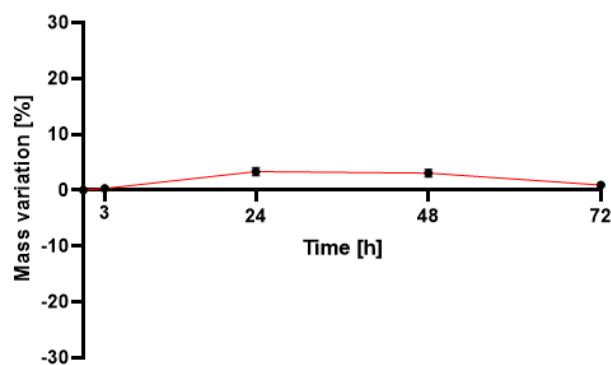
	G'' (0,44Hz)	Mean	Standard deviation	Increasing [%]
T0	4,7 5,3 4,7	4,9	0,3	0
T1	8,0 7,0 6,8	7,3	0,7	48,0
T4	8,8 8,7 7,6	8,4	0,6	69,8
T5	10,4 6,9 8,0	8,4	1,8	70,8
T7	6,3 5,4	5,8	0,6	18,2

**Table 4.14:** here reported the values of each measurement of  $G''$  (0,44Hz) during the shelf-life conducted at  $T_{amb}$ , its mean value, the calculated standard deviation and finally the increasing [%]

The stability test has been provided using the same protocol. Here reported the obtained results.



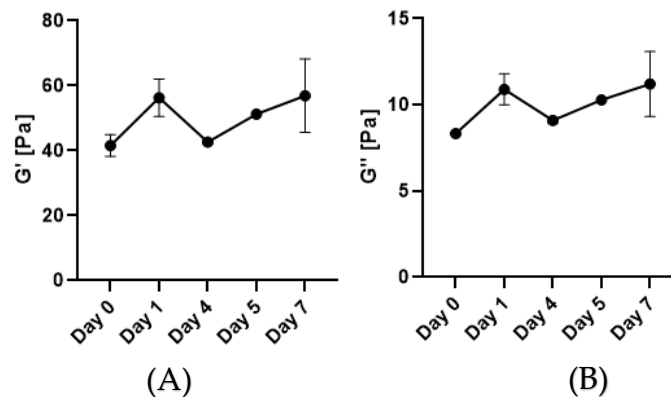
**Figure 4.48:** to provide the stability test, the gel was dispensed in transwells that fit 24 transwells support. Here reported the macroscopic observation of how Mu4Covid P 2.3 looked like and how it adapted to the walls



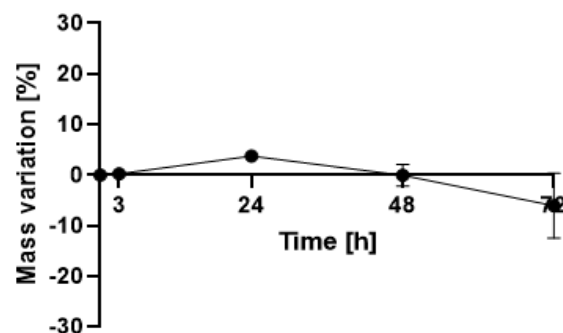
**Figure 4.49:** stability test provided at t = 0, 3, 24, 48, 72 hours of Mu4Covid P 2.3 in 24 transwells support by weighting the samples and calculating the mass variation [%]

## 4.5 Bacterial infection

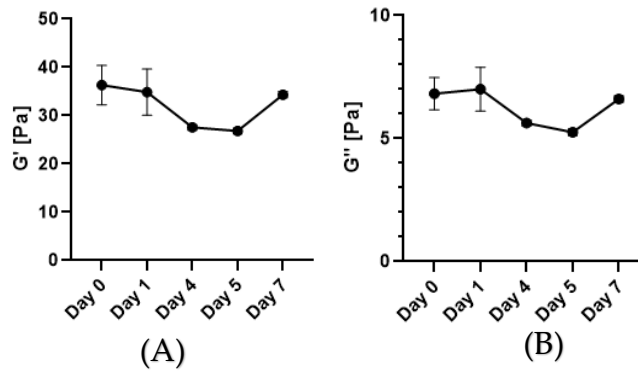
Through the delivered material from Pavia, it has been possible to study the shelf-life and stability at 37°C of the models whose medium was infected with *S. aureus* bacterial secretome.



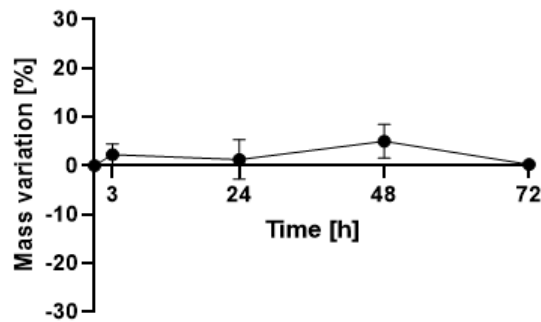
**Figure 4.50:** fixed the frequency of 0,44 Hz (A) reports the trend of  $G'$  (B) reports the trend of  $G''$  during the storage when as medium it is used EMEM 0.54. No statistical differences at  $G'$  (0,44 Hz) and  $G''$  (0,44 Hz) for  $p < 0.05$  have been found during the conducted shelf-life



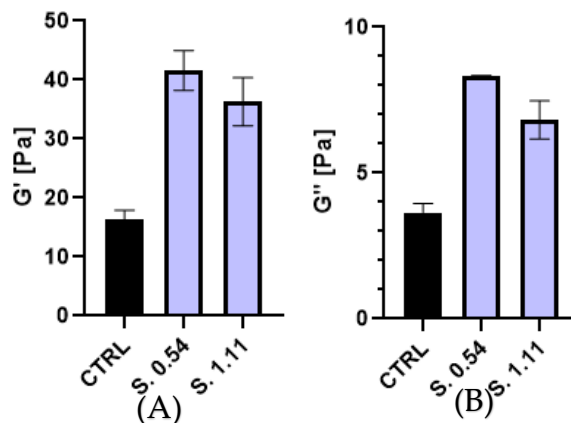
**Figure 4.51:** stability test provided at  $t = 0, 3, 24, 48, 72$  h of Mu4Covid P 2.3 dissolved in EMEM 0.54



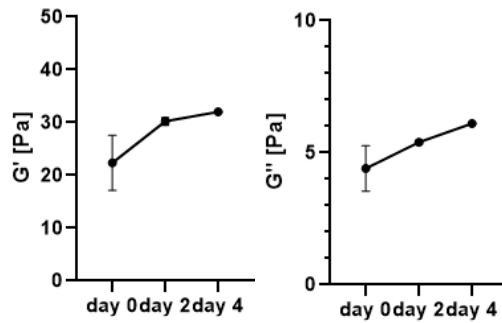
**Figure 4.52:** fixed the frequency of 0,44 Hz (A) reports the trend of  $G'$  (B) reports the trend of  $G''$  during the storage when as medium it is used EMEM 1.11. No statistical differences at  $G'$  (0,44 Hz) and  $G''$  (0,44 Hz) for  $p < 0.05$  have been found during the conducted shelf-life



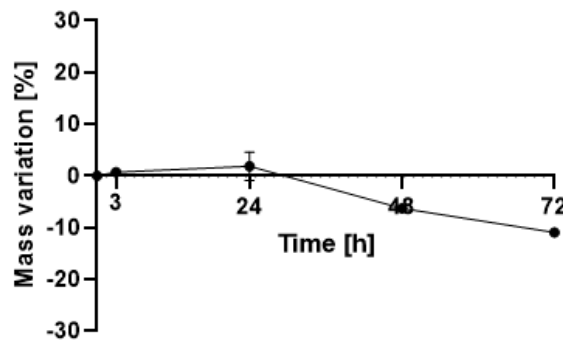
**Figure 4.53:** stability test provided at  $t = 0, 3, 24, 48, 72$  h of Mu4Covid P 2.3 dissolved in EMEM 1.11



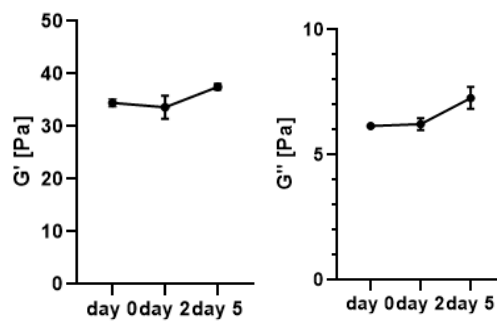
**Figure 4.54:** influence of the secretome in EMEM for the developed mucus model in (A)  $G'$ (0,44 Hz) and (B)  $G''$ (0,44 Hz) where the control is given by blank EMEM used as medium



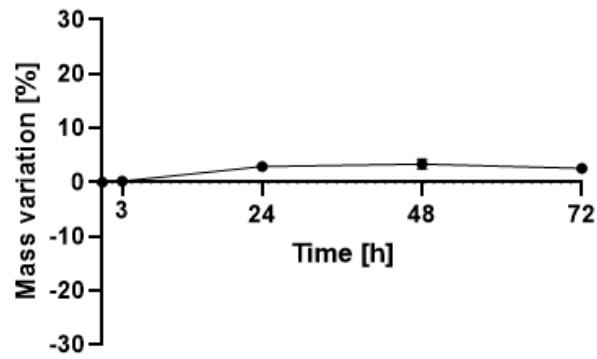
**Figure 4.55:** fixed the frequency of 0,44 Hz (A) reports the trend of  $G'$  (B) reports the trend of  $G''$  during the storage when as medium it is used TSB 0.5. No statistical differences at  $G'$  (0,44 Hz) and  $G''$  (0,44 Hz) for  $p < 0.05$  have been found during the conducted shelf-life



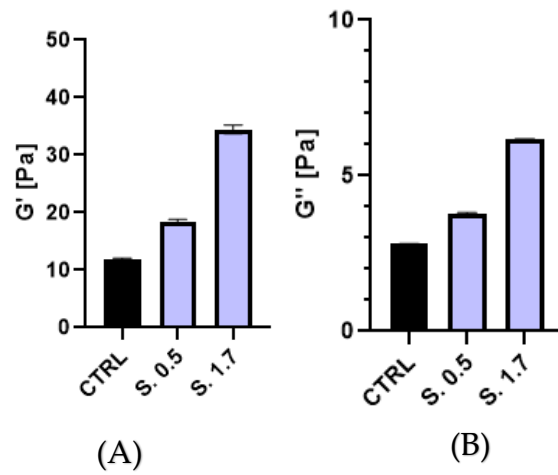
**Figure 4.56:** stability test provided at  $t = 0, 3, 24, 48, 72$  h of Mu4Covid P 2.3 dissolved in TSB 0.5



**Figure 4.57:** fixed the frequency of 0,44 Hz (A) reports the trend of  $G'$  (B) reports the trend of  $G''$  during the storage when as medium it is used TSB 1.7. No statistical differences at  $G'$  (0,44 Hz) and  $G''$  (0,44 Hz) for  $p < 0.05$  have been found during the conducted shelf-life



**Figure 4.58:** stability test provided at  $t = 0, 3, 24, 48, 72$  h of Mu4Covid P 2.3 dissolved in TSB 1.7



**Figure 4.59:** influence of the secretome in TSB for the developed mucus model in (A)  $G'(0,44 \text{ Hz})$  and (B)  $G''(0,44 \text{ Hz})$  where the control is given by blank TSB as medium

## 5. DISCUSSION

Mucus is a complex hydrogel that acts as a protective barrier in several parts of the human body such as the airway, gastrointestinal, cervicovaginal and in oculo-rhinotolaryngologic tracts. Depending on where it is placed, mucus has different functions. Focusing on the airway mucus, its main functions are to protect lungs against unsafe particles that may enter during inhalation and maintenance of epithelium's hydration level. Mucus is continuously transported from the lower respiratory tract to the more proximal airways thanks to the ciliary motion of the ciliated cells that lay on the epithelium. This transport is allowed only for adequate mucus clearance levels. However, control this parameter is not so easy because it's function of water and ion transport, mucin secretion, cilia action and cough. In fact, if the water content of the mucosal surface decreases brings to a clearance decreasing and to mucus adhesion to the epithelial surfaces. A similar undesired result is given by the increasing of secreted glycoproteins, as MUC5AC and MUC5B. When the critical threshold (> 6% of solids) is exceeded, the mucus osmotic pressure overcomes the one of the periciliary layer causing a cilia compression and so a decrease in transport that reflects as a mucus adhesion to the airway surface.

Healthy mucus references are very difficult to obtain because, in absence of trauma or diseases, very little amounts are produced by the lungs. Therefore, studies conducted on healthy subjects show some limitations: necessary dilution of the mucosal material and falsified rheological properties and poor reducibility due to subject-to-subject variability. Hence, the scientific community has progressed over the years in order to develop *in vitro* models that were able to mimic as much as possible the composition and structural properties of the natural mucus to provide robust experimental models.



However, due to its novelty, no mucus models are present for Coronavirus SARS-CoV-2 disease. The project "Mucus4Covid" has caught on this scenario. UniTO and UniPV collaborated with PoliMI to develop, characterize and validate prototypes of three-dimensional systems for the study of viral and bacterial infections and drug permeability.

In doing this analysis, several tests have been conducted. The first part of the work has dealt with optimization of different gels compositions in order to reach the one that better mimics the physiological and the SARS-CoV-2 pathological conditions. During the analysis, it was mandatory to observe some prerequisites. The first one was to obtain a 3D model that had rheological properties similar to the natural human sputum. Changing the concentration of alginate, mucin,  $\text{CaCO}_3$  and GDL it has been possible to vary those properties and study the effect of each element on the overall structure. Then, the gel had to be macroscopically similar to the native one. Therefore, it has been necessary to conduct a macroscopic analysis that results as some prototypes discarding because not complying. The macroscopic analysis has been conducted both when the gel was in the vial after the crosslinking, and when it was deposited on the rheometer plate. The characteristics that were taken into consideration have been if the surface was smooth and homogenous, if the overall compound was viscous enough to maintain its shape when flipped in the vial and the absence of the liquid phase. This was the case of Mu4Covid P 1.0 and Mu4Covid P 2.0 that showed, since the first day of production, coexistence of liquid and gel phase, and for this reason have been eliminated. It was also crucial to study the pH of the developed models because an environment similar to the one of the human bodies had to be set up in order to give the chance to their use in cells experiments. To provide this study, the pH of each 3D model was tested on a pH-meter after the reticulation. The final prerequisite was that the results from the other universities should have been promising too. This means

that the developed 3D model should certainly allow cells viability without impeding it and be performant in cytocompatibility test. Moreover, should shield viral and bacterial infections and allows drugs permeability.

Satisfied the prerequisites, it has been necessary to study the 3D model in terms of production, durability, adaptability and stability. In order to develop a system that was simple to manufacture and easily reproducible it has been conducted an analysis on the materials. Alginate has been selected as the main component together with mucin, main protein of the pulmonary mucus and involved in several physiological processes. For mucus production the method of the double syringe was performed. To develop the mucus model that better fits the native properties, it has been necessary to study separately the two main components: alginate and mucin. It has been discovered that varying the alginate concentration the overall mucus structure changes its properties too. Specifically, increasing the alginate concentration the gel tends to become more viscous reaching higher values of the storage and loss moduli. Moreover, have been conducted studies on blank alginate solution. Doing the frequency sweep tests it has been found that no variations in terms of  $G'$  and  $G''$  appear in the structure for 7 days from its production. In fact,  $G''$  always predominate over  $G'$  and the variations found during the days are not significative. Doing the viscosity test, instead, it has been investigated if there were changings in viscosity in time. No significant variations were discovered in this test too. Those results allow the preparation of the alginate solution in a huge amount in a single day and then use it during the following 4 days without have any change in properties. For a sake of completeness viscosity tests on alginate solution have been conducted also when the polymer is dissolved in TSB and EMEM. Neither in those cases significative differences have been found between the values of viscosity obtained the first and the fourth day of storage. Similarly, it has been investigated the mucin and how its changes affect the

final 3D model. Since the mucin at UniPV and PoliMI were stored differently, it has been necessary to study them separately and compare the results. Two gels have been prepared with the same component concentration, where the only difference was the mucin origin. No significant differences have been found between the two produced gels, so it has been possible to proceed with the studies. Therefore, have been produced gels with different mucin concentrations and have been compared. It has been discovered that no significant differences from the statistical point of view are provided in changing the mucin concentration. Therefore, depending on the study that it's wanted to begin, it is possible to increase or decrease the mucin amount indiscriminately. During the cytocompatibility studies it has been discovered that higher mucin concentrations bring to lower pH and less cells viability. For this reason, as the experiments continued, the mucin concentration was halved. In studying the main components of the system, it was necessary to verify the possibility to include medium in the gel and which was the best composition for this analysis. From the study appears that DMEM:dH<sub>2</sub>O, DMEM with 1% L-glut, 1% PS and 10% FBS, EMEM and TSB can all be used as mediums. This detection allows the use of EMEM and TSB as mediums during the bacterial studies. The study conducted on Mu4Covid 2.0 dissolved in DMEM, EMEM and TSB showed that some rheological differences are detected between the models, showing that the chemical composition of the model influences mechanical properties. Moreover, it has been investigated if the presence of 1:1 DMEM:dH<sub>2</sub>O prejudice the properties of the gel. Two gels were produced with the same compositions but in different medium, and it has been discovered that no changes there were in terms of rheological properties. Proceeding with the experiments and dripping the gel on a petri dish it has been found that there was no significative difference in terms of volume occupied by the drops. In order to avoid

any interference with cells studies, it was preferred to go on with the experiments without distilled water.

To allow the user to dispense the gel in the preferred modality, it has been necessary to study the extrudability of the 3D model. Three different ways of aliquoting have been investigated: using a pipette, a syringe or dripping the gel. Higher was the viscosity of the model, more difficult was its dripping, therefore for the compounds that had alginate concentration equal or higher than 0,6% was necessary to use a spatula and manually break the links. From these studies it has been discovered that macroscopically when dealing with dripped or syringe sample some clots are present. In those two conditions, the thickness of the testing sample increases a lot, and its dispensing appears more difficult for the user. Instead, using a pipette some links are broken during the sucking and pressurization phases so the sample on the rheometer plate appears thinner, homogenous and with a smoother surface. From the rheological point of view significant differences have been discovered between pipetting and dripping and pipetting and syringing but not between syringing and dripping. Higher values in  $G'$  and  $G''$  are reached when the prototypes were dripped or syringe. From these experiments emerged that the way the gel is extruded modifies the properties of the structure. Since no good results in terms of shape have been obtained dripping or syringing the gel, to use a pipette is revealed, for these studies, to be the best dispensing modality. Instead, pick up the sample from the vial using the spatula can be considered as the control.

The storage modalities have been then investigated. It is important to study the shelf-life of the developed 3D model in order to determine how the initial characteristics and performances vary among the conservation time. They have been conducted several studies about the shelf-life to understand which was the best storing modality. It has been discovered that the 3D model can be easily stored in vials and put in the

fridge at 4°C. During this analysis, some of the produced compositions were discarded because they don't comply the rheological requests. For some of them it was indistinguishable the gel-like phase and the liquid-like one. This is the case of Mu4Covid P 2.0 which showed a continuous alternation of storage and loss moduli. Some others, as Mu4Covid 1.0 and Mu4Covid P 2.1, showed too low mechanical characteristics that means  $G'$  and  $G''$  not in the range of physiological (the first) and pathological (the second) values. Finally, some others as Mu4Covid 2.0 and Mu4Covid P 2.2, were discarded because they were characterized by high variability. Those huge oscillations caused the prototype not to always be in the range. During all the shelf-life experiments, it has been found that all the prototypes showed, some first and some later, the presence of liquid and gel phase. In Mu4Covid P 2.0 and Mu4Covid P 1.0 it has been found the coexistence of the two phases since day 0, in Mu4Covid 1.0 since day 3 while for the more lasting, as Mu4Covid P 2.1 or Mu4Covid P 2.2, starting from day 5.

It has also been investigated to freeze the samples for 96 hours at -80°C and defrost them. From the obtained results it has been showed that for a defrosting modality that consists of 1 hour at -20°C and then 3 hours at 4°C, the freezing brought to  $G'$  values similar to the one found in the control, while  $G''$  values are much higher. This behaviour is due to the increasing in liquid-like phase that racks up during the freezing and consequent defrosting.

It has been showed that the implemented 3D model, is able to adapt itself to transwells of different sizes. During this thesis work, they have been used 6 and 24 transwells support. No differences have been found in terms of adaptability to the walls of the wells and permeability of the membrane between the two sizes. This result allowed the use of those prototypes for the stability test at 37°C. It has been discovered that the prototypes are stable when placed at 37°C in an oven for several days. After putting in

contact the mucus and the medium, every 24 hours the wells are lifted, lay 10 seconds on a clean napkin in order to dry the medium excess and weighted. To avoid any bacterial infection, after each weight analysis some grains of sodium azide were added to the water present in the empty wells of the multiwell. After collecting the data, they have been analyzed on Excel the average weight and its percentage and the standard deviation and its percentage. From the conducted studies it emerged that different mucus compositions behaves similarly: instantaneous increasing in mass variation [%] followed by its decreasing in time. Nevertheless, those increases and decreases aren't significative because never beyond  $\pm 7\%$ . Therefore, the mucus 3D models can be considered stable in medium at 37°C. During the studies of drug permeability, PAMPA membranes have been used. This implies that the 3D model is stable even using those kinds of membranes.

The cytocompatibility, viral activity, bacterial infections and drugs permeability studies conducted on Mu4Covid 2.0 at UniTO and UniPV have showed interesting results. Cytocompatibility tests quantified using Trypan blue coloration on VERO-E6 cellular line showed values of cell viability around 80%. This means that the produced model isn't toxic for the cells and promote their proliferation. In studying the viral activity with HCoV-OC43 on three different cellular lines of HCT8, it emerged that except for the concentration  $10^1$  no differences were revealed respect the control given by cells in mucus absence. Instead, when using SARS-Cov2, only without Mu4Covid 2.0 it's possible to observe the cytopathic effect while with the mucus barrier cells were compromised during the coloration. Evaluating the mucus permeability to antiviral drugs, it emerged that depending on drugs structure, different permeabilities have been obtained. Finally, an important limit overcame by this study is the production of a mucus model containing *Staphylococcus Aureus* secretome and placed in contact with

the virus. Those analysis showed that incorporating the bacterial secretome in the medium and then place virus on it doesn't affect significantly cells viability.

In healthy conditions airway mucus plays a fundamental role in protection of the lining epithelium against unsafe particles and chemicals that may enter during inhalation as air pollutants and cigarette smoke. Several experiments have been conducted on healthy mucus airway such as fluorescence microscopy analysis, which provide information on the mucus material, and porosity tests. In this contest also viscosity plays a key role: mucus is characterized by nonlinear and time-dependent viscoelastic behavior that is directly involved in mucus transport capacity. Therefore, several studies have been conducted in order to identify  $G'$  and  $G''$  of native healthy mucus and their dependence on strain and frequency. Performing tests at small strain magnitudes (0.02–10% strain) at physiological frequency, it was determined the strain at which the viscoelastic moduli deviate by more than 10% from the plateau value and so define the LVR. It has also been revealed that physiological ranges are  $14,9 \pm 9,2$  for  $G'$  and  $4,3 \pm 2,7$  for  $G''$  in a frequency domain between 0.2-1 Hz. Other important studied aspect are adhesiveness and wettability, and how they contribute to mucus properties. However, mucus changes are very common worldwide and are one of the main causes of early death. In case of structural modifications of mucus barrier some dangerous pathological conditions may arise such as CF, acute viral and bacterial infections such as primary ciliary dyskinesia, non-cystic fibrosis bronchiectasis and pan-bronchiolitis, common lung diseases such as asthma and COPD. All those conditions have in common reduction of mucociliary clearance and the increasing in mucus secretion, therefore also elevated morbidity and mortality rates. Generally, the amount of serum proteins, mostly MUC5AC and MUC5B expression, gets increased in pathological conditions resulting as a mucus adhesion to epithelium layer and duct obstructions. Currently, the main interest is given to respiratory disease caused by

novel coronavirus SARS-CoV-2 which, on March 11 2020, caused the declaration of pandemic state by WHO. Coronavirus infections were already studied worldwide since 1960s, but this infection stands out for its aggressivity and velocity in spreading. Disease severity increases with age and in case of other risk factors as diabetes, obesity, arterial hypertension, immunodeficiency and allergic, COPD or asthmatic history. To face this pathological condition, it has been showed MUC1 and MUC5AC increased levels in trachea sputum, hence in the whole airway tract MUC5AC, MUC1, and MUC1-CT are evaluated higher than the control. Hence it's evident a similarity in disease progression of SARS-CoV-2 with typical mucus hypersecretory diseases such as asthma, CF and COPD.

The prototype that has been chosen to mimic the healthy mucus is Mu4Covid 2.1 whose composition is: alginate 0,6%, mucin 2,5%, CaCO<sub>3</sub> 0,13% and GDL 1%. The macroscopic analysis conducted on the 3D model both when it is stored in the vial and on the rheometer plate shows great results. Waited the time for the crosslinking, the sample appears viscous enough to maintain its shape when the vial is inclined or upside down. Analysing the pH of the compound it is showed to be 5.84. Analyzing the dispensing modality it has been discovered that when pipetted, the gel appears with a smooth, compact and homogenous surface and is very easy to dispense. Instead, when dripped or syringe the gel is much thicker and has not homogenous surface. Therefore, it is recommended to the user to use a pipette for its dispensing in order to avoid the presence of any clots that can lead to rheological variability and surface discontinuity.

Analysing the storage modality, when the prototype is stored at 4°C, good values of shelf-life are detected. No statistical differences are noticed during the days until 7 days from its production in terms of  $G'$  and  $G''$ . Moreover, each day is characterized by very low variability, another sign of stability in time. However, after 5 days of



storage starts the coexistence of liquid and gel phases. One vial has been stored for 30 days in order to evaluate the properties of the mucus model after all this time. Before providing any test, the sample has been evaluated macroscopically: the appearance of the double phase is particularly evident both when the mucus is stored in the vial and when deposited on the rheometer plate resulting as a halo around the testing material. In terms of mechanical properties, have been found significative differences between the values of  $G'$  and  $G''$  detected at  $t = 0$  or  $t = 7$  and  $t = 30$ , sign of not stability.

Finally, the stability test has been provided. The mucus model was left reticulating in 24 transwell support and  $t = 0, 24, 48, 72, 96, 168$  hours have been selected as timepoints for the study. No significative variations have been found during the days in terms of mass variation [%]: its increasing and decreasing were always below 7%.

Instead, the prototype that has been chosen to mimic the Coronavirus SARS-CoV-2 pathological mucus condition is Mu4Covid P 2.3 whose composition is: alginate 0,7%, mucin 2,5%,  $\text{CaCO}_3$  0,13% and GDL 1%. The macroscopic analysis conducted on the 3D model when stored in the vial and on the rheometer plate shows remarkable results. The sample appears viscous enough to maintain its shape when the vial is inclined or upside down. Looking to its behaviour on the rheometer plate, it's able to maintain the shape avoiding the presence of a less viscous edge or of clots. Analyzing the pH of the prototype, it is showed to be 5.74. As before, from the extrusion tests it emerged that the best dispensing modality is by a pipette otherwise clots and discontinuities may be present. For this formulation, since the alginate amount is increased and the whole compound is shown more viscous, when dispensed by syringing or dripping, clots and extremely thick portions were particularly evident.

It has also been evaluated how the produced mucus adapts itself to the surface. Mu4Covid P 2.3 has been withdrawn using a pipette and deposited in different amounts on a petri dish. Using the software ImageJ it has been possible to calculate

the maximum height and the diameter of each drop and, through Excel, calculate the mean and the standard deviation. Thanks to this analysis it is possible to know how different amounts of mucus expand themselves on a flat surface. Moreover, during the test for proving the multiwells adaptability, 6 and 24 well plates have been filled of a known amount of mucus (respectively 1ml and 0,3ml) in order to fully cover the well surface. In this way, known the volume that it's wanted to fill, it is possible to obtain the amount of prototype that is necessary for the purpose.

Three different storage modalities have been investigated. When the prototype is stored at 4°C, good values of shelf-life are detected. The showed values of  $G'$  and  $G''$  are coherent with the ones typical of SARS-CoV-2 pathological condition. It's showed that the prototype preserves its rheological properties until 7 days from its production and is characterized by low standard deviation intrasample. However, after 5 days of storage starts the coexistence of liquid and gel phases. Moreover, also the freezing has been investigated as storage modality. Samples are left 96 hours at -80°C, then moved at -20°C for 20 minutes and left overnight at 4°C in order to provide a very smooth defrost. When the rheological properties have been evaluated it was appreciable that even if the values of the storage modulus were consistent with the ones found before the freezing, it wasn't the same for the ones of the loss modulus. In fact, much higher values were detected after freezing, sign of an increasing in the aqueous phase that wasn't reabsorbed by the sample. This result is also validated by the taken photos on the rheometer plate. It has also been investigated the storage leaving the samples at  $T_{amb}$  (22°C) in a room under controlled conditions. The most notable result is given by the presence of the double phase since the first day of storage. Even if high values of storage and loss moduli were detected, the data were characterized by an increasing in time and elevate variability up to over 70% more respect the values obtained at  $t=0$ , not proving to be a good substitute to the storage modality at 4°C.

Finally, the stability test has been provided. The mucus model was left reticulating in 24 transwell support and  $t = 0, 3, 24, 48, 72$  hours have been selected as timepoints for the study. No significative variations have been found during the days in terms of mass variation [%]: its increasing and decreasing were always below 7%.

It was also investigated if bacteria medium could be included in the medium. Therefore, it has been tested TSB containing *S. aureus* secretome grown in stationary phase 0.5 and grown in exponential phase 1.7, and EMEM containing VERO-E6 secretome 0.5 and 1.11. All the tested mediums showed to be suitable for alginate and mucin dissolution allowing the realization of Mu4Covid P 2.3 prototype. Experiments conducted on storage and stability for all the tested mediums showed stability in time in terms of maintenance of the rheological properties for at least 5 days but has to be considered the arising of the double phase after 4-5 days. Moreover, stability tests at 37°C display good outcomes about mass conservation in time. Making a comparison between blank TSB and TSB containing *S. aureus* secretome 0.5 and 1.7, it results evident the effect of the secretome on the overall compound: the secreted components bring to higher values of storage and loss moduli. Equal result was obtained comparing blank EMEM and EMEM containing VERO-E6 secretome 0.5 and 1.11.

## 6. CONCLUSION

In healthy conditions, mucus layer acts as a barrier for pathogens and unwanted substances, but sometimes this shield can be not enough, and viral or bacterial infections may arise. During the last years, due to the pandemic state, major interest is given to SARS-CoV-2 infection, but however mucus models able to mimic this disease aren't on the market yet. Mucus role is fundamental for the progress of this pathology: mucins overproduction causes networks entanglement that results as a steep and abnormal increasing in rheological properties. Instead, pH and mucociliary clearance decrease, leading to severe duct obstruction.

From the conducted studies, it has been revealed that prototypes composed by high amounts of mucin lead to an undesired reduction in cell viability and pH value. Therefore, it is essential to balance the amount of mucin in order to allow laboratory experiments with cells. Since it was mandatory to introduce limitations on mucin percentage, it was deeply studied the contribution of alginate in the developed model. It results that the alginate amount has a direct impact on models rheological properties. In fact, increasing the alginate percentage also the mechanical properties enhance. Therefore, it has been discovered that raising alginate concentration works well to mimic the viscosity and the network entanglement typical of SARS-CoV-2 pathological condition. During this analysis it was also found that alginate solution was able to preserve its characteristics in terms of viscosity and mechanical properties for several days after its production. Mucin instead, being a protein component susceptible to time and storage condition, but also the main determinant of pH value, should be prepared at the moment.

Another remarkable obtained result is that different mediums can be included in the prototype, but it has to be considered that when medium changes, and so chemical composition varies, some variations are appreciated also in the rheological properties of the produced gels. However, considering the mediums available for this study, those deviations can be considered not relevant.

Several prototypes have been developed and tested and two mucus models were selected as golden standard for the purpose: Mu4Covid 2.1, that mimics the healthy condition, and Mu4Covid P 2.3 that stands for the SARS-CoV-2 pathological disease. Both models showed to be stable in the tested mediums, allowing their use in biological experiments, and are characterized by coherent pH values respect the ones found in human airways mucus. The major importance is given to mechanical properties, which perfectly match the ranges found in human sputum studies. If correctly stored, mucus prototypes preserve their mechanical properties for 5 consecutive days after production, spent this time macroscopic changes arise. Investigations on stability conducted at 37°C were also extremely satisfying and give a chance to their use in cellular experiments. Finally, it has been appreciated that the developed models are easy to dispense and are able to adapt themselves to transwells and multiwells of different nature and sizes.

Biological studies conducted in Pavia and Torino prove elevated viability when cells are placed in contact with the developed mucus model, both in presence and absence of *S. aureus* secretome. Moreover, drug permeability tests open to different scenarios depending on the drugs structure, making the prototype effective also for those kinds of studies. Even if those experiments were conducted on intermediate mucus compositions, there are promising signs also with the final models.

Tests conducted in bacterial medium also showed meaningful results. Mediums containing *S. aureus* secretome can be adopted during the develop of the pathological

mucus model. In fact, components dissolution seems unchanged, but storage and stability tests showed encouraging outcomes. In doing rheological tests, it was also evident a steep increasing in mechanical properties of the prototypes in which bacterial secretome was included. This is sign that bacteria secreted components have consequences on mucus viscosity and network entanglement.

The main limitation encountered in this project is due to the currently commercially available mucins, such as porcine gastric mucin and bovine submaxillary mucin that, when combined with cross-linking agents, can't satisfy physiological pH and natural mucin concentrations. This drawback, encountered in several more studies, is presumably a result of the mucin processing [96], [97].

# Bibliography

- [1] Mucus: The Body's Unsung Hero The slimy stuff has a surprisingly wide array of beneficial biological functions By Diana Kwon, Knowable Magazine on June 28, 2019
- [2] Neutra M, Forstner J. Gastrointestinal mucus: synthesis, secretion, and function. In: Johnson L, editor. *Physiology of the gastrointestinal tract*, 2nd edn. New York, NY: Raven Press; 1987. Chapter 34.
- [3] Bansil R and Turner B. S. 2018 The biology of mucus: Composition, synthesis and organization *Adv. Drug Delivery*
- [4] R. Bansil, B.S. Turner, Mucin structure, aggregation, physiological functions and biomedical applications, *Curr. Opin. Colloid Interface Sci.* 11 (2006) 164–170.
- [5] Airway Mucus: Its Components and Function Erik P. Lillehoj and K. Chul Kim
- [6] [37] Models using native tracheobronchial mucus in the context of pulmonary drug delivery research: Composition, structure and barrier properties Author links open overlay panel Benedikt C. Huckab Xabier Murgiac Sarah Frischab Marius Hittingerd Alberto Hidalgo Brigitta Loretza Claus-Michael Lehr
- [7] The Role of Airway Mucus in Pulmonary Toxicology James M. Samet and Pi-Wan Cheng
- [8] Physiology of airway mucus clearance. Bruce K Rubin
- [9] Reduced mucociliary clearance in old mice is associated with a decrease in Muc5b mucin Barbara R. Grubb, Alessandra Livraghi-Butrico, Troy D. Rogers, Weining Yin, Brian Button
- [10] Nadel JA, Davis B, Phipps RJ. Control of airway secretion and ion transport in the airways.

- [11] Effective Mucus Clearance Is Essential for Respiratory Health Scott H. Randell, Richard C. Boucher
- [12] Airway mucus, inflammation and remodeling: emerging links in the pathogenesis of chronic lung diseases Zhe Zhou-Suckow, Julia Duerr, Matthias Hagner, Raman Agrawal & Marcus A. Mall
- [13] Lucas AM, Douglas LC. Principles underlying ciliary activity in the respiratory tract II. A comparison of nasal clearance in man, monkey and other mammals.
- [14] The Propulsion of Mucus by Cilia Michael A. Sleight, John R. Blake, and Nadav Liron
- [15] Sheehan JK, Thornton DJ, Somerville M, Carlstedt, I. Mucin structure. The structure and heterogeneity of mucin glycoproteins. (1991)
- [16] The particle in the spider's web: transport through biological hydrogels Jacob Witten and Katharina Ribbeck
- [17] X Murgia, B Loretz, O Hartwig, M Hittinger, C M Lehr 2017 The role of mucus on drug transport and its potential to affect therapeutic outcomes, *Advanced Drug Delivery Reviews*
- [18] Airway Mucus From Production to Secretion Olatunji W. Williams, Amir Sharafkhaneh, Victor Kim, Burton F. Dickey, and Christopher M. Evans
- [19] Joseph Z. Zaretsky and Daniel H. Wreschner 2018 Secreted and Membrane-Bound Mucins: Similarities and Differences
- [20] Airway Mucus Function and Dysfunction John V. Fahy, M.D., and Burton F. Dickey, M.D.
- [21] Airway Mucus and Asthma: The Role of MUC5AC and MUC5B Luke R. Bonser and David J. Erle



- [22] The Potential Role and Regulatory Mechanisms of MUC5AC in Chronic Obstructive Pulmonary Disease Jingyuan Li and Zuguang Ye
- [23] Mucins and their receptors in chronic lung disease Emma Denny, Jagdeep Sahota, Richard Beatson, David Thornton, Joy Burchell, Joanna Porter
- [24] [62] Defensive Properties of Mucin Glycoproteins during Respiratory Infections—Relevance for SARS-CoV-2 Authors: Maitrayee Chatterjee, Jos P. M. van Putten
- [25] Airway mucus: The good, the bad, the sticky Author links open overlay panel Christopher M. Evans and Ja Seok Koo
- [26] [3] The biology of mucus: Composition, synthesis and organization Author links open overlay Rama Bansila Bradley S. Turner
- [27] Visualization of the structure of native human pulmonary mucus Author links open overlay panel E. Meziab M. Kocha J. Fleddermann K. Schwarzkopf M. Schneiderb A. Kraegeloh
- [28] Models to evaluate the barrier properties of mucus during drug diffusion Author links open overlay panel Liu Liu Chunling Tiana Baoqi Donga Mengqiu Xia Ye Caia Rongfeng Hu Xiaoqin Chu
- [29] Role of the physicochemical properties of mucus in the protection of the respiratory epithelium S. Girod, J-M. Zahm, C. Plotkowski, G. Beck, E. Puchelle
- [30] Surface rheological properties alter aerosol formation from mucus mimetic surfaces Rania Hamed, Daniel M. Schenck and Jennifer Fiegel
- [31] Macro- and Microrheological Properties of Mucus Surrogates in Comparison to Native Intestinal and Pulmonary Mucus Benedikt C. Huck, Olga Hartwig, Alexander Biehl, Konrad Schwarzkopf, Christian Wagner, Brigitta Loretz, Xabier Murgia, and Claus-Michael Lehr

[32] A Rheological Evaluation of Various Mucus Gels for Use in In-vitro Mucoadhesion Testing F. Madsen, K. Eberth and D. Smart

[33] Effect of phospholipid mixtures and surfactant formulations on rheology of polymeric gels, simulating mucus, at shear rates experienced in the tracheobronchial tree Author links open overlay panel R. Banerje Jayesh R. Bellar R.R. Puniyani

[34] Mucociliary interactions and mucus dynamics in ciliated human bronchial epithelial cell cultures Patrick R. Sears, C. William Davis, Michael Chua, and John K. Sheehan

[35] Development of a functional airway-on-a-chip by 3D cell printing Ju Young Park, Hyunryul Ryu, Byungjun Lee, Dong-Heon Ha, Minjun Ahn, Suryong Kim, Jae Yun Kim, Noo Li Jeon and Dong-Woo Cho

[36] Endotracheal tube mucus as a source of airway mucus for rheological study X Matthew R. Markovetz, Durai B. Subramani, William J. Kissner, Cameron B. Morrison, Ian C. Garbarine, Andrew Ghio, Kathryn A. Ramsey, Harendra Arora, Priya Kumar, David B. Nix, Tadahiro Kumagai, Thomas M. Krunkosky, Duncan C. Krause, Giorgia Radicioni, Neil E. Alexis, Mehmet Kesimer, Michael Tiemeyer, Richard C. Boucher, Camille Ehre, and David B. Hill<sup>1</sup>

[37] Models using native tracheobronchial mucus in the context of pulmonary drug delivery research: Composition, structure and barrier properties Benedikt C. Huck, Xabier Murgia, Sarah Frisch, Marius Hittinger, Alberto Hidalgo, Brigitta Loretz, Claus-Michael Lehr

[38] Membrane-bound mucins: the mechanistic basis for alterations in the growth and survival of cancer cells S Bafna, S Kaur & S K Batra

[39] X. Cao, R. Bansil, K.R. Bhaskar, B.S. Turner, J.T. LaMont, N. Niu, N.H. Afdhal  
pH-Dependent Conformational Change of Gastric Mucin Leads to Sol-Gel Transition

[40] Acidic Submucosal Gland pH and Elevated Protein Concentration Produce Abnormal Cystic Fibrosis Mucus Author links open overlay panel Yuliang Xie, Lin Lu, Xiao Xiao Tang, Thomas O. Moninger, Tony Jun Huang, David A. Stoltz, Michael J. Welsh

[41] Asthma Christopher H. Fanta, M.D

[42] T-helper Type 2-driven Inflammation Defines Major Subphenotypes of Asthma Prescott G. Woodruff, Barmak Modrek, David F. Choy, Guiquan Jia, Alexander R. Abbas, Almut Ellwanger, Joseph R. Arron, Laura L. Koth, and John V. Fahy

[43] Takeyama K., Fahy J.V., Nadel J.A. Relationship of epidermal growth factor receptors to goblet cell production in human bronchi.

[44] Ex Vivo Sputum Analysis Reveals Impairment of Protease-dependent Mucus Degradation by Plasma Proteins in Acute Asthma, Anh L. Innes, Stephen D. Carrington, David J. Thornton, Sara Kirkham<sup>4</sup>, Karine Rousseau, Ryan H. Dougherty, Wilfred W. Raymond, George H. Caughey, Susan J. Muller, and John V. Fahy

[45] Management Of Pulmonary Disease In Patients With Cystic Fibrosis Bonnie W. Ramsey, M.D

[46] Patient-reported respiratory symptoms in cystic fibrosis C. H. Gossa T. C. Edwards B. W. Ramsey<sup>d</sup> M. L. Aitken<sup>a</sup> D. L. Patrick<sup>b</sup>

[47] Cystic fibrosis airway secretions exhibit mucin hyperconcentration and increased osmotic pressure Ashley G Henderson, Camille Ehre, Brian Button, Lubna H Abdullah, Li-Heng Cai, Margaret W Leigh, Genevieve C DeMaria, Hiro Matsui, Scott H Donaldson, C William Davis, John K Sheehan, Richard C Boucher, Mehmet Kesimer

[48] Roles of mucus adhesion and cohesion in cough clearance Brian Button, Henry P. Goodell, Eyad Atieh , Yu-Cheng Chen, Robert Williams, Siddharth Shenoy, Elijah

Lackey, Nathan T. Shenkute, Li-Heng Caid, Robert G. Dennisc, Richard C. Boucher, and Michael Rubinstein

[49] Expression of MUC5AC and MUC5B mucins in normal and cystic fibrosis lung D. A. Groneberg, P.R. Eynott, T. Oates, S. Lim, R. Wu, I. Carlstedt, A. G. Nicholson And K. F. Chung

[50] Molecular dynamics simulations to explore the structure and rheological properties of normal and hyperconcentrated airway mucus Andrew G. Ford Xue-Zheng Cao Micah J. Papanikolas Takafumi Kato Richard C. Boucher Matthew R. Markovetz David B. Hill, Ronit Freeman Mark Gregory Forest

[51] Micro- and macrorheology of mucus Author links open overlay panel Samuel K. Laia Ying-Ying Wang Denis Wirtz Justin Hanes

[52] World Health Organization. 2008–2013 Action Plan for the Global Strategy for the Prevention and Control of Noncommunicable Diseases. 2008.

[53] Beasley R, Weatherall M, Travers J, et al. Time to define the disorders of the syndrome of COPD. *Lancet* 2009

[54] Revisited role for mucus hypersecretion in the pathogenesis of COPD I. Cerveri and V. Brusasco

[55] Global Strategy for the Diagnosis, Management and Prevention of COPD. Global Initiative for Chronic Obstructive Lung Disease. July 2, 2009.

[56] Mucus pathophysiology in COPD: differences to asthma, and pharmacotherapy. Rogers DF

[57] Venkatakrisnan, V.; Thaysen-Andersen, M.; Chen, S.C.; Nevalainen, H.; Packer, N.H. Cystic fibrosis and bacterial colonization define the sputum N-glycosylation phenotype.

- [58] A machine learning model to identify early-stage symptoms of SARS-Cov-2 infected patients Author links open overlay panelMd. Martuza Ahamada Sakifa Aktara Md. Rashed-Alahfuzb Shahadat Uddinc Pietro Liòd Haoming Xuef Matthew A.Summersgh Julian M.W. Quinngi Mohammad Ali Monigj
- [59] Organization WH. Coronavirus disease 2019 (COVID-19): situation report-63. (2020)
- [60] Pathogenesis of COVID-19 from a cell biologic perspective Robert J. Mason
- [61] 4. Cone RA. 2009. Barrier properties of mucus.
- [62] M. Chatterjee, J. P. M. Van Putten, and K. Strijbisa, "Defensive Properties of Mucin Glycoproteins during Respiratory Infections — Relevance for SARS-CoV-2," vol. 11, 2020
- [63] Risk factors for severe and critically ill COVID-19 patients: A Review Ya-dong Gao, Mei Ding, Xiang Dong, Jin-jin Zhang, Ahmet Kursat Azkur, Dilek Azkur, Hui Gan, Yuan-li Sun, Wei Fu, Wei Li, Hui-ling Liang, Yi-yuan Cao, Qi Yan, Can Cao, Hong-yu Gao, Marie-Charlotte Brüggén, Willem van de Veen, Milena Sokolowska, Mübeccel Akdis, Cezmi A. Akdis
- [64] Alveolar macrophage dysfunction and cytokine storm in the pathogenesis of two severe COVID-19 patients Chaofu Wang, Jing Xie, Lei Zhao, Xiaochun Fei, Heng Zhang, Yun Tan, Xiu Nied, Luting Zhoua, Zhenhua Liue, Yong Ren, Ling Yuan, Yu Zhang, Jinsheng Zhan, Liwei Lian, Xinwei Chen, Xin Liu, Peng Wan, Xiao Han, Xiangqin Weng, Ying Cheng, Ting Yuh, Xinxin Zhang, Jun Cai, Rong Chenh, Zhengli Shig, Xiuwu Bian
- [65] Influence of SARS-CoV-2 on airway mucus production: A review and proposed model David K. Meyerholz, Leah R. Reznikov

[66] Effects of the Lower Airway Secretions on Airway Opening Pressures and Suction Pressures in Critically Ill COVID-19 Patients: A Computational Simulation Zhenglong Chen, Ming Zhong, Li Jiang, Nanshan Chen, Shengjin Tu, Yuan Wei, Ling Sang, Xia Zheng, Chunyuan Zhang, Jiale Tao, Linhong Deng & Yuanlin Song

[67] M. Bose, B. Mitra, P. Mukherjee, Mucin signature as a potential tool to predict susceptibility to COVID-19, *Physiol. Rep.* 9 (2021)

[68] Mucus targeting as a plausible approach to improve lung function in COVID-19 patients Author links open overlay panel Sarath S. Kumar<sup>1</sup> Aiswarya Binu<sup>1</sup> Aswathy. R. Devan<sup>1</sup> Lekshmi. R. Nath

[69] Biochemical and Biophysical Characterization of Respiratory Secretions in Severe SARS-CoV-2 (COVID-19) Infections Michael J. Kratochvil, Gernot Kaber, Pamela C. Cai, Elizabeth B. Burgener, Graham L. Barlow, Mark R. Nicolls, Michael G. Ozawa, Donald P. Regula, Ana E. Pacheco-Navarro, Carlos E. Milla, Nadine Nagy, Samuel Yang , Stanford COVID-19 Biobank Study Group, Angela J. Rogers, Andrew J. Spakowitz, Sarah C. Heilshorn and Paul L. Bollyky

[70] Significance of super spreader events in COVID-19 Sanjiv Kumar, Shreya Jha, Sanjay Kumar Rai

[71] Manfred Kansy, Frank Senner, and Klaus Gubernator, Physicochemical high throughput screening: Parallel Artificial Membrane Permeation Assay in the description of passive absorption processes

[71] Manfred Kansy, Frank Senner, and Klaus Gubernator, Physicochemical high throughput screening: Parallel Artificial Membrane Permeation Assay in the description of passive absorption processes

- [71] Evolutionary conservation of the antimicrobial function of mucus: a first defence against infection Cassie R Bakshani, Ana L Morales-Garcia, Mike Althaus, Matthew D Wilcox, Jeffrey P Pearson, John C Bythell & J Grant Burgess
- [72] Modulation of immune responses by commensal bacteria and intestinal helminth Herbst. Tina 2011
- [73] Ganz, T. 2002. Antimicrobial polypeptides in host defense of the respiratory tract. J. Clin.
- [74] Predisposing conditions to bacterial infections in chronic obstructive pulmonary disease. H M Jansen, A P Sachs, and L van Alphen
- [75] Bacterial Infection and the Pathogenesis of COPD Sanjay Sethi, MD
- [76] Combatting antibiotic-resistant bacteria using nanomaterials Akash Gupta, Shazia Mumtaz, Cheng-Hsuan Li, Irshad Hussain and Vincent M. Rotello
- [77] Evolutionary conservation of the antimicrobial function of mucus: a first defence against infection Cassie R Bakshani, Ana L Morales-Garcia, Mike Althaus, Matthew D Wilcox, Jeffrey P Pearson, John C Bythell & J Grant Burgess
- [78] Repairing The Broken Market For Antibiotic Innovation Kevin Outterson, John H. Powers, Gregory W. Daniel, and Mark B. McClellan
- [79] Reduced Three-Dimensional Motility in Dehydrated Airway Mucus Prevents Neutrophil Capture and Killing Bacteria on Airway Epithelial Surfaces Hirotohi Matsui, Margrith W. Verghese, Mehmet Kesimer, E. Schwab, Scott H. Randell, John K. Sheehan, Barbara R. Grubb, and Richard C. Boucher
- [80] Covid-19 induced superimposed bacterial infection Mohamed A. Hendaus & Fatima A. Jomha

- [81] Signatures of COVID-19 Severity and Immune Response in the Respiratory Tract Microbiome Carter Merenstein, Guanxiang Liang, Samantha A. Whiteside, Ana G. Cobián-Güemes, Madeline S. Merlino, Louis J. Taylor, Abigail Glascock.
- [82] D. lowy F and M.D. 1998 Staphylococcus aureus Infections N. Engl. J. Med. 339 520-32
- [83] The Staphylococcus aureus “superbug” Timothy J. Foster
- [84] Tong S Y C, Davis J S, Eichenberger E, Holland T L and Fowler V G 2015 Staphylococcus aureus infections: Epidemiology, pathophysiology, clinical manifestations, and management Clin. Microbiol. Rev. **28** 603–61
- [85] Goss C H and Muhlebach M S 2011 Review: Staphylococcus aureus and MRSA in cystic fibrosis J. Cyst. Fibros. 10 298–306
- [86] Localization of Staphylococcus aureus in Infected Airways of Patients with Cystic Fibrosis and in a Cell Culture Model of S. aureus Adherence Martina Ulrich, Silvia Herbert, Jürgen Berger, Gabriel Bellon, Dominique Louis, Gerd Münker, and Gerd Döring
- [87] Staphylococcus aureus biofilm: a complex developmental Organism Derek E. Moormeier and Kenneth W. Bayles Center for Staphylococcal Research, Department of Pathology & Microbiology, University of Nebraska Medical Center, Omaha, NE, USA.
- [88] von Eiff C 2008 Staphylococcus aureus small colony variants: a challenge to microbiologists and clinicians Int. J. Antimicrob. Agents **31** 507–10.
- [89] Approaches to the study of the cell secretome Yetrib Hathout
- [90] Secrets of the secretome in Staphylococcus aureus Author links open overlay panel Harald Kusch Susanne Engelmann



[91] Experimental models to study intestinal microbes-mucus interactions in health and disease Lucie Etienne-Mesmin, Benoit Chassaing, Mickaël Desvaux, Kim De Paepe, Raphaële Gresse, Thomas Sauvaitre, Evelyne Forano, Tom Van de Wiele, Stephanie Schüller, Nathalie Juge and Stéphanie Blanquet-Diot

[92] From tissue engineering to engineering tissues: the role and application of in vitro models Daniela Peneda Pacheco, Natalia Suárez Vargas, Sonja Visentin and Paola Petrini

[93] Development of a Primary Human Co-Culture Model of Inflamed Airway Mucosa Lael M. Yonker, Hongmei Mou, Kengyeh K. Chu, Michael A. Pazos, Huimin Leung, Dongyao Cui, Jinhyeob Ryu, Rhianna M. Hibbler, Alexander D. Eaton, Tim N. Ford, J. R. Falck, T. Bernard Kinane, Guillermo J. Tearney, Jayaraj Rajagopal & Bryan P. Hurley

[94] Kim HJ & Ingber DE (2013) Gut-on-a-Chip microenvironment induces human intestinal cells to undergo villus differentiation. *Integrative biology: quantitative biosciences from nano to macro*.

[95] Modeling Airway Dysfunction in Asthma Using Synthetic Mucus Biomaterials Daniel Song, Ethan Iverson, Logan Kaler, Shahed Bader, Margaret A. Scull, and Gregg A. Duncan

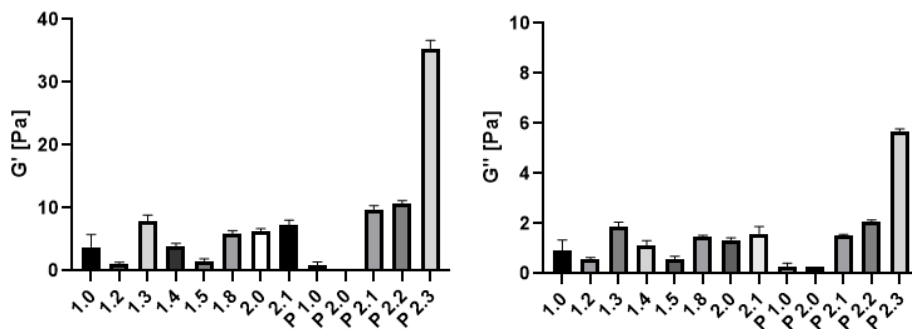
[96] A rational approach to form disulfide linked mucin hydrogels Katherine Joyner, Daniel Song, Robert F. Hawkins a, Richard D. Silcott a and Gregg A. Duncan Fischell Department of Bioengineering, University of Maryland, College Park, MD 20742, USA. Biophysics Program, University of Maryland, College Park, MD 20742, USA.

[97] Mucin Biopolymers and Their Barrier Function at Airway Surfaces Daniel Song, Devorah Cahn, and Gregg A. Duncan.

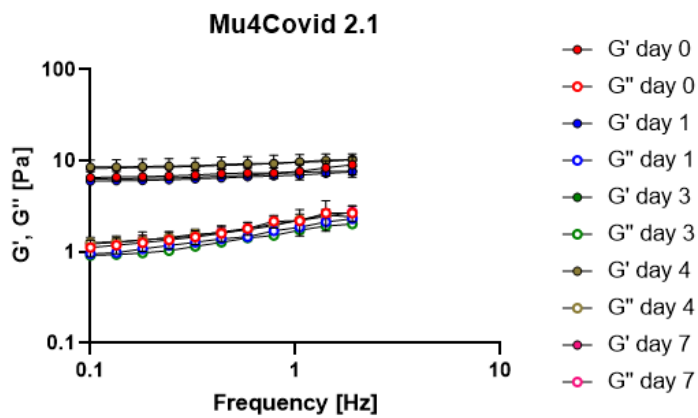


# A. Appendix A

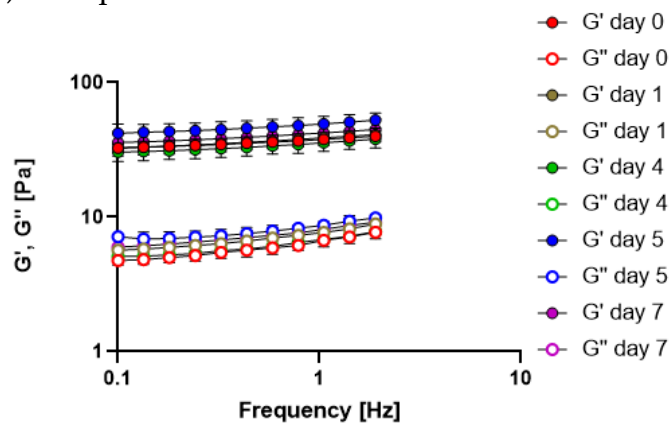
(1) Graphical behaviour at t=0 for each studied composition at  $G'(0,44\text{Hz})$  and  $G''(0,44\text{Hz})$



(3) Complete behaviour of Mu4Covid 2.1 during the shelf-life assessment



(4) Complete behaviour of Mu4Covid P 2.3 during the shelf-life assessment



## B. Appendix B

### HYDROGEL MU4COVID

#### **Considerazioni generali sul metodo della doppia siringa**

Nel protocollo si specifica di utilizzare il metodo della doppia siringa. Per mantenere la sterilità: si apre la siringa dalla busta sterile, si toglie il pistone e lo si appoggia in piedi dal lato dello stantuffo sotto la cappa, si chiude la siringa con un tappo per siringa, la si gira, in modo che l'apertura da dove entra il pistone sia rivolta verso l'alto e il tappo sia a contatto con il piano di lavoro della cappa. Successivamente si versa la soluzione da usare all'interno del foro da cui solitamente entra il pistone. Una volta che il fluido è colato in fondo, si inserisce il pistone e si spinge lentamente fino a sentire un "click". Al fine di non creare bolle, la siringa va girata molto lentamente (in modo che il tappo sia in alto e il pistone in basso) di modo che la soluzione possa bagnare uniformemente le pareti interne della siringa, fino a colare interamente verso il pistone. Si stappa la siringa con delicatezza (se lo si fa troppo velocemente il tappo può schizzare via) e si fa salire il pistone lentamente. Qualora durante questo procedimento ci si accorgesse della presenza di bolle bisogna provvedere alla loro eliminazione: muovere il pistone per posizionare la soluzione a metà della siringa, con una mano impugnare la siringa saldamente, con l'altra dare delle schicchere (il medio si comprime sul pollice e si rilascia il medio fino a farlo sbattere contro la siringa). A

questo punto si spinge il pistone verso l'alto finché la soluzione non raggiunge l'orlo dell'ugello della siringa.

Per il metodo della doppia siringa si prendono due siringhe (trattate come di cui sopra) con all'interno le due soluzioni che si vogliono miscelare: si avvita un connettore a una siringa e si procede a far salire la soluzione fino a 2/3 dell'altezza del connettore. Si aggancia quindi l'estremo libero del connettore all'ugello dell'altra siringa e si avvita. Si procede così alla miscela delle soluzioni premendo in modo alternato i pistoni delle due siringhe per un totale di 25 volte.

## Giorno 1

### **Preparare le soluzioni**

- Preparare sterilmente\*\* soluzione 4,2% di alginato (n.b. se X è la concentrazione finale desiderata nel gel, la soluzione da preparare il giorno prima deve essere 7X, nel nostro caso X=0.6%). Versare l'alginato poco alla volta, se occorre alzare gli rpm per pochi secondi in modo da far scendere eventuali accumuli di polimero, poi abbassare i giri. Lasciare agitare a circa 300 rpm o.n.
- Preparare sterilmente\*\* una soluzione di mucina al'8.8% (nel gel la concentrazione sarà 5%) versando piccole quantità di mucina nel solvente di interesse. Se occorre, alzare gli rpm per pochi secondi in modo da far scendere eventuali accumuli di proteina, poi abbassare i giri. Lasciare o.n a circa 300 rpm.
- Pesare il CaCO<sub>3</sub> in una vial di vetro in modo che il giorno dopo si possa aggiungere un definito volume di medium per ottenere una sospensione di CaCO<sub>3</sub> al 0.9%. Mettere o.n. la vial ben chiusa nella stufa a 120 °C SECCHI. (es. pesiamo 18 mg e il giorno dopo ci versiamo sterilmente 2 mL di medium). Se non è possibile lasciare o.n. si può mettere la vial al mattino e toglierla dopo 8 ore.

- Pesare GDL per fare una soluzione al 7% il giorno dopo (di solito 1 mL di soluzione sono sufficienti, quindi 70 mg, ad esempio).
- Mettere in etanolo 70% i tappi per siringhe e i connettori per il metodo della doppia siringa da fare sotto cappa.

**N.B.** tutte le soluzioni sono da fare nel medium che ci interessa, nel caso di Mu4OVID il medium selezionato è DMEM.

## Giorno 2

### **Preparazione MU4Covid**

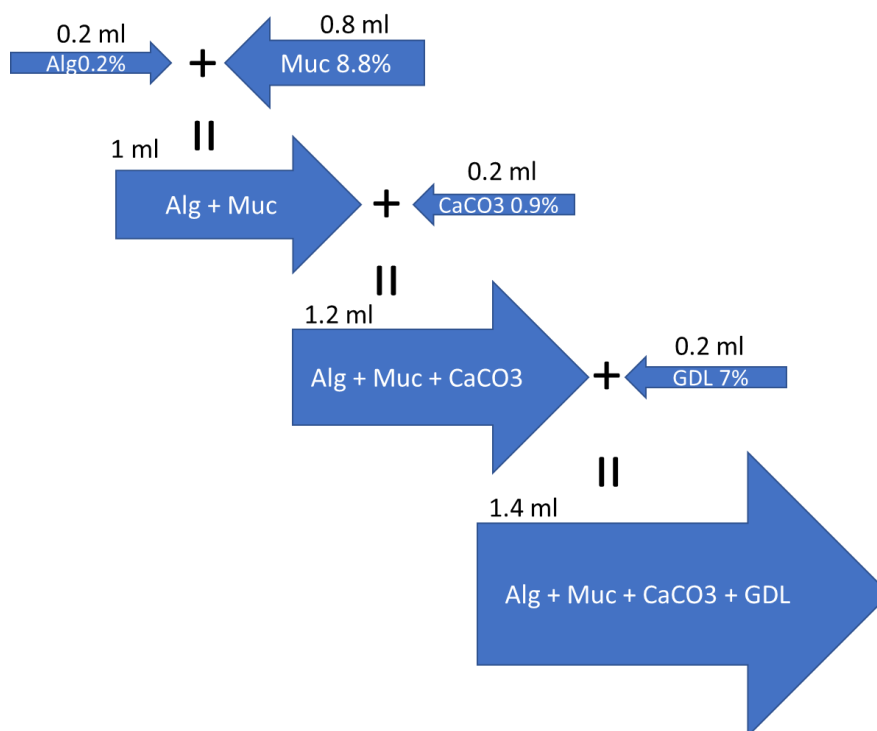
- Appoggiare sterilmente in una petri, almeno 1 h prima di fare i gel, i connettori e i tappi per siringa in modo che l'etanolo evapori. Se si vuole, è possibile far andare gli UV della cappa mentre evapora l'etanolo.
- Versare sterilmente il volume di medium nella vial con il calcio in modo da avere la sospensione a 0.9% sterile. Agitare vigorosamente al fine miscelare calcio e medium. (Procedura da fare prima di incominciare la procedura di preparazione dei gel, facilita l'omogeneità della sospensione).
- Prendere 0.2 mL di soluzione alginato 4,2% e inserirlo in una siringa (secondo il metodo descritto nel paragrafo "considerazioni generali sul metodo della doppia siringa"). Allo stesso modo versare in una seconda siringa 0.8 mL di soluzione di mucina 8.8% e su questa avvitare il connettore. Miscelare le soluzioni premendo in modo alternato i pistoni delle due siringhe per un totale di 25 volte.
- Versare 0.2 mL della sospensione di CaCO<sub>3</sub> in una nuova siringa (ancora una volta usando il metodo descritto nel paragrafo "considerazioni generali sul metodo della doppia siringa"). L'operatore avrà davanti a sé due siringhe, piene sino all'orlo: una di alginato + mucina (con connettore) e una di calcio. Tramite

il metodo doppia siringa si mescolano i 0.2 mL di calcio con 1 mL di alginato e mucina, ottenendo così una sola siringa con 1.2 mL di alginato, mucina e calcio.

- Preparare in modo non sterile la soluzione di GDL 7%, facendo attenzione a sciogliere tutti i grani. La soluzione di GDL deve essere preparata **subito prima** di essere impiegata (non devono trascorrere più di 5 minuti). Filtriamo con filtro 0,2 la soluzione e ne prendiamo 0.2 mL (sterili) da mettere in una siringa. Si miscela la siringa con 0.2 mL di GDL con la siringa avente 1.2 mL di alginato, mucina e calcio.
- Versare il volume desiderato di gel (1.4 mL totali) nei pozzetti.

**N.B. La soluzione finale ottenuta (1.4 mL totali) deve rimanere in frigo a 4°C per almeno 20 ore prima di procedere con gli esperimenti.**

N.B. Questo protocollo serve per produrre 1.4 mL. Se serve più o meno volume occorrerà mantenere inalterati i rapporti di volume 1:4:1:1 di alginato, mucina, CaCO<sub>3</sub> e GDL (Fig1)





Il gel ha un aspetto molto liquido, sul color sabbia-avorio. Si può utilizzare un ago per la sua deposizione nei pozzetti, oppure direttamente dalla siringa. Deve essere prestata molta attenzione a quando si va ad aggiungere il medium sopra il gel. Se infatti si pipetta il medium direttamente sopra, il gel si rompe. **È NECESSARIO colare il medium premendo il puntale sulla parete del pozzetto con ESTREMA lentezza.** Si consiglia di tenere sempre un pozzetto in più per tarare la mano su questo passaggio critico.

# List of Figures

Figure 1.1: Anatomic view of mucus coating of the tissues lining all the body internal organs and cavities (adapted from [1]) .....	7
Figure 1.2: mucus distribution in normal airways (adapted from [20]).....	9
Figure 1.3: impact of water amount in the clearance studies in a “two layers system” made of pericellular environment and overlying mucus layer. The left panel reports the condition of hyperhydration, the central panel reports the normal physiological condition, the right panel the dehydrated condition (adapted from [11]).....	11
Figure 1.4: beat cycle of the cilia seen from the side and top view. The recovery stroke starts on the left from the resting position (r) and continues unrolling clockwise. The effective stroke on right, shows how they remain extended until reaching the resting position (adapted from [14]).....	12
Figure 1.5: representation of the airways mucus layer focusing on MUC5AC and MUC5B, the most relevant membrane-bound mucins (adapted from [23]).....	14
Figure 1.6: : MUC5B distribution in mucus layer. WGA is referred to the samples that were treated with 10µg/mL of wheat germ agglutinin, while anti-MUC5B for the ones treated with antibodies (adapted from [27]).....	15
Figure 1.7: study on native airway mucus. $G'$ (white dots) and $G''$ (black dots) are here reported in function of frequency [Hz] (adapted from [32]).....	17
Figure 1.8: study on native airway mucus and modified one. $G'$ (red squares) and $G''$ (red squares) are referred to the modified artificial airway mucus, $G'$ (grey squares)	

and  $G''$  (grey squares) are referred to the native. Both the trends are reported in function of frequency [Hz] (adapted from [31]).....17

Figure 1.9: Shear rates experienced through the tracheobronchial tree (adapted from [33]).....18

Figure 1.10: Sources for native human pulmonary mucus (adapted from [37]).....19

Figure 1.11: Relationship between mucus gel protein concentration and elastic modulus and viscous modulus at pH 5 with 10-mM  $Ca^{2+}$  and at pH 9 without  $Ca^{2+}$  (adapted from [40]).....21

Figure 1.12: between elastic and viscous moduli of healthy subjects and asthmatic during studies about time and temperature dependence. Data are collected from four healthy subjects and five patients with asthma. (A) Airway mucus collected from patients with early asthma stage. \*\*\*P < 0.001 and \*\*P < 0.01 versus healthy control subjects. (B) Comparison of airway mucus collected during the acute asthma stage and after the recovery in the hospital. \*P < 0.05 versus acute asthma (adapted from [44]).....22

Figure 1.13: comparison between elastic and viscous moduli of healthy subjects and asthmatic ones during studies about frequency dependence (adapted from [44]).....22

Figure 1.14: SEM images of a network of mucus samples for the healthy condition at two different zoom levels (adapted from [50]).....24

Figure 1.15: SEM images of a network of mucus samples for the CF pathologic condition at two different zoom levels (adapted from [50]).....24

Figure 1.16: Macro-rheology of human cystic fibrosis sputum. (A) The frequency-dependent elastic and viscous moduli of CF samples (conducted on 6 patients). (B) Strain-dependent elastic and viscous moduli from 0.1–100% strain amplitude (adapted from [51]).....26

Figure 1.17: representation of the ciliated epithelial cells focusing on the produced mucins MUC1 (red), MUC4 (blue), and MUC16 (yellow) and how SARS-CoV-2 enters in binding to the receptor ACE2 (adapted from [62]).....27

Figure 1.18: age, gender and hypertension as risk factors on SARS-CoV-2 severity (adapted from [63]).....28

Figure 3.1: graphical representation of the mucus model production using the double syringe method: alginate and mucin solutions are firstly added in two different syringes that are put in contact using a connector, then CaCO<sub>3</sub> suspension is added and finally GDL solution.....38

Figure 3.2: graphical representation of how the stability test was carried out: using a pipette the transwells are filled of mucus solution and are left crosslinking in a fridge for 20 hours. Spent this time, they are put in contact with the medium deposited in the below multiwell and the structure is moved in an oven. At each timepoint the weight of each transwell is controlled.....41

Figure 4.1: frequency test of the alginate solution 0,6% conducted on the same alginate solution stored for 7 days from its production.....50

Figure 4.2: viscosity test of the alginate solution 0,6%. (A) reports the viscosity [mPa\*s] against the shear rate [1/s], (B) selected the shear rate value at 6,81 [1/s] it has been reported the correspondent viscosity value during the testing days.....50

Figure 4.3: viscosity test of the alginate solution 0,6% dissolved in EMEM. Comparison between day 0 and day 4.....51

Figure 4.4: viscosity test of the alginate solution 0,6% dissolved in TSB. Comparison between day 0 and day 4.....51

Figure 4.5: comparison between Mu4Covid 1.5 and Mu4Covid 1.8 in which the respective alginate concentrations are 0,4% and 0,5%, while mucin is kept constant at 2,5%. (A) Reports the whole curve, (B) fixed the frequency at 0,44 Hz reports the correspondent storage and loss moduli. Statistical differences at  $G'$  (0,44 Hz) and  $G''$  (0,44 Hz) for  $p < 0.05$  have been found between the two compositions.....52

Figure 4.6: comparison between Mu4Covid 2.1 and Mu4Covid P 2.3 in which the respective alginate concentrations are 0,6% and 0,7%, while mucin is kept constant at 2,5%. (A) Reports the whole curve, (B) fixed the frequency at 0,44 Hz reports the correspondent storage and loss moduli. Statistical differences at  $G'$  (0,44 Hz) and  $G''$  (0,44 Hz) for  $p < 0.05$  have been found between the two compositions.....52

Figure 4.7: how mucin appears after weighted.....53

Figure 4.8: comparison between two gels produced with the same components amount, the only difference is the used mucin: the one present at Politecnico di Milano and the one from Università di Pavia. (A) shows the whole curve, (B) fixed the frequency at 0,44 Hz reports the correspondent storage and loss moduli. No statistical differences at  $G'$  (0,44 Hz) and  $G''$  (0,44 Hz) for  $p < 0.05$  have been found between the two compositions.....53

Figure 4.9: comparison between Mu4Covid 1.2 and Mu4Covid 1.5 in which the respective mucin concentrations are 5% and 2,5%, while alginate is kept constant at 0,4%. (A) shows the whole curve, (B) fixed the frequency at 0,44 Hz reports the correspondent storage and loss moduli. No statistical differences at  $G'$  (0,44 Hz) and  $G''$  (0,44 Hz) for  $p < 0.05$  have been found between the two compositions.....54

Figure 4.10: comparison between Mu4Covid 2.1 and Mu4Covid P 2.1 in which the respective mucin concentrations are 1,25% and 2,5%, while alginate is kept constant at 0,6%. (A) shows the whole curve, (B) fixed the frequency at 0,44 Hz reports the

correspondent storage and loss moduli. No statistical differences at  $G'$  (0,44 Hz) and  $G''$  (0,44 Hz) for  $p < 0.05$  have been found between the two compositions.....54

Figure 4.11: Mu4Covid 2.0 produced in DMEM, TSB and EMEM as mediums. Here reported a comparison in terms of (A)  $G'$  (0,44 Hz) and (B)  $G''$ (0,44 Hz).....55

Figure 4.12: comparison between two gels of the same composition but dissolved in different medium: one using DMEM with 1% L-glut, 1% PS and 10% FBS and the other in distilled water 1 : 1 DMEM : dH<sub>2</sub>O. No statistical differences at (A)  $G'$  (0,44 Hz) and (B)  $G''$  (0,44 Hz) for  $p < 0.05$  have been found between the two compositions.....57

Figure 4.13: macroscopic view of the gels on the rheometer plate immediately before providing the frequency test. (A) pipetted gel, (B) dripped and (C) syringe.....57

Figure 4.14: comparison of the same gel (Mu4Covid 1.0) dispensed by pipetting and dripping. (A) shows the whole curve, (B) fixed the frequency at 0,44 Hz reports the correspondent values of storage and loss moduli. Statistical differences at  $G'$  (0,44Hz) and  $G''$  (0,44Hz) for  $p < 0.05$  have been found between the two compositions.....58

Figure 4.15: comparison of the same gel (Mu4Covid 2.1) dispensed by pipetting, dripping and syringing. (A) shows the whole curve, (B) fixed the frequency at 0,44Hz reports the correspondent values of storage and loss moduli. No statistical differences at  $G'$  (0,44Hz) and  $G''$  (0,44Hz) for  $p < 0.05$  have been found between the syringe and dripped modalities, while statistical differences have been found between the syringe and dripped respect pipetted.....58

Figure 4.16: comparison of the same gel (Mu4Covid P 2.2) dispensed by pipetting, dripping and syringing. (A) shows the whole curve, (B) fixed the frequency at 0,44 Hz reports the correspondent values of storage and loss moduli. No statistical differences at  $G'$  (0,44 Hz) and  $G''$  (0,44 Hz) for  $p < 0.05$  have been found between the syringe and

dripped modality, while statistical differences have been found between the syringe and dripped respect pipetted.....59

Figure 4.17: the presence of the double phase didn't spare any gel production, here reported how Mu4Covid P 2.3 looks like after being stored for 7 days at 4°C.....61

Figure 4.18: macroscopic view of frozen and successively defrosted samples when pipetted on the rheometer plate.....61

Figure 4.19: comparison between rheological properties of the mucus Mu4Covid 1.0 at  $t_0$  and after the freezing and the defrosting in terms of  $G'$  (A) and  $G''$ (B). No statistical differences at  $G'$  (0,44 Hz) for  $p<0.05$  have been found between the two storage modalities, while statistical differences at  $G''$  (0,44 Hz).....62

Figure 4.20: macroscopic view of how the 3D model adapt itself to transwell of different size. (A) 6 transwells support, (B) 24 transwells support.....62

Figure 4.21: stability test provided at  $t = 0, 1, 3, 24, 48, 72$  hours of Mu4Covid 2.0 in a 6 transwells support by weighting the samples and calculating the mass variation [%].....63

Figure 4.22: stability test provided at  $t = 0, 24, 48, 72, 96, 168$  hours of Mu4Covid P 2.0 in 24 transwells support by weighting the samples and calculating the mass variation [%].....63

Figure 4.23: stability test provided at  $t = 0, 3, 24, 48, 72$  hours of Mu4Covid P 2.2 in a 6 transwells support by weighting the samples and calculating the mass variation [%].....63

Figure 4.24: cellular activity at 24 and 72 hours of VERO-E6 cellular line. Cell viability has been quantified using Trypan blue coloration.....64

Figure 4.25: comparison of the cellular viability of VERO-E6 cellular line using Trypan blue coloration when the dissolving agent is DMEM and TSB. The control is given by the cells culture in absence of Mu4Covid 2.0.....65

Figure 4.26: virucidal test using HCoV-OC43 on three different cellular lines.....65

Figure 4.27: virucidal test using Sars-CoV-2 with different mucin amounts (A) 2,5% and (B) 1,25% and in absence of Mu4Covid 2.0 (C).....66

Figure 4.28: drug permeability tests. Blu, reports data when mucus is absent while red in mucus presence.....66

Figure 4.29: cytocompatibility using VERO-E6 present in Mu4Covid 2.0 containing *S. aureus* secretome in exponential phase (S. 0.5) and stationary phase (S. 1.7) dissolved in TSB and comparison with Mu4Covid 2.0 in only TSB and the control in absence of Mu4Covid 2.0.....67

Figure 4.30: macroscopic view of Mu4Covid 2.1 when inside the vial used for the storage. (A) shows how the gel is like when the vial that contains it is slightly inclined (B) shows how it is like when the vial is put upside down.....68

Figure 4.31: macroscopic view of how Mu4Covid 2.1 appears when dispensed in different ways: (A) pipetted, (B) dripped and (C) syringed.....68

Figure 4.32: comparison of Mu4Covid 2.1 dispensed by pipetting, dripping and syringing. Fixed the frequency at 0,44 Hz (A) shows the trend of  $G'$ , while (B) the trend of  $G''$ . No statistical differences at  $G'$  (0,44 Hz) and  $G''$  (0,44 Hz) for  $p < 0.05$  have been found between the syringe and dripped modality, while statistical differences have been found between the syringe and dripped respect pipetted.....69

Figure 4.33: fixed the frequency of 0,44 Hz (A) reports the trend of  $G'$  during the 7 days of storage (B) reports the trend of  $G''$  during the 7 days of storage. No statistical



differences at  $G'$  (0,44 Hz) and  $G''$  (0,44 Hz) for  $p < 0.05$  have been found during the conducted shelf-life.....69

Figure 4.34: macroscopic view of how the mucus model appears after 30 days of storage in the vial and on the rheometer plate before providing the test.....70

Figure 4.35: fixed the frequency of 0,44 Hz (A) reports the trend of  $G'$  at  $t = 0, 7, 30$  days (B) reports the trend of  $G''$   $t = 0, 7, 30$  days. Statistical differences at  $G'$  (0,44 Hz) and  $G''$  (0,44 Hz) for  $p < 0.05$  have been found between the obtained values at  $t = 30$  days and  $t = 0$  day or  $t = 7$  days.....70

Figure 4.36: to provide the stability test, the gel was dispensed in transwells that fit 24 transwells support. Here reported the macroscopic observation of how Mu4Covid 2.1 looked like and how it adapted to the walls.....70

Figure 4.37: stability test provided at  $t = 0, 24, 48, 72, 96, 168$  h of Mu4Covid 2.1 in 24 transwells support by weighting the samples and calculating the mass variation [%].....71

Figure 4.38: macroscopic view of Mu4Covid P 2.3 in the vial for the storage showing how the gel is like when (A) the vial is on a flat surface (B) the vial is upside down.....71

Figure 4.39: macroscopic view of Mu4Covid P 2.3 when is put on the rheometer plate before performing any experiment (A) and when the experiment is concluded and the upper plate of the rheometer is rising up (B).....72

Figure 4.40: macroscopic view of how Mu4Covid P 2.3 appears when dispensed in different ways: (A) pipetted, (B) dripped and (C) syringe.....72

Figure 4.41: comparison of Mu4Covid P 2.3 dispensed by pipetting, dripping and syringing. Fixed the frequency at 0,44 Hz (A) shows the trend of  $G'$  (B) the one of  $G''$ .

Statistical differences at  $G'$  (0,44 Hz) and  $G''$  (0,44 Hz) for  $p < 0.05$  have been found between the three dispensing modalities.....73

Figure 4.42: macroscopic view of 1mL of gel in a well of the 6 multiwells and 0,3 mL of gel in a well of the 6 multiwells.....74

Figure 4.43: fixed the frequency of 0,44 Hz (A) reports the trend of  $G'$  during the days (B) reports the trend of  $G''$  during the days. No statistical differences at  $G'$  (0,44 Hz) and  $G''$  (0,44 Hz) for  $p < 0.05$  have been found during the conducted shelf-life.....75

Figure 4.44: appearance of the liquid phase in Mu4Covid P 2.3 after being stored at 4°C after 5 days.....75

Figure 4.45: macroscopic view during the freezing/defrosting process: (A) when vials were freeze at -80°C, (B) mucus in the vial after leaving the sample overnight at 4°C to provide the defrost, (C) mucus deposited on the rheometer plate before performing any operation .....76

Figure 4.46: comparison between rheological properties of Mu4Covid P 2.3 at  $t=0$  and after the freezing and the defrosting in terms of (A)  $G'$ (0,44Hz) and (B)  $G''$ (0,44Hz). No statistical differences at  $G'$ (0,44Hz) for  $p < 0.05$  have been found between the conducted shelf-lives, while statistical differences have been found in terms of  $G''$ (0,44Hz).....76

Figure 4.47: fixed the frequency of 0,44 Hz (A) reports the trend of  $G'$  (B) reports the trend of  $G''$  during the storage at  $T_{amb}$ . Statistical differences at  $G'$  (0,44 Hz) and  $G''$  (0,44 Hz) for  $p < 0.05$  have been found during the conducted shelf-life.....77

Figure 4.48: to provide the stability test, the gel was dispensed in transwells that fit 24 transwells support. Here reported the macroscopic observation of how Mu4Covid P 2.3 looked like and how it adapted to the walls.....79

Figure 4.49: stability test provided at t = 0, 3, 24, 48, 72 h of Mu4Covid P 2.3 in 24 transwells support by weighting the samples and calculating the mass variation [%].....	79
Figure 4.50: fixed the frequency of 0,44 Hz (A) reports the trend of G' (B) reports the trend of G'' during the storage when as medium it is used EMEM 0.54. No statistical differences at G' (0,44 Hz) and G'' (0,44 Hz) for $p<0.05$ have been found during the conducted shelf-life.....	80
Figure 4.51: stability test provided at t = 0, 3, 24, 48, 72 h of Mu4Covid P 2.3 dissolved in EMEM 0.54.....	80
Figure 4.52: fixed the frequency of 0,44 Hz (A) reports the trend of G' (B) reports the trend of G'' during the storage when as medium it is used EMEM 1.11. No statistical differences at G' (0,44 Hz) and G'' (0,44 Hz) for $p<0.05$ have been found during the conducted shelf-life.....	81
Figure 4.53: stability test provided at t = 0, 3, 24, 48, 72 h of Mu4Covid P 2.3 dissolved in EMEM 1.11.....	81
Figure 4.54: influence of the secretome in EMEM for the developed mucus model in (A) G'(0,44 Hz) and (B) G''(0,44 Hz) where the control is given by blank EMEM used as medium.....	81
Figure 4.55: fixed the frequency of 0,44 Hz (A) reports the trend of G' (B) reports the trend of G'' during the storage when as medium it is used TSB 0.5. No statistical differences at G' (0,44 Hz) and G'' (0,44 Hz) for $p<0.05$ have been found during the conducted shelf-life.....	82
Figure 4.56: stability test provided at t = 0, 3, 24, 48, 72 h of Mu4Covid P 2.3 dissolved in TSB 0.5.....	82

Figure 4.57: fixed the frequency of 0,44 Hz (A) reports the trend of  $G'$  (B) reports the trend of  $G''$  during the storage when as medium it is used TSB 1.11. No statistical differences at  $G'$  (0,44 Hz) and  $G''$  (0,44 Hz) for  $p < 0.05$  have been found during the conducted shelf-life.....82

Figure 4.58: stability test provided at  $t = 0, 3, 24, 48, 72$  h of Mu4Covid P 2.3 dissolved in TSB 1.7.....83

Figure 4.59: influence of the secretome in TSB for the developed mucus model in (A)  $G'$ (0,44 Hz) and (B)  $G''$ (0,44 Hz) where the control is given by blank TSB as medium.....83

# List of Tables

Table 4.1: some of the more interesting tested gels and their composition .....	45
Table 4.2: all the tested pH values obtained during the analysis.....	46
Table 4.3: macroscopic view of several tested gels: the first column reports the nomenclature, the second how the gel looks like inside the vials used for the storage, and the third one how it looks like when pipetted and placed on the rheometer plate before performing any test.....	48
Table 4.4: macroscopic view of the mucus dissolved in DMEM and in 1:1 DMEM:dH <sub>2</sub> O. Each drop has been deposited withdrawing 20µl of gel after its reticulation.....	56
Table 4.5: diameter and height of each drop calculated using the App ImageJ. Here reported the mean and the standard deviation.....	56
Table 4.6: shelf-life over a maximum of 7 consecutive days of several mucus compositions. Fixed the frequency at 0,44 Hz, all the data are reported in terms of storage and loss moduli and their time evolution.....	60
Table 4.7: here reported the composition of Mu4Covid 2.0 used for the tests in UniTO and UniPV.....	64
Table 4.8: here reported the composition of Mu4Covid 2.1, the mucus model that has showed to better mimic the physiological healthy condition.....	67
Table 4.9: here reported the composition of Mu4Covid P 2.3, the one that has showed to better mimic the SARS-CoV-2 pathological condition.....	71

Table 4.10: macroscopic observation of several mucus quantities on a petri dish using a pipette. Each drop has been pipetted three times. For each mucus quantity, here reported the photos of the side and top view.....74

Table 4.11: diameter and height of each drop calculated using the App ImageJ. Here reported the mean and the standard deviation.....74

Table 4.12: macroscopic view on the rheometer plate and inside the vials of Mu4Covid P 2.3 when stored at  $T_{amb}$ .....77

Table 4.13: here reported the values of each measurement of  $G'$  (0,44Hz) during the shelf-life conducted at  $T_{amb}$ , its mean value, the calculated standard deviation and finally the increasing [%].....78

Table 4.14: here reported the values of each measurement of  $G''$  (0,44Hz) during the shelf-life conducted at  $T_{amb}$ , its mean value, the calculated standard deviation and finally the increasing [%].....78

